CHARACTERISING AMR PLASMID TRANSMISSION IN THE GUT MICROBIOME

By

CELIA KESSLER

A thesis submitted to

the University of Birmingham

for the degree of

MSC BY RESEARCH

Institute of Microbiology and Infection

College of Medical and Dental Sciences

University of Birmingham

May 2021

ABSTRACT

Antimicrobial resistance poses an urgent threat to global health. In particular, strains of the bacterial family *Enterobacteriaceae* resistant to last-line carbapenem antibiotics have been identified by the World Health Organisation as a critical priority for drug development. The spread of carbapenem resistance is aided by the horizontal transfer of resistance genes to susceptible bacteria on plasmids, which is commonplace in environments of high bacterial density such as the human gut microbiome. Reducing the transfer and stability of such plasmids is an attractive strategy for tackling antibiotic resistance, especially in the gut microbiome as only resistant bacteria are targeted whilst the rest of the microbiome is left intact: a quality lacking from traditional antibiotic therapy. Here, an investigation was begun to understand the conjugative dynamics of a carbapenemase-encoding plasmid in *Klebsiella pneumoniae* with and without co-culture with members of the commensal gut microbiota, in a simple *in vitro* model of the gut microbiome, wherein *Bacteroides fragilis* was not found to affect conjugation frequency. In parallel, an investigation into natural extracts of the culinary spices turmeric and black pepper as potential anti-plasmid agents was undertaken, to characterise them as potential agents for targeting conjugation in the gut microbiome. A literature review explored more complex established *in vitro* models with the potential for incorporation into such investigations into plasmid conjugation.

COVID-19 IMPACT STATEMENT

Following UK Government guidelines concerning the SARS-CoV-2 global pandemic, laboratory access ceased from Friday 20th March 2020. Access resumed from Monday 13th July 2020 at low capacity and with strict restrictions in place in consideration of the safety of all lab members. As a result of this significant amount of lost lab time, the wet-lab components of this project were unable to progress as far as had been initially planned. Instances where parts of the project would have benefited from better access to equipment and more time in the lab to perform, optimise and repeat experiments have been clearly indicated in the thesis where applicable. In addition, an in-depth literature review was conducted in the months working remotely, and has formed much of Chapter 4 of this thesis.

ACKNOWLEDGMENTS

With credit to Luuk Earl for provision of a UoB Thesis LaTeX Template upon which the formatting of this thesis was based, and modified in this instance with no endorsement by the template provider. Available at https://www.overleaf.com/latex/templates/uob-thesis-latex-template/dqgzvjpfsvfs?fbclid=IwAR3ZZ8kxKNNyrLiTgkuUpZBadPxKlC9NHHAoomEnuBLp7197OWQ2_a_Z9q4 under the Creative Commons CC BY 4.0 public license.

More personally, I'd like to thank my primary supervisor, Dr. Michelle Buckner, for her guidance and support throughout the project in what has been a somewhat difficult year, and my secondary supervisor, Prof. Willem van Schaik, for his feedback and support. Thanks also to past and present members of the Buckner Lab, T102 and G7 for all of their help and encouragement.

Contents

List of Figures

List of Tables

List of Abbreviations

AFR	Aerobic fluorescence recovery
AMR	Antimicrobial resistance
APH	Aminoglycoside phosphotransferase
ARG	Antibiotic resistance gene
ATCC	American Type Culture Collection
ATP	Adenosine triphosphate
Az^R	Azide-resistant
BHIS	Brain Heart Infusion- Supplemented
CDAD	*Clostridioides difficile*-associated diarrhoea
CFS	Cell-free supernatant
CFU	Colony forming unit
CRE	Carbapenem-resistant *Enterobacteriaceae*
COP	Colonising opportunistic pathogen
DMSO	Dimethyl sulfoxide
DNA	Deoxyribonucleic acid
EEA	Euorpean Economic Area
ECDC	European Centre for Disease Prevention and Control
ESBL	Extended-spectrum β-lactamase
EU	European Union
EUCAST	European Committee on Antimicrobial Susceptibility Testing
ExPEC	Extraintestinal pathogenic *Escherichia coli*
GBD	Global Burden of Disease Project
GFP	Green Fluorescent Protein

GI	Gastrointestinal
GLASS	Global Antimicrobial Surveillance Scheme
HGT	Horizontal gene transfer
HIV	Human Immunodeficiency Virus
ICU	Intensive care unit
Inc	Incompatibility
KPC	*Klebsiella pneumoniae* carbapenemase
LB	Luria-Bertani
LD_{50}	Lethal dose
LMIC	Low- to middle- income country
MDR	Multi-drug resistant
MGE	Mobile genetic element
MIC	Minimal inhibitory concentration
MLST	Multi-locus sequence typing
MOB	Mobility
MPF	Mating pair formation
MRS	De Man, Rosa and Sharpe
NCTC	National Collection of Type Cultures
NDM	New Delhi metallo-β-lactamase
NE	Natural extract
OD	Optical density
PBS	Phospho-buffered saline
PCR	Polymerase Chain Reaction
R&D	Research and development
ROS	Reactive oxygen species
RFLP	Restriction fragment length polymorphism

SCFA	Short-chain fatty acid
SDW	Sterile distilled water
SHIME®	Stimulator of the Human Intestinal Microbial Ecosystem
ST	Sequence type
T4CP	Type 4 coupling protein
Tn	Transposon
UTI	Urinary tract infection
WHO	World Health Organisation

1. Introduction

1.1 Antimicrobial Resistance

The threat of untreatable infections is no longer a concern of the past. Drug-resistant pathogens have been projected to threaten 10 million lives per year by 2050, with a cumulative global cost of 100 trillion US dollars (O'Neill, 2016). This projection covers not just the morbidity and mortality of infections, but also the increased risk of many clinical practices such as chemotherapy, invasive surgeries and parturition procedures, with the most severe impacts predicted on low- and middle-income countries.

1.1.1 A global crisis

Bacteria can cause a vast range of morbidities from local infections such as gastroenteritis, meningitis and dermal infections to systemic complications such as septicaemia. Antimicrobial resistance (AMR)[1] has already begun to restrict the available treatment and prevention options for such infections (MacLean and San Millan, 2019). For example, surveillance of invasive isolates in the EU/EEA in 2018 reported that 11% of *Staphylococcus aureus* isolates were resistant to two or more antibiotic groups, with rates reaching 19.2% for *Pseudomonas aeruginosa* and 30% for *Klebsiella pneumoniae* (ECDC, 2019). These values are largely either decreasing (e.g. *S. aureus*; *P. aeruginosa*) or stabilising (e.g. *K. pneumoniae*) in many European countries, thanks to active surveillance and national guidance. However, observed increases in resistance of some bacteria to "last resort" antibiotics, such as carbapenems are concerning. Comparison of total AMR burden in the EU/EEA between 2007

[1] The term 'AMR' covers all manner of drug-resistant microbes, such as bacteria, viruses, fungi and parasites. This project focuses on antibiotic resistant bacteria, and so 'AMR' in this context refers specifically to antibiotic resistance.

and 2015 showed that AMR-attributed deaths rose by a factor of 2.46 from 11,000 to 27,000, with deaths attributed to carbapenem-resistant *K. pneumoniae* infection rising by 6.6-fold (Cassini et al., 2019).

Such stringent data on global AMR burden are difficult to synthesise, due to different local governmental, healthcare, data collection and surveillance systems providing incomparable data. An estimate from O'Neill (2016) attributed 700,000 global deaths per year to AMR bacterial infections, though the estimates had to be extrapolated from USA figures due to scarcity of comparable data from low- to middle-income countries (LMICs), and therefore are likely to be less representative of the latter (Limmathurotsakul et al., 2019). Multiple large-scale projects have been set up in recent years to collect and standardise global AMR data, such as the Global Antimicrobial Surveillance Scheme (GLASS) by the World Health Organization (WHO) in 2015, and integration of AMR into the Global Burden of Disease (GBD) project (O'Neill, 2016; Limmathurotsakul et al., 2019).

Indeed, the AMR crisis is a complex issue with many contributing factors. Low financial returns and high risk are deterrents for pharmaceutical companies to invest in the research and development (R&D) of new therapies, requiring novel funding strategies (Towse et al., 2017). Overuse and misuse of antibiotic drugs in both high-income countries and LMICs accelerate the development and spread of resistance, requiring tailored stewardship schemes (Fleming-Dutra et al., 2016; M. M. Nair et al., 2021). But the evolutionary ability of microorganisms to withstand challenges to their survival underpins the AMR crisis, and attention to and investment in the research and discovery of novel antibiotic therapies is critical for staying ahead in this evolutionary arms race.

1.1.2 Biological origins

An antibiotic is, by definition, a medicine used for the prevention and treatment of bacterial infection (WHO, 2020). Historically, antibiotic discovery and design has been based

on natural antibacterial compounds, since these have already been evolutionarily selected and refined (Hutchings et al., 2019). A significant proportion of these have been isolated from soil-dwelling organisms, hypothesised to result from soil environments harbouring high biomass and biodiversity, and therefore competition for resources across kingdoms (Traxler and Kolter, 2015). The evolution of this form of biological warfare naturally included evolution of resistance to such compounds.

Resistance to antibiotic compounds evolves through genetic changes in individual cells, often providing a survival advantage over more sensitive population members. Changes contributing to AMR include mutations in genes encoding antibiotic targets, upregulation of expression or activity of efflux pumps, downregulation of porin expression reducing membrane permeability and drug uptake, and expression of drug-inactivating enzymes (Blair et al., 2015). Also contributing to AMR are the increased ability of bacteria to form protective biofilms (Høiby et al., 2010), and the ability to transiently become metabolically inactive persisters (Fisher et al., 2017), though the genetic bases of these traits are less well understood.

Acquisition of many of these traits occurs by two main pathways (Blair et al., 2015; MacLean and San Millan, 2019): *de novo* mutations and horizontal gene transfer (HGT). *De novo* mutations result from naturally-occurring errors in DNA replication, and are the sole mechanism of AMR evolution in some key pathogens, such as *Mycobacterium tuberculosis* (MacLean and San Millan, 2019). HGT is the acquisition of novel genetic material from an external source, and arguably contributes more significantly to AMR in the majority of human pathogens.

1.1.3 Genetic mobility in prokaryotes

Foreign genetic material can be introduced into bacterial cells by several means, the key three being transformation, transduction and conjugation (Soucy et al., 2015). Transformation describes the uptake of foreign DNA from the environment, usually from nearby lysed

microbes. Transduction is the injection of DNA into bacteria by bacteriophages, and conjugation is direct bacteria-bacteria transfer of DNA through a specialised mating pair formation (MPF) complex.

The majority of successful HGT events are understood to occur between closely related organisms (Soucy et al., 2015). However, the stochastic and often non-specific nature of HGT allows DNA transfer between even very distantly related bacterial species in the same niche (Smillie et al., 2011). The resulting "floating pangenome" shared, in theory, between the vast majority of bacteria illustrates how, in the context of AMR, mobilisable antibiotic resistance genes (ARGs) can easily transfer into and between pathogenic strains.

Conjugation in particular has contributed significantly to many of today's key AMR pathogens, such as carbapenem-resistant *Enterobacteriaceae* (Section 1.3.3). DNA segments that can be mobilised are known as mobile genetic elements (MGEs), notably plasmids and conjugative transposons. Plasmids, the largest of bacterial MGEs at a median size of 80 kb (ranging between 744 bp and 2.58 Mb; Shintani et al., 2015), are best able to carry multiple ARGs, as well as genes conferring resistance to other antibacterial substances, such as biocides and heavy metals (Pal et al., 2015). Plasmids have also been observed to contain additional mobile elements such as transposons within them, in a nested Russian doll-like format (Sheppard et al., 2016). Carrying multiple resistance genes on a single MGE allows for co-selection by any condition the MGE encodes resistance to. This has instigated a rise in multi-drug resistant (MDR) bacterial strains, which threaten to become a significant global health challenge in coming decades (Blair et al., 2015; Ventola, 2015; Tacconelli et al., 2018; MacLean and San Millan, 2019).

Plasmid conjugation requires several core elements: a relaxase protein to recognise the origin of transfer (*oriT*) in *cis* and form a complex with the plasmid DNA, an MPF system to transfer the complex to a recipient cell, and a type 4 coupling protein (T4CP) to pair the processes (Smillie et al., 2010; Shintani et al., 2015). These elements define the mobility

potential of a particular plasmid, and form the basis of classification into three categories: conjugative, mobilisable and non-mobilisable, respectively based on whether they code for their own MPF system, use another in *trans*, or cannot mobilise at all (Smillie et al., 2010).

Conjugative and mobilisable plasmids within genera can be further classified by relaxase sequence (MOB types) and replication machinery (replicon types), both of which employ both PCR-based and *in silico* methods for classification (Orlek et al., 2017). Within replicon typing, incompatibility (Inc) grouping is used in some genera to further simplify classification: plasmids with similar replication and partitioning systems are unstable in the same host cell, since these mechanisms cross-interfere and cannot sustain the persistence of both plasmids over time (Carattoli, 2009). For example, the family *Enterobacteriaceae* exhibits 27 known Inc groups at the time of review (Shintani et al., 2015; Kopotsa et al., 2019). Since Inc groups represent different replication systems, they also provide information on the host range in which a plasmid can be stably maintained, as host-encoded genes are often necessary for replication (Carattoli, 2009). For instance, IncQ plasmids have a much broader host range than IncF (which are restricted to the family *Enterobacteriaceae*), because IncQ plasmids can replicate independently of several host-encoded genes that are required for IncF replication (Carattoli, 2009).

Host specificity can provide important insight into the dynamics of AMR genes, since these are often associated with specific plasmid types (Carattoli, 2009), and therefore specific host ranges. This is not an absolute rule however, since other mechanisms of plasmid gene mobility such as transposition and chromosomal integration can cause discrepancies in gene dynamics (Sheppard et al., 2016). Nevertheless, this insight can guide predictions of the dissemination of certain genes and explain observed epidemiological patterns.

1.1.4 Plasmid persistence and evolution

Plasmid carriage can reduce the fitness of its host by a combination of factors, including but not limited to: RNA polymerase and ribosome sequestration, amino acid depletion and, in the case of conjugative plasmids, the high ATP consumption of and increased vulnerability to phage infection caused by the conjugation process (San Millan and MacLean, 2017). In the absence of countering effects, these burdens have the potential to condemn plasmids to be lost from bacterial populations in the long term by purifying selection.

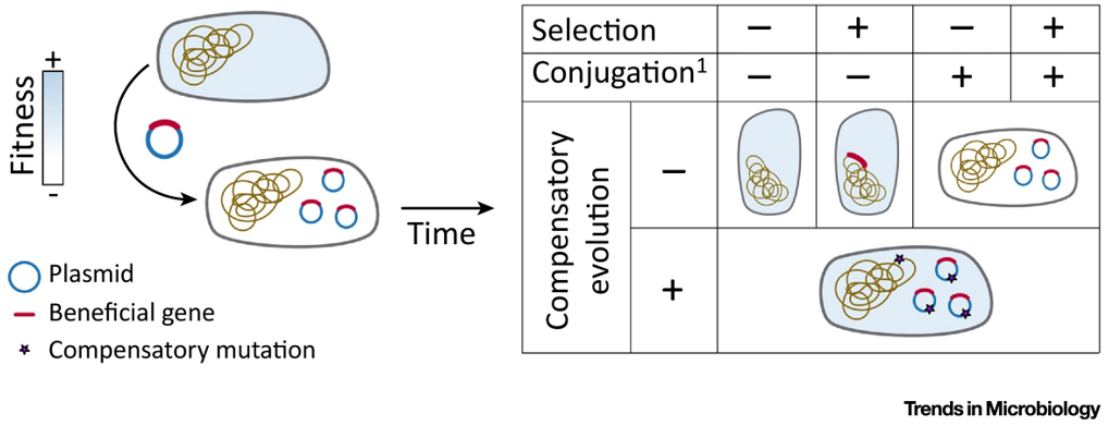

Figure 1.1: Plasmid stability after acquisition. Acquisition causes an initial drop in fitness. The table outlines how three factors affect plasmid stability over time: selection, conjugation ([1]high enough conjugation frequency for persistence despite fitness costs), and compensatory evolution. Figure © San Millan (2018). Published by Elsevier Ltd, doi: 10.1016/j.tim.2018.06.007. Shared under https://creativecommons.org/licenses/by-nc-nd/4.0/.

Three countering effects have been identified which combat this purifying selection: selection, conjugation and compensatory evolution (Figure 1.1). Positive selection pressure, for example by the presence of antibiotics in a niche, promotes the retention of advantageous genes, and advantageous gene-carrying plasmids in a population (San Millan, 2018). It is widely accepted that this phenomenon has driven the rise and spread of antibiotic resistance genes in response to antibiotic use (Ventola, 2015). However as displayed in Figure 1.1,

plasmids and AMR genes can be maintained in bacterial populations in the absence of positive selection. This requires a particular plasmid to either minimise the burden it causes to its host (compensatory evolution), be able to conjugate efficiently into plasmid-free cells, or both (San Millan, 2018).

Mathematical models of plasmid dynamics in bacterial populations support that these factors, as well as additional factors such as biofilm formation, can prolong persistence in the absence of selective pressure (Bergstrom et al., 2000; Imran et al., 2005; Lili et al., 2007; Zwanzig et al., 2019). Long-term co-culture experiments in the absence of selection, reviewed by Harrison and Brockhurst (2012), demonstrate that plasmid persistence is often associated with decreased burden and the reduction in strength of purifying selection. This was observed to occur by a number of evolutionary adaptations, including bacterial suppression of conjugation (Dahlberg and Chao, 2003), loss of unnecessary plasmid accessory genes (Modi et al., 1991) and downregulated plasmid gene expression (Heuer et al., 2007). Interestingly, the observation that non-mobilisable plasmids could also be maintained in the absence of selection (Modi et al., 1991) suggested that in these cases, conjugation frequency (Figure 1.1) may not contribute as significantly to long-term plasmid stability and persistence as selection and compensatory evolution. However, recent work on a range of conjugative plasmids in *E. coli* concluded that conjugation was pivotal in the persistence of these plasmids over time, emphasising that strategies developed to inhibit conjugation and promote plasmid loss would be effective for reducing the persistence of AMR plasmids (Lopatkin et al., 2017).

Compensatory evolution can consist of mutations in both the plasmid and chromosome, and of both genomic and transcriptional changes (Harrison et al., 2015; Buckner et al., 2018b). Regions of interest that have been identified as potential contributors to plasmid compensatory evolution include the chromosomally encoded *gacA/gacS* two-component regulator system (Harrison et al., 2015; Stevenson et al., 2018), and plasmid-encoded insertion sequences (Porse et al., 2016).

Research into plasmid-host evolution contributes important insight into how plasmid transfer affects host bacteria, and how plasmids themselves evolve in new hosts. This has key implications in understanding how bacteria and plasmids behave in both *in vitro* laboratory and clinical settings, as well as how this drives pathogen evolution. Understanding how these interactions differ with different degrees of antibiotic selection could help identify where interventional strategies, such as restriction of antibiotic use, could reduce the clinical implications of conjugation by the reduction of plasmid stability in new hosts (Buckner et al., 2018b).

1.2 Interventional Strategies

1.2.1 Going forward

The rate of antibiotic drug discovery has largely declined since the 1980s, with most new compounds derived from existing antibiotic classes (Ventola, 2015; O'Neill, 2016). This multifaceted problem includes barriers in funding and pharmaceutical investment, but also in finding and designing compounds that are effective against infection with minimum host toxicity (Ventola, 2015). This has fuelled interest in alternative approaches to preventing and treating bacterial infections, especially those that are multi-drug resistant, for which limited treatment options are available.

An alternative approach of interest is the targeting of the drug resistance itself, rather than the fitness of the organism. Rendering drug-resistant bacteria susceptible to existing antibiotics increases the usefulness of tried and tested existing drugs, and could mean that there is less reliance on the development of new drugs in the future (Buckner et al., 2018a). With mobile ARGs playing a major role in disseminating resistance globally, bacterial plasmids have been identified as attractive targets to tackle AMR.

1.2.2 Targeting plasmids

Plasmid curing (removing a plasmid from a batcerial population) is used in experimental laboratory contexts, where it is advantageous to obtain a plasmid-free version of an existing strain. Although there is no standard protocol to achieve this due to inconsistencies in plasmid properties such as stability (Trevors, 1986), methods include exposure to sub-inhibitory concentrations of chemical curing agents, elevated temperature or use of Inc systems to promote plasmid segregation, instability and loss. Chemical curing agents typically work by intercalating, breaking or interfering with the replication or transcription of plasmid DNA (Trevors, 1986; Buckner et al., 2018a).

The *in vitro* success of various curing methods has made it an attractive strategy for tackling AMR by removing mobile ARGs from a population over time. As well as theoretically rendering pathogenic bacteria susceptible to available treatments in the case of infection, plasmid curing could also be used to reduce AMR prevalence in the absence of infection (Buckner et al., 2018a). For example, administration of a plasmid curing agent to a hospitalised patient could help prevent drug-resistant hospital-acquired infections, or could remove resistance genes residing in gut commensals without perturbing the rest of the microbiome. The latter is a common issue with broad-spectrum antibiotics, as these can promote the selection of resistant organisms, and disruption of microbiomes allows invasion of opportunistic pathogens such as *Clostridioides difficile*[2] (Dicks et al., 2019). Additionally, routine treatment in animal husbandry or waste treatment contexts could reduce AMR transmission through food chains and the environment (Buckner et al., 2018a), contributing to the 'One Health' approach to tackling AMR across clinical, agricultural, farming and environmental sectors.

As well as the compound- and Inc-based mechanisms mentioned previously, additional curing systems are being explored for therapeutic use, including using MPF-targeting phage

[2]Referred to in the references by its previous name, *Clostridium difficile*.

to infect and kill MPF-expressing bacteria (Jalasvuori et al., 2011), and CRISPR-Cas9 to specifically cleave ARGs (Kim et al., 2016) or plasmid maintenance genes (Citorik et al., 2014). However, despite ongoing research into plasmid curing compounds as well as approaches based on conjugation inhibition, plasmid incompatibility, phage and CRSIPR/Cas, no system has proved successful or safe enough for routine use as of yet (Buckner et al., 2018a). Challenges include delivery, compound toxicity in humans, and lack of research into efficacy and side-effects *in vivo*. Another concern is that of the potential for resistance to evolve, as is inevitable if a treatment agent causes a fitness defect. Finally, it may also promote the chromosomal integration of resistance genes under selective pressure as demonstrated in Figure 1.1 (San Millan, 2018). Nevertheless, promising progress is being made: recent work on pectin-coated platinum nanoparticles (although a mechanism is still unclear; Bharathan et al., 2019); a plasmid-encoded curing "cassette" containing genes designed to block replication and maintenance of the target plasmid (Lazdins et al., 2020); and the repurposing of existing nucleoside analogue HIV drugs to block conjugation (Buckner et al., 2020). The two formerly mentioned studies incorporated *in vivo* models, key to the development of this research area in the future.

1.3 Carbapenem Resistance

Several of the strains of interest in this AMR project (Section 2.2) were clinically relevant *K. pneumoniae* strains isolated from localised nosocomial infections, and exhibiting resistance to last resort carbapenem antibiotics. Reduced susceptibility to carbapenems was attributed to plasmid-associated ARGs, representative of the observation that carbapenem resistance is predominantly plasmid-mediated (Meletis, 2016; Kopotsa et al., 2019). As a result, plasmid targeting strategies for tackling AMR are highly relevant in the fight against carbapenem-resistant organisms, and these organisms are increasingly central to anti-plasmid research

(Bharathan et al., 2019; Lazdins et al., 2020; Buckner et al., 2020).

1.3.1 Carbapenem antibiotics

Carbapenems are broad-spectrum β-lactam antibiotics, irreversibly inhibiting transpeptidase enzymes which contribute to cell wall synthesis. Since the bacterial cell wall is continuously renewed in a synthesis-hydrolysis cycle, inhibition of synthesis leads to a reduction in wall integrity and cell lysis (Tomasz, 1979).

In the last decades, carbapenems have typically been considered as valuable last resort antibiotics. This is mainly due to their attractive stability in the face of many extended-spectrum β-lactamase (ESBL) enzymes (Meletis, 2016) that confer resistance to earlier β-lactam antibiotics such as penicillins. ESBLs target the β-lactam ring structure within the drug molecule, cleaving it and rendering the drug unable to bind transpeptidases. Despite these strengths however, resistance to carbapenem antibiotics has inevitably arisen and disseminated globally, critically threatening antibiotic therapy (Tacconelli et al., 2018).

1.3.2 Carbapenem resistance mechanisms

Several resistance mechanisms have been uncovered in Gram-positive and Gram-negative bacteria, decreasing susceptibility to carbapenems to various degrees (Meletis, 2016). Gram-positive bacteria can acquire mutations in transpeptidase genes, reducing antibiotic binding affinity to and inhibition of the proteins. As well as this, resistant Gram-negative bacteria can display reduced outer membrane permeability to carbapenems by means of reduced expression of membrane porin proteins, such as *ompK35*, *ompK36* or *oprD* (Kaczmarek et al., 2006; Quale et al., 2006). MDR efflux pumps, when overexpressed, can also act to reduce periplasmic concentrations of carbapenems, reducing their effectiveness (Quale et al., 2006; Blair et al., 2014). Finally, expression of modified β-lactamase enzymes that can hydrolyse carbapenems, termed carbapenemases, confer what is potentially the most significant mech-

anisms of resistance: these enzymes are primarily coded for by horizontally transferrable genes and confer resistance to the majority of β-lactams, not just carbapenems (Poirel et al., 2007).

Analysis of clinical isolates with reduced susceptibility to carbapenems demonstrate that this phenotype tends to arise from a combination of mechanisms, though this is not always consistent. For example, complex interplay of β-lactamase, porin and efflux pump expression has been observed in carbapenem-resistant *Pseudomonas aeruginosa* isolates (Quale et al., 2006). Kaczmarek et al. (2006) compared related carbapenemase-encoding *K. pneumoniae* that exhibited different carbapenem MIC profiles, attributing these to a significant downregulation in expression of porin genes in the more resistant strain, but with no difference in efflux activity. However in a separate clinical isolate, curing of a carbapenemase- ($bla_{\text{KPC-3}}$) encoding plasmid led to a complete loss of carbapenem resistance, with expression of key porins showing similar profiles to susceptible controls (Leavitt et al., 2010b). These studies firstly demonstrated the variety of ways in which carbapenem susceptibility can be reduced in bacteria, but the latter study additionally highlights the particular importance of mobilisable carbapenemase genes, as they have the potential to be sufficient for clinically significant increases in carbapenem MICs.

Different types of carbapenemase enzyme span several of the four Ambler molecular classes of β-lactamase A to D, based on sequence and structural differences (Ambler et al., 1980). Of all carbapenemases, the Class A serine carbapenemase KPC (*K. pneumoniae* carbapenemase) is the most globally prevalent (Castanheira et al., 2017), with Class B zinc-coordinating metallo-β-lactamases including NDM (New Delhi Metallo-β-lactamase) and Class D serine carbapenemases such as OXA-type enzymes also exhibiting global spread (Meletis, 2016; Khan et al., 2017). The epidemiology of carbapenemases is further discussed in Section 1.3.3.

1.3.3 Carbapenem-Resistant *Enterobacteriaceae*

Clinical carbapenem resistance is most prevalently detected among Gram-negative pathogens such as *P. aeruginosa*, *Acinetobacter baumannii* and members of the *Enterobacteriaceae* family (Cai et al., 2017). Carbapenem-resistant *Enterobacteriaceae* (CRE) can cause a range of infections from urinary tract infections (UTIs), skin and soft tissue infections, pneumonia, intra-abdominal infections and blood infections (bacteremia) (Adar et al., 2021). The prevalence and transmission of CRE in hospitals is concerning, with as many as 58% of hospitalised CRE infections having been acquired from within the hospital setting (Adar et al., 2021), likely in part due to invasive procedures such as ventilation or catheterisation opening portals for infection (Vincent, 2003; Adar et al., 2021). Additionally, CRE infections are associated with a four-times greater risk of mortality for bacteremia patients (Tamma et al., 2017). Treatment options for CRE are limited, with CRE often also exhibiting resistance to unrelated drug classes such as fluoroquinolones and aminoglycosides (Morrill et al., 2015). As a consequence, CRE are classified as a critical priority for new drug development by the WHO (Tacconelli et al., 2018), and are a growing threat as their resistance mechanisms continue to evolve (Logan and Weinstein, 2017).

CRE epidemiology is heterogeneous, with different carbapenemases and carbapenemase-producing strains often showing different patterns of spread. For example, clonal expansion of *K. pneumoniae* sequence type (ST) 258 encoding $bla_{\text{KPC-2}}$ or $bla_{\text{KPC-3}}$ on a Tn*4401* transposon accounts for approximately 70% of bla_{KPC} dissemination in *K. pneumoniae* (Kitchel et al., 2009), whereas bla_{NDM} producers do not seem to associate with any particular dominant sequence type (Logan and Weinstein, 2017). Kopotsa et al. (2019) reviewed papers published in English between 2013 and 2018 on plasmid-mediated carbapenem resistance in *Enterobacteriaceae*, reporting that KPC- and OXA- type β-lactamases were most prevalent in a range of observed countries, with an overall rise in prevalence of all carbapenemase types.

This review also reported that IncF plasmids accounted for almost 40% of plasmid-borne carbapenemases, possibly explaining the propensity of these genes to the family *Enterobacteriaceae*, to which the IncF group is restricted (Carattoli, 2009).

Since carbapenem resistance is predominantly plasmid-mediated (Meletis, 2016; Kopotsa et al., 2019), novel plasmid-targeting strategies are an attractive approach to tackling this particular threat. Indeed, recent research published on plasmid targeting highlights the importance of mobile carbapenemases in *Enterobacteriaceae* as research motivations (Bharathan et al., 2019; Lazdins et al., 2020; Buckner et al., 2020), and feature IncF plasmids as curing targets. However plasmid-targeting approaches will not come without their setbacks, as several carbapenemases are commonly associated with active transposons (Logan and Weinstein, 2017), with Tn*4401*-mediated chromosomal integration of bla_{KPC} having been observed in clinical *K. pneumoniae* isolates (Sheppard et al., 2016; Mathers et al., 2017). Purifying selection against plasmid carriage coupled with the positive selection of therapeutic carbapenem use may promote chromosomal integration of these genes, and drive the dissemination of plasmid-free CRE.

Unfortunately, there can be no perfect solution to AMR. Nevertheless, although all interventional strategies will inevitably fall in the face of bacterial evolution, innovative and effective new solutions are the only way to keep the global AMR burden as manageably low as possible.

1.4 The Human Gut Microbiome

Several of the antibiotic resistant pathogenic species that are classified as high or critical priority by the WHO (Tacconelli et al., 2018), including CRE, reside commensally in the human gut (Price et al., 2017). The human gut microbiome has been identified as a key environment for HGT events and the generation of new AMR strains (Huddleston, 2014; van

Schaik, 2015; Zeng and Lin, 2017; San Millan, 2018; McInnes et al., 2020). Investigating and understanding the factors by which plasmid-mediated transfer of AMR is affected by the gut microbiome and its components is key to designing interventional strategies to tackle this phenomenon.

1.4.1 Composition

The human gastrointestinal (GI) tract contains the majority of the bacterial symbionts that inhabit the human body, with numbers ranging from less than 10^3 ml^{-1} in the stomach and duodenum, to 10^{11}-10^{12} ml^{-1} in the colon (Sekirov et al., 2010). The sum of these and other microorganisms in the gut is referred to as the gut microbiota and, along with their genomes and the surrounding environment, are collectively known as the gut microbiome (Marchesi and Ravel, 2015). The microbiota consists of a complex and dynamic community of mutualistic, commensal and parasitic symbionts, which respectively benefit, do not affect, and cause detriment to their human host. Swain Ewald and Ewald (2018) argue that these symbioses are better understood as a continuum rather than discreet categories, since fitness effects on the host are often difficult to measure and establish as net positive or negative.

The bacterial composition of the human gut microbiome consists predominantly of the phyla *Bacteroidetes* and *Firmicutes*, typically with either of the two dominating in healthy adults (Huttenhower et al., 2012). The majority of strains residing in the GI tract are strict anaerobes and difficult to isolate, with the sheer diversity of gut bacteria revealed with the onset of metagenomic and other "omic" approaches (Lagier et al., 2012) overcoming the limitations of traditional culture-based methods. These approaches are not without their own limitations however, with low sensitivity to organisms of low abundance (Lagier et al., 2012) discussed as a potential confounding factor in studies investigating microbiome characteristics such as long-term stability (Martinson et al., 2019).

Mutualistic bacteria play a key role in the nutrition and metabolism of their host, with

their vast range of metabolic genes contributing to and increasing the metabolic potential of the human digestive system (Sekirov et al., 2010). For instance, the microbiota is chiefly responsible for the digestion of indigestible dietary fibres into short-chain fatty acids (SCFAs), converting these into a human-digestible form (Sekirov et al., 2010). Beneficial anti-inflammatory properties of SCFAs have also been reported, for example by promoting the maturation of regulatory T cells (Arpaia et al., 2013). Indirect benefits of commensals, as well as mutualists, include aiding in intestinal maturation in early life, immunomodulation, and restricting growth and colonisation of opportunistic pathogens by competitive exclusion (Sekirov et al., 2010). For example, the commensal *Bacteroides fragilis* has been shown to modulate the $CD4^+$ T-cell inflammatory response through the expression of polysaccharide A (Mazmanian et al., 2008).

1.4.2 Dysbiosis and disease

The distinction between mutualistic, commensal and parasitic symbionts is further complicated by many commensals such as *B. fragilis* causing systemic infections upon translocation outside of the GI tract, caused by injury, impaired intestinal mucosal homeostasis or preexisting inflammatory conditions such as type 2 diabetes (Sekirov et al., 2010). Also often harmlessly residing in the gut are *Enterobacteriaceae* such as *K. pneumoniae* and extra-intestinal pathogenic *E. coli* (ExPEC) which can also cause disease when translocated outside of the gut and can be referred to as colonising opportunistic pathogens (COPs; Price et al., 2017). These COPs can cause a range of diseases as discussed in Section 1.3.3, with comparative genomics of ExPEC isolates revealing no site-specific genetic variation between infection sites (Ranjan et al., 2017). Although low in abundance (Rajilić-Stojanović et al., 2010), such *Enterobacteriaceae* are considered as normal residents of the healthy gut microbiota, with *E. coli* observed to dominate within the family (Martinson et al., 2019). The risk of disease from opportunistic pathogens residing in the gut is generally higher for hospitalised patients

who are more likely to be immunocompromised, exposed to pathogenic strains from other patients, subject to invasive procedures such as catheterisation which provide ports of entry for pathogens, and finally subject to antibiotic administration, causing dysbiosis and selective pressure for drug-resistant strains (Vincent, 2003; van Schaik, 2015).

Additionally dysbiosis, or disruption of the "normal" balance of the microbiota, often caused by broad-spectrum antibiotic use, dampens the effect of competitive exclusion of other opportunistic pathogens. This can result in their overgrowth, preceding pathologies such as antibiotic-associated diarrhoea attributed to *C. difficile* (Dicks et al., 2019). There is ongoing research into "probiotic" strains, typically taken as supplements to increase microbial diversity and the competitive exclusion of pathogenic strains (Wilkins and Sequoia, 2017). Primarily researched are *Lactobacillus* and *Bifidobacterium* spp., which produce and secrete host-benefiting SCFAs as well as compounds such as organic acids which reduce the growth rate of other nearby strains (Parkes et al., 2009). This has been demonstrated with *Lactobacillus* spp. on CRE isolates (C.-C. Chen et al., 2019), where the *Lactobacillus* strains and their supernatant alone both significantly reduced the viability of CRE, but the effect of the supernatant was abolished upon pH neutralisation. Further details on the probiotic effects of and competitive inhibition by Lactobacilli are discussed in Section 3.5.2. Probiotic strains are of particular interest as both treatment and prophylaxis options for *C. difficile*-associated diarrhoea (CDAD), with a 2017 systematic review of 31 trials in adults and children suggesting that probiotic administration reduced the risk of CDAD by 60% (Goldenberg et al., 2017). These studies demonstrate that probiotic treatment can be successful, but the mechanisms and host interactions involved in these treatments are not yet well understood. Additionally, these otherwise mutualist strains have the potential to themselves cause morbidities such as bacteremia upon translocation outside of the gut, with Yelin et al. (2019) matching identical genomic data of *Lactobacillus* genomes between hospital-administered probiotic capsules and isolates from intensive care unit (ICU) patients with bacteremia.

1.4.3 Conjugation and the gut microbiome

The potential for HGT in the gut is vast and widely accepted, with the factors influencing this phenomenon being continually investigated. The gut microbiome is an ideal medium for the transfer of MGEs such as plasmids, due to high bacterial density facilitated by biofilm-promoting mucoid structures, and stresses such as pH, immune modulation, inflammation and antibiotic use (Stecher et al., 2012; Huddleston, 2014; Zeng and Lin, 2017). Stecher et al. (2012) demonstrated that inflammatory responses in the gut promoted transient blooms of *Enterobacteriaceae* in mice, increasing the proximity of (and consequently HGT between) these strains which would be otherwise inhibited by the commensal microbiota. Details of investigations into the inhibition of conjugation by the commensal microbiota are further discussed in Section 3.1.1. Additionally, a shared ecology has been demonstrated to be a key driving factor in HGT, with transfer enriched among bacteria that share the same niche, even when phylogenetically distanced (Smillie et al., 2011). Transduction, transformation and conjugation have all been demonstrated to contribute to this HGT (McInnes et al., 2020), however conjugation is by far the best characterised mechanism of HGT in the gut. Equally, investigations have also uncovered particular host-derived features exhibiting repression of HGT: Machado and Sommer (2014) co-cultured *E. coli* strains with the human intestinal cell line Caco-2, and demonstrated inhibition of conjugation of an ESBL plasmid by an uncharacterised peptide-based factor.

High incidence of HGT in combination with the relative long-term stability of the gut microbiome have coined this environment as a "melting pot" for mobile ARGs, with the collective set of ARGs in a single gut referred to as the gut resistome (van Schaik, 2015). This reservoir of ARGs with the potential to transfer between commensal and pathogenic bacteria, even if only transiently present in the microbiome, has significant clinical implications with regards to the emergence of new AMR strains. Observed examples of this have

been identified using genomic analysis of AMR clinical isolates, such as the tracing of a transposon-containing vancomycin resistance gene in *Enterococcus faecium* isolates to the same transposon found in gut anaerobes (Howden et al., 2013). Husain et al. (2014) characterised a conjugative transposon in a clinical isolate of *B. fragilis* from an infected appendix, which contained a mosaic of ARGs with >99% identity to sequences from three distinct Gram-positive bacteria, including the gut anaerobe *Eubacterium ventriosum*. Examples of direct evidence of HGT events between *Enterobacteriaceae* within individual hospital patients have also been published, and are described in detail in Section 4.3.2.

Our current understanding of the effects of various components of the microbiome on bacterial conjugation is far from complete. Research into this particular area is challenging due to the complex, dynamic and spatially diverse nature of the gut microbiome, which makes it difficult to study directly or recreate in models. Investigating and understanding the factors by which transfer of AMR is affected by the gut microbiome and its components is key to designing interventional strategies to tackle the emergence of new resistant strains.

1.5 Studying and tackling conjugation in the gut microbiome

1.5.1 Rationale

AMR is a serious global challenge, perpetuated by the transfer of ARG-encoding plasmids in bacteria (Section 1.1). Tackling this plasmid transmission is a promising strategy that can re-sensitise AMR bacteria to existing antibiotic therapies, and merits further research for the development of both clinical and environmental treatments (Section 1.2). CRE in particular, as critical priority pathogens for new drug development, have been the subjects of such anti-plasmid research, as the HGT of carbapenemase genes is significant to the dissemination of these pathogens (Section 1.3). CRE are typically found as members of the resident gut microbiota, which is a known reservoir of ARGs and melting pot for HGT (Sec-

tion 1.4). Characterising AMR plasmid dynamics in the gut microbiome is therefore important for both anti-plasmid research and tackling the spread of key groups of pathogens such as CRE. Understanding how various elements of the microbiome affect the conjugation of plasmids is beneficial in order to develop anti-plasmid therapies targeting conjugation in this environment. The lack of *in vivo* research has been identified as a limitation in the field of anti-plasmid research, and is necessary for the potential development of these therapeutic strategies for reducing the global burden of AMR. In addition to *in vivo* research, exploring the range of methods and models available for investigating plasmid dynamics in the gut microbiome could also contribute valuable insight into this field.

1.5.2 Research questions

Question 1) Does co-culture impact the growth of opportunistic pathogens or the transmission of their AMR plasmids?

This research question is addressed in Chapter 3, and the specific hypotheses addressing this research question are detailed in Section 3.1.6.

Question 2) How can *in vitro* models of the human gut microbiome be used in anti-plasmid research?

This research question is addressed in Chapters 4 and 5, and the specific hypotheses addressing this research question are detailed in Section 4.1.3.

2. Materials and Methods

2.1 Materials

2.1.1 Antibiotics

The antibiotics and antibacterial agents used in this project are listed in Table 2.1. All items listed were purchased as dry solids, and prepared with the relevant solvent at the appropriate concentration when needed. Prepared antibiotic solutions were stored at -20°C in 1 ml aliquots.

Table 2.1: Antibiotics used in this project. *Non-antibiotic antibacterial agents, but used as antibiotics in this project.

Antibiotic	**Abbreviation**	**Stock concentration (μg/ml)**	**Working concentration (μg/ml)**	**Solvent**	**Source**
Ampicillin	AMP	10,000	100	1% $NaCO_3$ solution	MP Biomedicals
Cephalothin	CEF	10,000	100	SDW	Sigma Aldrich
Doripenem	DOR	10,000	0.25 or 1	SDW	Sigma Aldrich
Kanamycin	KAN	10,000	50	SDW	Sigma Aldrich
Rifampicin	RIF	10,000	100	DMSO	TCI
$HgCl_2$*	-	1000	-	SDW	Sigma Aldrich
NaN_3*	-	10,000	100	SDW	Sigma Aldrich

2.1.2 Bacterial Strains

The strains used in this project are listed in Table 2.2. Strains were stored and grown as described in Section 2.2.1.

Table 2.2: Bacterial strains used in this project. Only antibiotics to which resistance was relevant to the project are shown; antibiotic abbreviations outlined in Table 2.1. ATCC = American Type Culture Collection.

Lab code	Species	Strain	Plasmid(s)	Resistance	Origin
H203	*K pneumoniae*	ST468	pKpQIL-UK	DOR	Prof. N. Woodford
H207	*K. pneumoniae*	ST258	-	AMP	Prof. B.N. Kreiswirth
H218	*K. pneumoniae*	ST258	pKpQIL-UK	DOR	Buckner et al. (2018b)
H222	*K. pneumoniae*	Ecl8	-	RIF	Buckner et al. (2018b)
H234	*K. pneumoniae*	Ecl8 mCherry	-	KAN	Buckner et al. (2020)
H235	*K. pneumoniae*	Ecl8	pKpQIL-*gfp-aph*	KAN	Buckner et al. (2020)
CPE01	*K. pneumoniae*	ST147	pCPE01_2	DOR	Dr. C McMurray
I448	*E. coli*	ATCC 25922	-	-	ATCC
I967	*E. coli*	J53	-	RIF	Prof. L.J.V. Piddock
Az^R J53	*E. coli*	J53	-	NaN_3	Prof. A. McNally
-	*B. fragilis*	ATCC 25285	-	-	ATCC
K1	*L. casei*	Shirota	-	-	Yakult

2.1.3 PCR Primers

The oligonucleotide primers used for colony PCR (Section 2.2.3) are listed in Table 2.3. Primers were ordered from Sigma-Aldrich, suspended in nuclease-free water (Invitrogen) to a stock concentration of 100 mM and stored at -20°C. Primer stocks were diluted to 25 mM with nuclease-free water before use, and stored at -20°C in 500 μl aliquots.

Table 2.3: PCR primers used in this project: (F) refers to forward primers, and (R) to reverse. T_M is the primer-specific melting temperature, and T_A is the annealing temperature used for a pair of forward and reverse primers.

Primer	**Sequence 5'-3'**	**Product size (bp)**	**T_M (°C)**	**T_A (°C)**
pKpQIL-UK backbone (F)	CAGCATGACAGAATAGCGAGGCTT	383	58.7	56
pKpQIL-UK backbone (R)	TACAAGGAGATGTGCCATGACCGT	383	59.3	56
KPC-2 (F)	AGCTACCGCTTGAAGGACAA	1600	51.7	49
KPC-2 (R)	GGATTGCGTCAGTTCAGCAT	1600	52.5	49
pCPE01_2 backbone (F)	TTCACACGACGCTCCACTTC	161	66.5	59.5
pCPE01_2 backbone (R)	TAAGTCCCGTGGAATAAAACG	161	62.5	59.5
NDM-5 (F)	ATGCCGACACTGAGCACTAC	290	63	59.5
NDM-5 (R)	GAATTCGAGCTGCAAACCGC	290	69	59.5

2.1.4 Culture Media

The media used for bacterial culture in this project are listed in Table 2.4. Media was prepared by mixing solid powdered media with distilled water at the appropriate concentration, followed by sterilisation by autoclaving at 121°C for 15 minutes. Media for use in agar plates was purchased with agarose already incorporated. Prepared media was stored at room temperature prior to use.

Table 2.4: Culture Media used in this project

Medium	Abbreviation	Preparation	Source
Luria-Bertani	LB	37.5 g/l	Sigma-Aldrich
Supplemented Brain-Heart Infusion	BHIS	Appendix C	Appendix C
de Man, Rogosa and Sharpe	MRS	51 g/l with 1 ml/l Tween®80	Sigma-Aldrich

2.2 Methods

2.2.1 Bacterial storage and culture

Strains were stored at -20°C in Protect cryoprotective fluid (Technical Service Consultants Ltd). To prepare an agar plate, a single bead was spread over a plate of appropriate agar media for incubation, using aseptic technique throughout. Liquid cultures were made by adding single colonies from these plates into 5ml appropriate broth media in a sterile 30ml universal tube for incubation. Plates were stored at 4°C for two weeks maximum, after which a new plate was streaked from the Protect stock. Long-term storage of strains at -80°C was also in Protect cryoprotective fluid.

Unless specified otherwise, bacterial plates and liquid cultures were incubated aerobically at 37°C. When specified, anaerobically incubated plates were first placed in a sealed anaerobic jar, with anaerobic conditions established and maintained by an Anaerogen sachet (Oxoid).

Aerobic liquid cultures were incubated in a rotary shaker at 200 rpm, with the universal tube lids secured. Anaerobic liquid cultures were incubated statically in universal tubes in the anaerobic jar, with lids loose to allow depletion of oxygen within the universal tube.

2.2.2 Gram staining

A sterile loop was used to place a small amount of a bacterial colony onto a drop of water on a clean glass slide. The bacterial cells were heat fixed by briefly passing the glass slide through a bunsen flame.

Using a Pasteur pipette, a few drops of crystal violet (Sigma Aldrich) were added to cover the bacteria on the slide, and this was left for one minute before rinsing off with water. To fix the crystal violet, Gram's iodine (Sigma Aldrich) was pipetted onto the fixed bacteria, left for one minute and rinsed with water. Next, a 1:1 mixture of ethanol and acetone was pipetted, drop by drop, onto the stain, until the eluent ran clear, and the slide was immediately rinsed with water. Finally, a safranin counter-stain (Sigma Aldrich) was added, left for one minute, and rinsed off with water. The slide was then left to dry completely.

Oil-immersion light microscopy was used to visualise the fixed and stained bacteria. The colour and morphology of the cells seen under the microscope were noted.

2.2.3 Colony PCR

A lysate was prepared from a single colony in 100 μl nuclease-free water, incubated in a heat block at 100°C for 10 minutes. PCR tubes were set up to contain 25 μl PCR mix, consisting of 12.5 μl (50%) MYTaq Red Mix (Bioline), 1 μl (4%) of each of the forward and

reverse primers (Table 2.3), 7.5 μl (30%) nuclease-free water and 3 μl (12%) colony lysate. A control tube was also prepared, containing 3 μl nuclease-free water instead of lysate. A thermocycler was set up for 1 cycle of 95°C for 1 minute, followed by 30 cycles of 3 stages: 95°C for 15 seconds; the relevant annealing temperature for the primers (Table 2.3) for 15 seconds; and 72°C for the length of time corresponding to the target sequence length (using a rule of thumb of one minute per kb). A final single cycle of 72°C for 10 minutes concluded the reaction, after which the thermocycler held the PCR tubes at 4°C until switched off.

To visualise the products by gel electrophoresis, 12.5 μl of the contents of each PCR tube was pipetted into a set 1% agarose gel (made with 1x TBE buffer diluted with distilled water from a 10x stock; Invitrogen) containing 0.006% SYBR Safe DNA Stain (EDVOTEK), alongside 6 μl of a 1kb Hyperladder (Bioline), and run for 40 minutes at 120V. The gel was imaged using a transilluminator (Amersham Imager; Cytiva).

2.2.4 Broth microdilution MIC assay

Three biological replicates of overnight liquid cultures were prepared in the working concentration of the relevant antibiotic (Section 2.1) in broth media, alongside one control universal tube containing media only, to check for contamination in the preparation process. After overnight incubation, 1 ml of each culture was centrifuged for 4 minutes at 8000 rpm, the supernatant containing the antibiotic discarded, and the pellet re-suspended in 1 ml fresh LB. This was diluted 1:100 to approximately 10^7 colony forming units (CFU) /ml in ISO-sensitest LB broth (Sigma-Aldrich).

Antibiotic/antibacterial compound (Table 2.1) was diluted in ISO-sensitest broth. Using aseptic technique throughout, doubling dilutions of antibiotic were pipetted along the rows of a 96-well plate for final well volumes of 50 μl, with the final column not containing any antibiotic as a positive control. Unless otherwise specified, the values of antibiotic concentrations tested ranged from 0.5 μg/ml to 512 μg/ml. 50 μl of diluted bacterial culture was

pipetted into each well, with one biological repeat per row. A row was left free of diluted culture as a negative control, in order to check for contamination in the preparation process. The plate was covered, incubated statically for 18 hours at 37°C and the wells then checked for growth.

The MIC of a particular strain was taken as the lowest concentration of antibiotic in which no growth was observed. If biological repeats differed by one doubling dilution, the MIC was reported as being within a range of two successive tested concentrations.

The control *E. coli* strain ATCC 25922 (Laboratory code I448 in Table 2.2) was tested alongside as an additional control, and the results were only accepted if the MIC for this strain was within the range of MIC values as defined by the European Committee on Antimicrobial Susceptibility Testing (EUCAST, 2020b), where applicable.

When testing for the MIC of $HgCl_2$, this protocol was modified to account for the safety risks posed by the hazardous nature of inorganic mercury. All steps using this compound were performed within a fume hood, and the plate carefully wrapped in cling-wrap and left to incubate under the hood for up to six days to account for slower growth at room temperature. Lower concentrations of $HgCl_2$ (64 μg/ml to 0.0625μg/ml) were tested than those specified in the protocol, since 50 μg/ml was considered as a relatively high concentration for mercury resistance (De et al., 2003), and to account for the expected low MIC values of the sensitive strains.

2.2.5 Conjugation on filters

Three biological replicates of overnight liquid cultures were prepared in the working concentration of the relevant antibiotic (Section 2.1) in LB broth, alongside one control universal tube containing LB only, to check for contamination in the preparation process.

After overnight incubation, 1ml of each culture was spun down for 4 minutes at 8000 rpm, the supernatant containing the antibiotic discarded, and the pellet re-suspended in 1 ml LB.

This suspension was diluted 1:10 by adding 100 μl to 900 μl sterile phosphate buffered saline (PBS) (Invitrogen), and the Optical Density at 600nm (OD_{600}) of the resulting suspension measured using a spectrophotometer (Thermo Electron Corporation). A calculated volume of the undiluted suspension was added to 5 ml LB for a final OD_{600} of 0.5. Three donor/recipient mixtures were made, one for each biological replicate of the donor and recipient. Unless otherwise stated, a donor:recipient ratio of 1:1 was used.

To transfer the bacteria to the filters, 100μl of each mixture was pipetted onto a sterile filter paper disk (Cytiva Whatman) on a plate of plain LB agar, and incubated overnight at 37°C. Donor alone, recipient alone or LB alone, all 100 μl, were also added to disks and incubated on LB agar as control plates. After overnight incubation, the filter disks were then placed into separate universal tubes containing 1 ml LB broth using sterilised foreceps, and vortexed vigorously to resuspend the cells.

To select for transconjugants, 100 μl of this neat suspension, as well as of 10^{-1} and 10^{-2} dilutions in sterile PBS, was plated onto double selective plates containing antibiotics to select for both the recipient and plasmid. These plates were grown overnight, or left in the incubator for an additional night in the case of no initial growth. Control plates (from suspensions of disks prepared, with donor only, recipient only or LB only) were expected to show no growth, and were incubated for as long as the other plates. Colonies that appeared on the experimental plates (referred to as putative transconjugants) were replica plated by using sterile toothpicks to transfer the colonies onto clean double selective plates, and were tested for presence of the plasmid by colony PCR (Section 2.2.3).

To calculate the true donor:recipient ratio of the mixture used in the conjugation, the mixed suspensions used to inoculate the filters were also then diluted 1 in 10 in PBS as above. 100μl of the 10^{-4} to 10^{-7} dilutions of each mixture were plated onto plain LB agar, and grown overnight. Following this the CFUs were counted, and plates of the dilutions that contained a number of colonies between 20 and 100 (enough colonies to count easily,

but few enough to minimise clustering and difficulties distinguishing between cultures) were replica plated using velvet squares onto the relevant antibiotic selective plates to select for the donor and recipient, respectively. After overnight growth, the number of CFUs on each plate was counted, and a ratio of donor:recipient cells in the original mixture calculated by first correcting for the dilution by converting the CFU count to CFU/ml of original suspension, and then dividing both CFU/ml values by that of the donor to get a ratio.

To calculate the mutation rate of the donor and recipient strains, 100 μl of the neat suspension of each biological replicate was plated onto the antibiotic selective plates that the strain should be sensitive to. After overnight growth, any CFUs present were counted. For experiments where transconjugants were incubated for longer, mutant selection plates were also incubated for that period of time. To calculate mutation rate, viable counts of the original OD_{600} suspensions were calculated by making 1 in 10 dilutions up to 10^{-7}, and plating 100 μl of the 10^{-4} to 10^{-7} dilutions onto plain LB agar. After overnight growth, the CFUs on the plates were counted, and from this the approximate number of viable CFU/ml of the original OD_{600} suspensions were calculated by correcting for the dilution. The mutation rates for each biological repeat were calculated by dividing the estimated number of mutated cells by the number of viable cells.

2.2.6 Conjugation in liquid

Three biological replicates of overnight cultures as well as one control tube were prepared, using the same protocol as for conjugation on filters (Section 2.2.5). Similarly, the overnight cultures were centrifuged, their OD_{600} corrected and donor/recipient mixtures made.

To prepare the plate, 180 μl of LB broth was added to individual wells of a 96-well plate. Added to these was 20 μl of mixed bacterial suspension, for a final dilution of 1 in 10. Control wells were prepared using 20 μl donor alone, recipient alone or LB broth alone instead of the mixture. The plate was then covered and incubated with gentle agitation (80 rpm) at 37°C

for 18 hours.

To select for transconjugants after incubation, the well contents were serially diluted 1 in 10 in sterile PBS to 10^{-7} (by adding 20 μl of the previous dilution into 180 μl PBS), and 100 μl of dilutions 10^{-4} to 10^{-7} were spread on double antibiotic plates. These were incubated overnight, or left in the incubator for longer in the case of no initial growth. Control plates containing donor only, recipient only or LB only were expected to show no growth, and were incubated for as long as the other plates. The putative transconjugants from the experimental plates were replica plated using sterile toothpicks to transfer the colonies onto clean double selective plates, and were tested for presence of the plasmid by PCR (Section 2.2.3).

True donor:recipient ratios and mutation rates were calculated using the same protocol as used for conjugation on filters (Section 2.2.5).

2.2.7 Measuring plasmid transmission by flow cytometry

This transmission assay was performed as described by Buckner et al. (2020): four biological replicates of overnight liquid cultures were prepared in the working concentration of the relevant antibiotic (Section 2.1) in LB broth, alongside one control universal tube containing LB only, to check for contamination in the preparation process.

After overnight incubation, 1 ml of each culture was centrifuged at 8000 rpm for three minutes, the supernatant discarded and the pellet resuspended in 1 ml sterile PBS. The OD_{600} was adjusted to 0.5, and donors and recipients mixed. Ratios were strain-dependent: 3:1 for conjugation of the plasmid pCT-*gfp-aph* in *E. coli*, and 1:2 for conjugation of the plasmid pKpQIL-*gfp-aph* in *K. pneumoniae* (Table 2.2). Control wells included LB only, donor only and recipient only for each biological replicate. Incubation was at 37°C on a shaking platform (80 rpm), with incubation times differing by strain: 12 hours for *E. coli* conjugating pCT-*gfp-aph*, and six hours for *K. pneumoniae* conjugating pKpQIL-*gfp-aph*.

After incubation, the cultures and controls were diluted 1:1000 in filter-sterilised (filtered

through 0.2 μm pores) PBS (Sigma-Aldrich) in sterile 96-well plates. The samples were then analysed using an Attune NxT acoustic focusing flow cytometer with Autosampler (Thermo Scientific), using excitation wavelengths of 488 nm (blue) and 561 nm (yellow). Voltages and thresholds were established using the donor only and recipient only controls, to check for clear separation of GFP and mCherry emission data. Gates were set to capture total bacteria, GFP only, mCherry only and transconjugants (GFP + mCherry). 10,000 total events were collected for each sample. After data collection, the percentage of total events that were identified as transconjugants (expressing both GFP and mCherry) were recorded.

2.2.8 Anaerobic end-point growth assay

Three biological replicates of overnight liquid cultures were prepared in the working concentration of the relevant antibiotic (Section 2.1) in broth, alongside one control universal tube containing broth only, to check for contamination in the preparation process. Also incubated overnight was a universal tube with 10 ml prepared BHIS broth, with the lid on but loose, in an anaerobic jar with an Anaerogen sachet.

The next day, the cells were first grown to exponential phase, by making a 1% subculture in plain LB media until the OD_{600} reached within the range of 0.4-0.6, checked with a spectrophotometer. The control overnight was also subcultured and incubated. To pellet the cells, 1 ml of each subculture was then centrifuged at 8000rpm for four minutes. The supernatant was carefully removed, and the pellet resuspended in the anaerobic BHIS prepared the day before, and pipetted up and down gently to mix. Into separate universal tubes, 900 μl of each biological replicate and control was transferred, and these were placed with the lid loose in the anaerobic jar and immediately incubated at 37°C for four hours. The remaining suspensions and control were serially diluted 1:10 (20 μl in 180 μl) in sterile PBS in a 96-well plate. The 10^{-6} and 10^{-7} dilutions (100 μl) were plated onto selective LB agar, to give the viable counts at time point zero.

Once the four hour incubation was complete, the universal tubes were vortexed to resuspend any settled cells, and the contents serially diluted 1:10 in sterile PBS as above. 100μl of the 10^{-6} and 10^{-7} dilutions were plated onto selective LB agar, to give the viable counts at the time point of four hours. Both sets of viable counts plates were incubated overnight, and counted the following day. The fold-change in viable counts over four hours was calculated using the ratio of these counts. Plates inoculated with the control were checked for growth.

2.2.9 Anaerobic co-culture, conjugation in liquid, and co-culture conjugation in liquid

The co-culture, conjugation and co-culture conjugation protocols were set up similarly to the anaerobic growth kinetics protocol (Section 2.2.8), with a conjugation being prepared as a co-culture of donor and recipient strains. Experiments involving a conjugation included an extra OD_{600} check, and additional plating steps to investigate muation and conjugation frequencies.

Three biological replicates of each strain to be co-cultured, as well as an uninoculated control and 10 ml anaerobic BHIS broth, were prepared as in the anaerobic end-point growth kinetics protocol (Section 2.2.8). Once the cells were deemed to be at exponential phase (Section 2.2.8), 1.4 ml of each replicate and control were spun down at 8000 rpm for four minutes to pellet the cells. The supernatant was carefully removed, and the pellets resuspended in 700 μl anaerobic BHIS broth. This step concentrated the cells by a factor of two, and was done for co-cultures and conjugations, which used two strains. Co-culture conjugations, which involved three strains, were concentrated by a factor of three (i.e. a pellet from 1.5 ml of subculture was resuspended in 500 μl anaerobic BHIS broth). Here, for conjugations and co-culture conjugations, the concentrated donors and recipients were OD_{600} checked again, and biological replicates paired by similarity of values to get the ratios as close to 1:1 as possible.

The strains were then mixed in equal proportions in a universal tube for a final volume of 1ml, and incubated, lids loose, in the anaerobic jar at 37°C for four hours. The remaining suspensions and control (20μl) were serially diluted 1:10 in sterile PBS in a 96-well plate. The 10^{-6} and 10^{-7} dilutions (100 μl) were plated onto selective LB agar, to give the viable counts at time point zero. For experiments involving a conjugation, mutant selection plates were also prepared, with 100 μl (or 50 μl, depending on how much suspension was left) of each strain plated onto agar containing the counter-selective antibiotic/antibacterial agent.

Once the four hour incubation was complete, the universal tubes were vortexed to re-suspend any settled cells and separate mating pairs, and the contents serially diluted 1:10 in sterile PBS as above. The 10^{-6} and 10^{-7} dilutions (100μl) were plated onto selective LB agar, to give the viable counts at the time point of four hours. For experiments involving a conjugation, 100 μl of the neat, 10^{-1} and 10^{-2} dilutions were plated onto double selective plates to select for transconjugants.

Both sets of viable counts plates, as well as mutant and transconjugant selection plates if applicable, were incubated overnight and counted the following day. Transconjugant selection plates were left for another day to account for slow growth. The fold-change in viable counts over four hours was calculated using the ratio of the counts, by first calculating the CFU/ml at zero and four hours by correcting for the dilutions, and then dividing both values by the CFU/ml at zero hours. Plates inoculated with the control were checked for growth. Any growth on the mutant selection and transconjugant selection plates was counted. 16 putative transconjugants were selected from the double selective plates, with care taken to sample all morphologies present. These were replica plated onto UTI agar containing antibiotic selecting for the plasmid, and were tested for the presence of plasmid by colony PCR.

Once transconjugants were confirmed, conjugation frequency per donor was calculated, using the viable counts. Mutation frequencies were also calculated using viable counts. Calculations were made by first converting the CFUs counted to CFU/ml by correcting for the

dilution factors, and conjugation and mutation frequencies calculated as in Section 2.2.5.

3. Conjugation in co-culture with microbiome strains

3.1 Introduction

3.1.1 Impact of co-culture on the transfer of AMR plasmids

As detailed in Section 1.4.3, recent literature has supported the significance of the human gut microbiome as a medium for HGT of AMR genes, with particular emphasis on plasmid conjugation being the most significant means of these transfers. However, we do not yet have a full understanding of how individual elements of the microbiome may promote or repress conjugation. Research is ongoing into both host-derived and microbiota-derived factors, since these both constitute the microbiome (Marchesi and Ravel, 2015).

Little research has been conducted, either *in vitro* and *in vivo*, on the impact of the microbiota on conjugation of AMR plasmids between gut-dwelling strains. J. D. Anderson (1975) co-cultured donor and recipient *E. coli in vitro* with large amounts of faeces-derived *B. fragilis* for four hours, and observed that *B. fragilis* had a density-dependent inhibitory effect on the transfer of two multi-drug resistance plasmids: 3-5x10^9/ml *B. fragilis* resulted in a conjugation frequency of one half of that of the control conjugations (no co-culture), and 2x10^{10}/ml resulted in no detection of conjugation. Anderson additionally tested the effect of culturing the donor and recipient together with 2x10^{10}/ml formalin-killed *B. fragilis*, as well as culture supernatant from a live 2x10^{10}/ml *B. fragilis* culture. These latter experiments were only performed with one experimental replicate for each plasmid, with the resulting conjugation frequencies lower than the mean conjugation frequencies of the controls, but still withing their range. These limited experiments therefore suggested that it was presence of

live bacteria that had the most prominent effect on conjugation rates, and the author suggested suppression of metabolism in the *E. coli* as a plausible explanation. This was also supported by the observation that dense culture of *B. fragilis* almost completely inhibited the growth of the *E. coli* in mixed culture.

Similarly, Moubareck et al. (2007) tested the effect of strains of bifidobacteria on conjugation of ESBL-encoding plasmids from *K. pneumoniae* and *Salmonella enterica* donors into *E. coli*, testing the effects of co-culture, heat-killed cells and supernatant *in vitro*. Where Anderson centrifuged and resuspended the *B. fragilis* for all experiments, Moubareck and colleagues made the distinction between bifidobacterial "co-culture" and "pellet", whereby the former condition consisted of adding a 48h culture of *Bifidobacterium* directly to the conjugation mixture, and the latter of washing the cells and resuspending in fresh broth beforehand, as Anderson did. Interestingly, Moubareck and colleagues found that the pellet did not significantly change the conjugation rate in relation to the control (broth only) after five hours, but the co-culture did, as well as the supernatant and heat-killed cells. In contrast to Anderson's findings, these authors concluded that the factors reducing conjugation rate came not from live cells, but from thermostable metabolites. Distinguishing between co-culture and pellet could introduce a confounding variable; the co-culture conditions using broth cultures may have had depleted nutrients relative to the pellet conditions where fresh broth was added. Nevertheless, when investigating the viable counts of donors and recipients after the five-hour incubation, the authors found no significant change in the numbers of donors and recipients across the conditions, and so growth inhibition as a result of nutrient availability was not a significant factor affecting these results.

Kunishima et al. (2019) also compared the effect of presence and absence of supernatant from live cultures of individual microbiota strains including *B. fragilis* and *Bifidobacterium longum* on conjugation of an ESBL plasmid between *E. coli*. Supernatant of four of the seven strains- *C. difficile*, *E. faecium* and two strains of *Clostridium butyricum*- significantly

reduced conjugation frequency compared to a control (no supernatant added) over two hours. In these experiments, Kunishima and colleagues found no effect exerted by *B. longum* supernatant, in contrast to observations by Moubareck et al. (2007) that *B. longum* supernatant significantly affected the transfer of two different plasmids between *E. coli*. These studies are not directly comparable due to differing materials and experimental design, but this comparison highlights the complexity of the effects the studies are trying to uncover.

These studies all report interesting findings, demonstrating that elements of the gut microbiome may impact plasmid dynamics in that environment. The papers suggest potential mechanisms behind their findings, for example suppression of growth and metabolism by live cells (J. D. Anderson, 1975) or metabolites or other substances present in culture media (Moubareck et al., 2007; Kunishima et al., 2019), but invite further investigations into elucidating the mechanisms at play. Designing experiments to investigate these effects is difficult, since *in vitro* methods are highly reductionist for studying an environment as complex and dynamic as the gut microbiome, producing results with low translatability.

Work has also been done *in vivo* in animal models to compare rates of conjugative transfer with and without various elements of the microbiome. Here of course, the microbiome environment is incorporated into the model, making the results of such studies much more translatable, but the variables more difficult to control. Duval-Iflah et al. (1980) investigated the transfer of a MDR plasmid from *Serratia liquefaciens* to *E. coli* in the intestines of gnotobiotic mice inoculated in various conditions: with human faecal flora, no flora, or a dense population of unspecified *Bacteroides* (10^{10} viable counts per gram of faeces) with heat-killed flora. The authors observed that, in the conditions of no flora and *Bacteroides* with heat-killed flora, transconjugants appeared in the mouse faeces quickly (within 24 hours) and at similar levels (10^3-10^4 per gram of faeces), suggesting that the *Bacteroides* in this case did not have a significant effect on the rate of conjugative transfer. When the mouse intestinal tract was inoculated with human faecal flora, transconjugants became established at similar

levels, however after a longer delay of 12 days, suggesting some inhibition. All of these observations were made in the absence of antibiotic selective pressure.

Moubareck et al. (2007) also extended their study of bifidobacteria to gnotobiotic mice, testing two bifidobacterial strains that had shown inhibitory effects in *in vitro* co-culture. Both strains led to a 3.3-log decrease in number of isolated transconjugants from faeces compared with the control mice (inoculated with donor and recipient only) after 17 days. The conclusion from these *in vivo* experiments that the bifidobacteria had an inhibitory effect on conjugation was consistent with that of their *in vitro* experiments.

All of the aforementioned studies used different approaches to address the same research question: how does the presence of micobiota strains affect the conjugation of AMR plasmids? Importantly, even studies that used similar experimental designs and microbiota strains came to different conclusions, alluding to the answers to this research questions being complex and perhaps varying contextually across different donor and recipient strains or plasmids.

3.1.2 Plasmid background: pKpQIL-like plasmids

Plasmid pKpQIL was first isolated in a national outbreak of $bla_{\text{KPC-3}}$-producing *K. pneumoniae* in Israel in 2006 and, through curing and transformation experiments, was found to be responsible for the cephalosporin and carbapenem resistance phenotype of these strains (Leavitt et al., 2010b). Subsequent sequencing of the plasmid uncovered that, based on its *repA* sequence, it belongs to the IncFII-like incompatibility group (Leavitt et al., 2010a). The $bla_{\text{KPC-3}}$ gene was nested within Tn*4401*, an active transposon frequently associated with bla_{KPC} genes (Naas et al., 2008). Additional regions of interest of this plasmid included $bla_{\text{TEM-1}}$ and several genes of the mercury resistance (*mer*) operon (Figure 3.1). Other ARG sequences were identified, such as $bla_{\text{OXA-9}}$ and *aadA*, though these were predicted to be inactive due to a nonsense mutation and truncation respectively (Leavitt et al., 2010a).

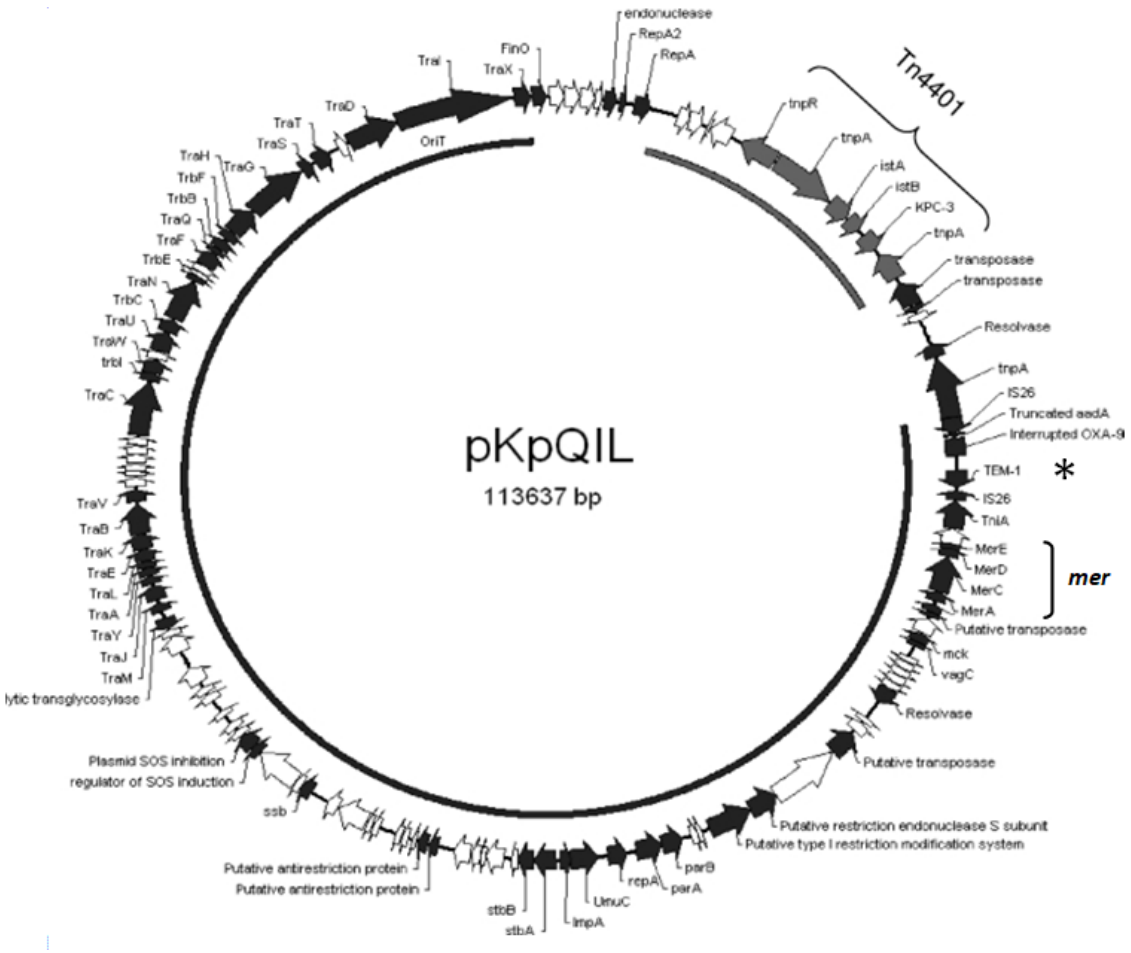

Figure 3.1: Annotation of plasmid pKpQIL. The *bla*$_{\text{KPC}}$-containing transposon Tn*4401* is indicated with a curly bracket, the *mer* operon with a square bracket and the *bla*$_{\text{TEM-1}}$ location with an asterisk. Arrows indicate gene orientation, with filled arrows indicating predicted ORFs of known functions. Figure adapted from Leavitt et al. (2010a), copyright © 2010, American Society for Microbiology.

Initial *in vitro* experiments performed to characterise the plasmid confirmed its ability to conjugate between *K. pneumoniae* strains (Leavitt et al., 2010b). Indeed, pKpQIL-like plasmids were globally identified in subsequent nosocomial outbreaks of *bla*$_{\text{KPC}}$-carrying *Enterobacteriaceae* (Richter et al., 2012; L. Chen et al., 2014; Doumith et al., 2017). These plasmids quickly became the dominant *bla*$_{\text{KPC}}$ vectors in many regions, including in the UK where, in a sample of 44 KPC-positive isolates between 2008 and 2010, 84.1% carried *bla*$_{\text{KPC}}$ on IncFII$_{\text{K2}}$ plasmids, and all 11 of a sequenced subset were substantially similar to published

pKpQIL sequences (Doumith et al., 2017). The study identified some of the key dominant UK variants of pKpQIL, including the $bla_{\text{KPC-3}}$-carrying variant included in this project, pKpQIL-UK.

pKpQIL-like plasmids isolated from these outbreaks contained either $bla_{\text{KPC-2}}$ or $bla_{\text{KPC-3}}$, and were predominantly associated with the ST258 sequence type of *K. pneumoniae*, suggesting significant clonal expansion of this sequence type in addition to horizontal transmission of pKpQIL-like plasmids (L. Chen et al., 2014). An epidemiological investigation into the USA Center for Disease Control and Prevention's (CDC) database revealed that ST258 was likely to account for 70% of KPC-producing *K pneumoniae* between 1996 and 2008 (Kitchel et al., 2009). In addition to clonal expansion of KPC-producing strains and dissemination by plasmid transmission, the mobile Tn*4401* transposon also provides a mode of horizontal transmission, with Mathers et al. (2017) observing chromosomal integration rates of bla_{KPC}-containing Tn*4401* of 5%. Furthermore, short- and long-read sequencing analysis of KPC-positive strains from a single US hospital over five years identified that the Tn*4401* transposon was frequently found nested within insertion sequences of another mobile transposon, a Tn2-like element (Sheppard et al., 2016). Variation between Tn2-like elements suggested that Tn*4401* had frequently transposed into different pre-existing Tn2-like elements, providing further evidence for Tn*4401* mobility. These analyses have not been conducted on pKpQIL-like plasmids, and so it cannot be concluded that Tn2 transposition occurs in pKpQIL-carrying strains. Nevertheless, the nested mobility of bla_{KPC} genes has certainly contributed to their rapid dissemination (Sheppard et al., 2016), and influenced the genetic contexts of these ARGs with the potential for chromosomal integration or movement between different MGEs.

Previous work investigating the pKpQIL-UK variant as a clinically relevant plasmid confirmed successful conjugation from clinical isolates of *K. pneumoniae* into both a plasmid-naive ST258 strain and a laboratory-adapted strain Ecl8, with conjugation frequencies per

donor of $3.3x10^{-4}$ and $1.57x10^{-5}$ respectively (Buckner et al., 2018b). Additional conjugation experiments using a transformed *E. coli* DH10B donor strain and other Enterobacteriaceae recipients, such as *E. coli* NCTC10418, *Salmonella typhimurium* ATCC14028s and *Serratia marcescens* NCTC10211, also resulted in successful conjugations of pKpQIL-UK with frequencies per donor cell of $1.4x10^{-5}$, $1.7x10^{-5}$ and $1.9x10^{-5}$ respectively (Saw, 2015). Buckner et al. (2018b) also found that plasmid acquisition by naive *K. pneumoniae* resulted in altered gene expression in both the plasmid and recipient chromosome. These changes were hypothesised to contribute to ameliorating the fitness costs of the plasmid, given that the plasmid was then able to persist in its new *K. pneumoniae* host in the absence of positive selection pressure.

Plasmid pKpQIL-UK was used as the AMR plasmid of interest in this project both because of its dominance in CRE epidemiology in the UK (Doumith et al., 2017), and because its conjugative behaviours had been well studied (Saw, 2015; Buckner et al., 2018b). pKpQIL-like plasmids are well-adapted to their *K. pneumoniae* hosts (Buckner et al., 2018b), especially ST258, where pKpQIL-like plasmids are suggested to have contributed to its fitness, survival and global dissemination (Pitout et al., 2015). With CRE classified as a critical priority by the WHO (Tacconelli et al., 2018), and many of these residing commensally in humans as COPs (Price et al., 2017), AMR transfer between these gut-dwelling strains is of great research interest, reflected in the relatively large proportion of observational studies focused on these strains (discussed in Section 4.3.2). Therefore, as an Enterobacteriaceae-restricted, clinically relevant and widespread plasmid, pKpQIL-UK was considered as an ideal model with which AMR transfer between Enterobacteriaceae COPs in the human gut microbiome could be studied.

3.1.3 Dual-fluorescence plasmid tracking

Strain H235, a laboratory adapted reference *K. pneumoniae* Ecl8 strain, was the result of a previous transformation of Ecl8 (Fookes et al., 2013; laboratory code H222) with a modified version of pKpQIL-UK, pKpQIL-*gfp-aph* as described in Buckner et al. (2020). pKpQIL-*gfp-aph* contained a *gfp-aph* cassette inserted into the $bla_{\text{KPC-3}}$ locus of pKpQIL-UK (Figure 3.1), thus disrupting the $bla_{\text{KPC-3}}$ gene. The cassette rendered H235 able to synthesise Green Fluorescent Protein (GFP) and the aminoglycoside-3'-phosphotransferase (APH) protein, the latter of which conferred resistance to aminoglycoside antibiotics such as kanamycin. Further details on these strains, as well as on those described in the following sections, are outlined in Table 2.2.

Use of a *gfp*-encoding plasmid allowed metabolically active cells containing this plasmid to synthesise GFP and be detected by flow cytometry, therefore rendering them distinguishable from non-fluorescent cells. For this system a recipient *K. pneumoniae* strain, H234, was generated (as described in Buckner et al. (2020)) by inserting an *mcherry* cassette into the H222 chromosome, with the resulting expressed mCherry protein also detectable by flow cytometry. The objective was to exploit these fluorescence to trace conjugation of the plasmid to recipients (Figure 3.2). Flow cytometry could be used in a medium throughput assay to rapidly assess the proportion of dual-fluorescent transconjugants in a mixed bacterial population (Section 2.2.7) (Buckner et al., 2020).

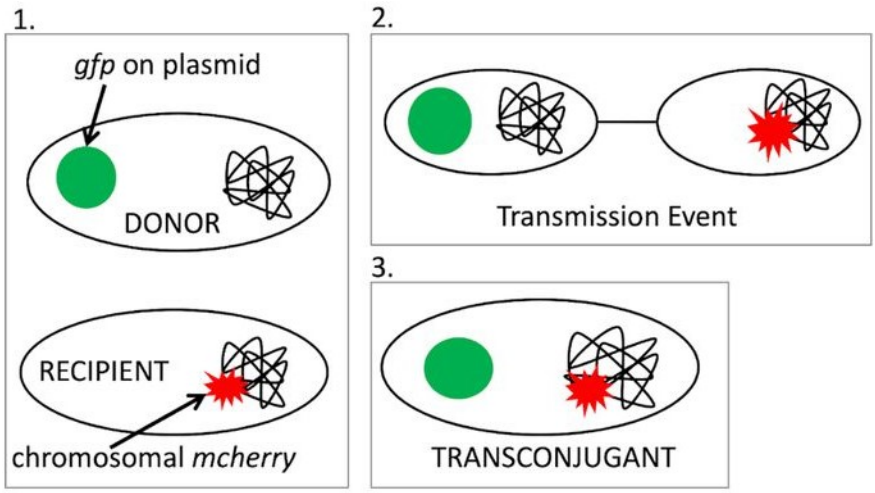

Figure 3.2: Dual fluorescence system. 1. The donor contains a *gfp-aph* casette on the plasmid of interest, conferring fluorescence and resistance to kanamycin. The plasmid-free recipient strain is chromosomally tagged with *mcherry*. 2. Donors and recipients are incubated together to allow conjugation. 3. Transconjugants are dual-fluorescent and can be distinguished from mono-fluorescent donors and recipients using flow cytometry. Figure from Buckner et al. (2020).

This dual-fluorescence system was chosen for this project because of its medium-throughput capacity, and because it has been well-characterised in the context of investigating plasmid transmission inhibition (Buckner et al., 2020). Using this established model in a new context opens avenues for further research into the effect of components of the microbiome, whether cellular- or small-molecule-based, on conjugation of AMR plasmids.

Fluorescent strains

pKpQIL-like plasmids have been characterised in lab-adapted strains such as *K. pneumoniae* Ecl8 (Fookes et al., 2013; Buckner et al., 2018b). However, these lab-adapted strains do not necessarily emulate how clinically relevant strains behave (Fux et al., 2005; Buckner et al., 2018b). In this project, strain H207, a carbapenem-susceptible plasmid-free clinical isolate of *K. pneumoniae* ST258 from the USA (provided by Prof. B.N. Kreiswirth) was used. The first step planned was to conjugate pKpQIL-*gfp-aph* into this strain, and then to

use this transconjugant as the donor strain for subsequent flow cytometry-based conjugation experiments.

The generation of new mCherry-encoding recipient strains was also planned for this project. *E. coli* was chosen as the species of choice because of the relevance of many of its strains as COPs (Section 1.4.2), and its high abundance relative to other *Enterobacteriaceae* in the human gut microbiome (Martinson et al., 2019), therefore a likely clinically relevant recipient for such plasmids. Saw (2015) demonstrated that pKpQIL-UK could successfully conjugate into *E. coli*. I967 (courtesy of Prof. L.J.V. Piddock), a rifampicin-resistant variant of the laboratory-adapted *E. coli* J53 strain, was used for the initial experiments. J53 is a widely used recipient strain for *in vitro* conjugation experiments (Yi et al., 2012), and its widespread use and adaptation to laboratory environment made it a good candidate for establishment of this fluorescent assay. Once successful conjugations were characterised using mCherry-encoding I967, more clinically relevant opportunistic pathogenic isolates of *E. coli* were to be obtained to increase the translatability and clinical relevance of the assay.

Aerobic Fluorescence Recovery (AFR)

The dual-fluorescence system described above was designed for conjugation experiments performed in aerobic environments. Since the focus of this project is on the human gut microbiome, however, the conjugation experiments were designed to be performed anaerobically. This posed an obstacle to the detection of fluorescence, since both GFP and mCherry (a derivative of DsRed) proteins depend on the presence of oxygen in the environment for their complete maturation (Craggs, 2009; Strack et al., 2010). Pinilla-Redondo et al. (2018) investigated the recovery of fluorescence of these proteins, by first growing *E. coli* expressing the genes *gfp* or *mcherry* in anaerobic conditions, and then transferring them to PBS in the presence of oxygen, and testing for recovery of fluorescence by flow cytometry. Their results indicated that, at pH 7, detection of GFP exhibited a near-complete recovery by the one-hour

time point, and mCherry by two hours.

The AFR design for this project was based on the experiments of Pinilla-Redondo et al. (2018), with the AFR incubation set up at 4°C, in PBS containing chloramphenicol at a concentration above the MICs of the strains. The rationales behind the respective conditions were that the proteins were thought to mature more efficiently at this lower temperature (Scott et al., 1998), and that chloramphenicol, as a bacteriostatic translation inhibitor, would halt the translation of additional fluorescent proteins during the AFR stage. Pinilla-Redondo et al. (2018) also investigated the effect of pH on the recovery of these fluorophores after suppression by acid, and observed that both proteins displayed greater fluorescence at higher pH values when incubated in conditions up to pH 8. However, GFP detection decreased with decreasing pH, displaying less than 50% fluorescence intensity at pH 4.4. Although a very low pH, and unlikely to be encountered in these experiments, the PBS used in the AFR step was to be buffered to pH 7 to account for organic acid secretion by certain microbiota strains such as lactic acid bacteria, in order to keep the AFR step consistent between experiments investigating different microbiota strains.

3.1.4 Adding co-culture components to conjugation experiments

Designing a co-culture element to the model (Section 2.2.9) was based primarily on a similar set of experiments by J. D. Anderson (1975), who used pellets of 40h cultures of faeces-derived *B. fragilis* in *in vitro* co-culture with donor and recipient *E. coli* strains for four hours to investigate the effect on rate of transfer of two MDR plasmids, or "R factors". As previously discussed (Secion 3.1.1) Anderson observed a dose-dependent inhibitory effect using *B. fragilis* pellets. This study and others (Moubareck et al., 2007; Kunishima et al., 2019) also explored other forms of bacterial co-culture, such as non-pelleted culture, killed cells or supernatant. In this project, bacterial pellets were chosen as the method of co-culture, as this included the addition of fresh broth to all conditions (both control and experimen-

tal), meaning that nutrient availability would not be a confounding factor when investigating growth. The focus of these experiments was the effect of the cells themselves, and so the effect of supernatant was not investigated, though this was noted as an area of interest for further work.

For the purposes of this project, several changes were made to Anderson's original protocol based on the equipment available and to increase reproducability. The donor and recipient strains were grown to exponential phase before use rather than making dilutions of stationary phase cultures, to ensure cells going into the experiment were in the same metabolically active state. This was because cells in stationary phase have been shown to have significantly reduced conjugation frequencies (Headd and S. A. Bradford, 2020), and it would be difficult to control for the metabolic state of recently diluted stationary phase cells. The exponential phase cultures were then corrected to an OD_{600} of between 0.4-0.6, to ensure that the donor:recipient ratio remained as consistent as possible between experiments.

Supplemented BHI (BHIS) broth was used as the culture medium (Table 2.4). Although not designed to represent the microbiome environment, BHI media has been demonstrated to retain more intestinal microbial diversity when used to culture microbiome samples, compared to three other media commonly used to grow members of the microbiota (gut microbiome media, bacterial growth media and fastidious anaerobe broth) for between 4-48 hours (Yousi et al., 2019). Supplementation of BHI (Appendix C) increased levels of Vitamin K and hemin: nutrient groups which BHI lacked respective to the other media tested by Yousi et al. (2019). Additionally added was the reducing agent L-cysteine, measurable by the redox indicator L-resazurin, to contribute to replication of the anaerobic and highly reducing conditions of the gut lumen (Bacic and C. J. Smith, 2008). It was noted that Pinilla-Redondo et al. (2018) had omitted resazurin from their anaerobic media when investigating AFR of fluorescent proteins, because of the potential of interference with the emission spectrum of mCherry. Despite the dilution steps taken before analysis using the flow cytometer (Section

2.2.7), L-resazurin was not to be included in experiments using the dual-fluorescence system to eliminate the risk of fluorescence interference.

Two microbiota strains were chosen for investigation in this project: *B. fragilis* and *L. casei*. Members of their respective phyla, *Bacteroidetes* and *Firmicutes*, form the bulk of the gut microbiome in the majority of human adults (Huttenhower et al., 2012). Within the phylum *Bacteroidetes*, the majority of commensals fall under the order *Bacteroidales* with a longitudinal study by Zitomersky et al. (2011) detecting between $5x10^8$ to $8x10^{10}$ *Bacteroidales* per gram of the subjects' faeces. *B. fragilis* was chosen for this project as a representative strain for this dominant order as it is a widely studied microbiota member, used by J. D. Anderson (1975) and chosen with the intention of comparing the results from the subsequent experiments to those yielded by Anderson. *L. casei*, a Gram-positive species of the phylum *Firmicutes*, is a well-studied probiotic. The strain used in this project was the strain Shirota isolated from the commercial probiotic yoghurt drink Yakult (Douillard et al., 2013). Further details on *L. casei* and previous work on this strain in this research context are described in Section 3.5. Investigating the effect of a probiotic on conjugative transfer of AMR genes could guide potential use of these strains as interventional strategies to tackle the spread of AMR. Similarly to J. D. Anderson (1975), the microbiota strains used were stationary phase cultures taken after 40h of anaerobic incubation. The bacterial density for each experiment was measured both by OD_{600} and by viable counts.

Lastly, preparation of strains was performed at a lab bench with incubation in an anaerobic jar (Section 2.2.1), which was also used to pre-reduce the media overnight prior to the experimental set-up. Pre-reduction of media, preparation of strains and the main incubation step would have been ideally performed inside of an anaerobic cabinet to ensure anaerobic conditions throughout, keeping the media more reduced and minimising any confounding impact of the presence of oxygen on the experiment. However, restricted availability of the cabinet (see COVID-19 Impact Statement) meant that this was not possible during this

project. *B. fragilis* and *L. casei* were suited to this experimental design since both are aero-
1015 tolerant (Bacic and C. J. Smith, 2008; Zotta et al., 2017), meaning that the oxygen exposure when being handled on a lab bench would not be detrimental, as is often the case with strictly anaerobic organisms.

3.1.5 Controlling for growth rate

An important factor to consider when testing conjugation frequencies is the relative growth
1020 rates of the strains. Slower-growing strains would appear to conjugate less in the same time frame as faster-growing strains, ultimately because there are fewer cells present for conjugation overall. Additionally, if the donor and recipient strains in a conjugation have significantly different growth rates, the donor:recipient ratio may be impacted and subsequently affect the conjugation frequency.

1025 To address these potentially confounding effects, the growth rate of each strain was investigated by end-point viable counts under the same experimental conditions as the conjugations (Section 2.2.8), so that the results were comparable to those of the viable counts of the conjugation experiments. After the growth rate of each strain was established under these conditions, the donor and recipient strains were individually grown in co-culture with the mi-
1030 crobiome strains, to assess the effect of co-culture on growth rate (Section 2.2.9). Lastly, the conjugation experiments included calculation of viable counts using culture dilution and selective plating, just as for the growth tests. This setup would make the growth data consistent and comparable between all growth, co-culture and conjugation experiments. Additionally, this took into account that a conjugation is essentially a co-culture (between the donor and
1035 recipient strains), and any growth effect these strains may have on each other could also be observed.

3.1.6 Hypotheses

The aim of this chapter was to investigate the efficiency of conjugation of a carbapenem resistance-determining plasmid, pKpQIL-UK, between a clinically relevant *K. pneumoniae* donor and various *E. coli* recipients in the presence of members of the human gut microbiota. This chapter addresses research questions 1 (Section 1.5.2). This was planned using an established dual-fluorescence system using flow cytometry and AFR, which would be supported by more traditional selective plating-based conjugation experiments and growth tests.

Elucidating how the presence of members of the gut microbiota affects the conjugation of this plasmid between COPs would further our understanding of the significance of the microbiota on AMR transmission and dissemination. These experiments could also identify the role of particular gut-dwelling organisms, with probiotic strains of particular interest in the context of designing interventional strategies to tackle the spread of AMR.

The specific hypotheses devised in this chapter were as follows:

- That conjugation experiments using the dual-fluorescence system and AFR method, used together to monitor conjugation of pKpQIL-*gfp-aph* between a clinically relevant *K. pneumoniae* donor and a variety of *mcherry*-expressing *E. coli* recipient strains, would successfully reflect relative conjugation frequencies observed using the same strains in selective plating experiments. For example, that a donor-recipient combination with a higher conjugation frequency relative to other combinations would retain a comparatively higher frequency across both experimental designs, even if the absolute frequencies for each combination differed between designs.

- That pellets of the microbiota strains *B. fragilis* and *L. casei* at stationary phase slow the growth of the donor and recipient strains when incubated in co-culture, and that this may therefore account for any change in conjugation frequency observed.

- That the conjugation frequency of pKpQIL between *K. pneumoniae* and *E. coli* would be lower in the presence of microbiota strains, and that this could be observed both by flow cytometry/AFR and selective plating.

3.2 Experiments and Results: pKpQIL-*gfp-aph*

3.2.1 Initial characterisation of strains

All strains used in this section (Table 2.2) were, unless specified, taken from long-term cold storage at -80°C and characterised by selective plating on agar containing antibiotic to check for resistance, Gram staining (Section 2.2.2) to check the cellular morphology and tested for the presence or absence of the pKpQIL backbone by colony PCR (Section 2.2.3; Table 2.3).

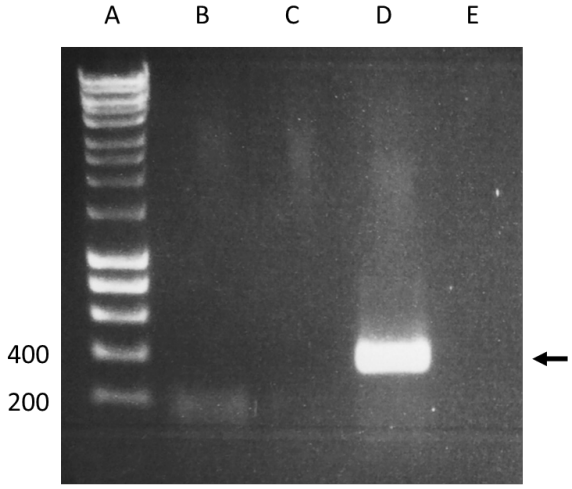

Figure 3.3: Colony PCR of the strains I967 (recipient *E. coli* J53), H207 (*K. pneumoniae* ST258) and H235 (*K. pneumoniae* Ecl8 containing pKpQIL-*gfp-aph*) using primers specific to the pKpQIL backbone.
Lanes A: 1kb hyperladder, B: I967, C: H207, D: H235, E: PCR negative control (water). Appropriate hyperladder band sizes (in base pairs) are indicated on the left. Band of interest has a size of 383bp and is identified with an arrow.

The recipient strains I967 (*E. coli* J53) and H207 (*K. pneumoniae* ST258) were confirmed by PCR to be negative for the pKpQIL backbone, and therefore free of the pKpQIL plasmid

(Figure 3.3). The donor strain *K. pneumoniae* Ecl8, H235, tested positive for the pKpQIL backbone, confirming presence of the plasmid. The strains grew on their respective selective conditions on LB agar (I967 in 100μg/ml rifampicin; H207 in 100μg/ml ampicillin; H235 in 50μg/ml kanamycin). All three strains were confirmed as Gram-negative with a rod-shaped morphology when observed under oil immersion light microscopy after Gram staining. The results of the three tests were consistent with the expected observations for these organisms.

3.2.2 Testing selective markers

aph

To confirm the selective conditions used to isolate putative transconjugants from a conjugation of pKpQIL-*gfp-aph* from H235 into H207, broth microdilution MIC testing was performed for the two strains with kanamycin (Section 2.2.4). H207, as a recipient, would have to be sensitive to kanamycin so that *aph*-encoding transconjugants could be selected.

Counterintuitively, the observed MIC value of kanamycin for H207 (256 μg/ml) was equal to H235 (128-256 μg/ml) (Table 3.1), despite H235 containing pKpQIL-encoded *aph*. The control strain I448 had a low MIC value of 2 μg/ml, however target MIC values for kanamycin are not available for validation of this experiment (EUCAST, 2020b). Despite this, kanamycin was clearly not suitable for use in selecting H207 transconjugants, as the plasmid-free recipient was already highly resistant to kanamycin.

Table 3.1: MIC values for the conjugation of pKpQIL-*gfp-aph* into H207.
Antibiotic abbreviations are outlined in Table 2.1. Where biological replicates gave different values, the MIC is indicated as a range. *Range as accepted by EUCAST (2020b); N/A indicates that recommendations are not available for that antibiotic. - indicates that the MIC assay was not performed.

Strain	MIC (μg/ml) of antibiotic		
	KAN	CEF	AMP
I448	2	16-32	2
I448 range*	N/A	N/A	2-8
H207	256	256	-
H222	-	-	32-64
H235	128-256	2-4	64-128

bla$_{\text{TEM-1}}$

Other loci of the pKpQIL plasmid were investigated to use as selectable markers in a H207 background. A literature search revealed that the *bla*$_{\text{TEM-1}}$ gene may confer resistance to early cephalosporin antibiotics such as cephalothin (P. A. Bradford, 2001). A subsequent broth microdilution MIC assay for cephalothin demonstrated that H207 (MIC value of 256 μg/ml) was again more resistant than H235 (MIC value of 2-4 μg/ml; Table 3.1). Unfortunately there was also no EUCAST target value for cephalothin for the control strain I448, which exhibited a relatively high value of 16-32μg/ml. However, given the 10-fold difference in apparent MIC values of the two *K. pneumoniae* strains and the negligible amount of resistance apparently conferred by the *bla*$_{\text{TEM-1}}$ gene in pKpQIL, cephalothin was not pursued further in this case.

To check if these results were at least in part due to the inactivity of the *bla*$_{\text{TEM-1}}$ gene,

an MIC assay was performed for ampicillin, a β-lactam antibiotic targeted by β-lactamase enzymes, for H235 and the plasmid-free Ecl8 strain, H222 (Table 2.2). The only difference between H222 and H235 was the presence of pKpQIL-*gfp-aph* in H235, and so any difference in ampicillin MIC was expected to be as a result of plasmid-encoded factors. H222 was confirmed to be plasmid-free by colony PCR, testing negative for the pKpQIL backbone (Figure 3.4). H222 had an MIC of 32-64 μg/ml, and H235 a value of 64-128 μg/ml (Table 3.1). The I448 control strain presented a value of 2 μg/ml, which was within the expected range as defined by EUCAST. Both H207 and H235 appeared resistant to ampicillin, with higher MICs than the EUCAST breakpoint for resistance of 8 μg/ml for *Enterobacterales* (EUCAST, 2020a). Despite an apparent slight elevation of MIC exhibited by H235, biological replicates of both strains had MICs of 64 μg/ml. Overlapping values indicated no significant difference in MIC between H222 and H235 for ampicillin, and that the $bla_{\text{TEM-1}}$ gene provided insufficient β-lactamase activity to provide a selective advantage for cells encoding this gene, making it a poor selectable marker for pKpQIL-*gfp-aph*.

mer operon

The *mer* operon (Figure 3.1) was the third locus investigated as a potential selectable marker for pKpQIL-*gfp-aph*. It was difficult to predict just from the genes present whether this operon was functional, as *mer* operons differ in their genetic composition across different taxa (Boyd and Barkay, 2012), but the pKpQIL *mer* operon did encode the key mercuric reductase protein, MerA, along with the inner membrane spanning proteins MerC and MerE, and the regulatory protein MerD. To the best of our knowledge, the mercury resistance phenotype had not yet been tested or characterised in pKpQIL-like plasmids, and so the success of this approach was uncertain. An MIC assay was carried out using mercury(II) chloride ($HgCl_2$). The broth microdilution MIC protocol was modified to account for the risks posed by the hazardous nature of inorganic mercury (Section 2.2.4). As a control, the kanamycin broth

MIC test was also repeated under these conditions in a separate plate.

Table 3.2: MIC values testing the *mer* operon, with the assay plate incubated in a fume hood at room temperature checked at 24 hour intervals for a total of six days.
Antibiotic abbreviations are outlined in Table 2.1. Where biological replicates gave different values, the MIC is indicated as a range. *Range as accepted by EUCAST (2020b); N/A indicates that recommendations are not available for that antibiotic. - indicates that the MIC was not performed.

Strain	MIC (μg/ml) of antibiotic	
	KAN	$HgCl_2$
I448	0.125	1
I448 range*	N/A	N/A
H207	0.125-0.25	1-2
H235	0.125	1-2

After checking for growth in the plate every 24 hours for six days, both H207 and H235 exhibited identical MIC values of 1-2 μg/ml (Table 3.2), indicating that the putative *mer* operon did not provide any benefit to host bacteria under these selective conditions. The results of the kanamycin MIC control under these conditions were inconsistent with the first test, with values of 0.125-0.25 μg/ml for H207, 16 μg/ml for H235 and 0.125 μg/ml for I448 (Table 3.2). Despite not being an optimised experiment, the results were consistent between biological replicates and indicated that there was no significant difference between the two strains. Furthermore, the modifications needed to safely work with the $HgCl_2$ were clearly having an impact on bacterial growth, behaviour or compound stability, as indicated by the unexpected results from the kanamycin MIC. Taken together, these preliminary results

indicated against the use of the *mer* operon as a selectable marker, and in combination with the safety concerns of using this compound, this approach was not pursued further.

3.2.3 Alternative approaches

Overall, testing the selective potential of pKpQIL-*gfp-aph* indicated that this particular plasmid could not be selected for when conjugated into *K. pneumoniae* H235. There were no other known selectable markers on the plasmid other than the *gfp* gene, and although screening for GFP-producing transconjugants by colony-based fluorescence microscopy (after killing off the donor population with e.g. cephalothin) was theoretically possible, it would be very labour-intensive and there would be no way to select for maintenance of the plasmid in any future experiments. The above experiments showed that the pKpQIL-UK plasmid contained no other functional selectable markers into which the *gfp-aph* cassette could be cloned into, to leave the $bla_{\text{KPC-2}}$ gene intact for use as a selectable marker. Short of cloning an alternative resistance gene elsewhere on the plasmid, selecting for H207 transconjugants would be unsuccessful. Therefore, in the interest of time, it was decided to revert the focus of the project towards the original, unmodified, $bla_{\text{KPC-2}}$-encoding plasmid pKpQIL-UK, and not employ the use of the dual-fluorescence system for this part of the project. This was preferable to using H235 as the donor strain for flow-cytometry-based conjugation experiments, since a prioritised focus of the project was on investigating clinically relevant donor and recipient strains. Clinical isolates of *K. pneumoniae* containing pKpQIL-UK were available, and so the step of creating a clinically relevant donor was circumvented.

3.3 Experiments and Results: pKpQIL-UK

3.3.1 Initial characterisation of strains

The pKpQIL-UK-carrying donor strain in this case was H218 (Table 2.2), a *K. pneumoniae* ST258 clinical isolate into which pKpQIL-UK had previously been conjugated in the lab (Buckner et al., 2018b). Colony PCR testing using pKpQIL backbone-specific primers confirmed carriage of pKpQIL-UK (Figure 3.4). Growth on 0.25 μg/ml doripenem confirmed carbapenem resistance, and Gram staining presented the expected Gram-negative bacilli under oil-immersion light microscopy.

The recipient *E. coli* I967 had been previously characterised (Section 3.2.1) as being devoid of pKpQIL (Figure 3.3), growing on 100 μg/ml rifampicin, and presenting as Gram-negative bacilli when Gram stained, which is consistent with *E. coli*.

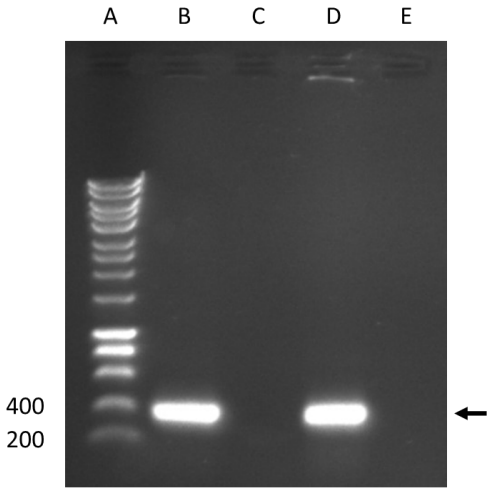

Figure 3.4: Colony PCR of the strains H218 (*K. pneumoniae* ST258 containing pKpQIL-UK) and H222 (*K. pneumoniae* Ecl8), using primers specific to the pKpQIL backbone. H235 was used as a positive control for the plasmid.
Lanes A: 1kb hyperladder, B: H218, C: H222, D: H235, E: PCR negative control (water). Appropriate hyperladder band sizes (in base pairs) are indicated on the left. Band of interest has a size of 383bp and is identified with an arrow.

3.3.2 Conjugating pKpQIL-UK into I967

Conjugation was initially done by the filter mating method (Section 2.2.5) to compare the results with previous experimental work done on this plasmid (Saw, 2015; Buckner et al., 2018b) and ensure that the work was consistent. It has also been established that solid and liquid media are both appropriate for IncF plasmid conjugation (Rodriguez-Grande and Fernandez-Lopez, 2020). Doripenem (0.25 μg/ml) was used to select for H218 and 400 μg/ml rifampcin to select for I967: a higher rifampicin concentration than the standard working concentration (Table 2.1) was chosen due to the risk of spontaneous mutation in susceptible donor strains. Rifampicin is a specific inhibitor of the β-subunit of bacterial RNA polymerase, and variable levels of resistance can arise from single mutations in the β-subunit-encoding *rpoB* gene, which render the enzyme still functional but less susceptible to binding and inhibition by rifampicin (Wehrli, 1983). Using a higher concentration would theoretically reduce the number of *rpoB* mutants tolerant to the working concentration of rifampicin, thus reducing the appearance of false positive results when selecting for transconjugants on double-antibiotic agar. A mutant selection window of *K. pneumoniae* for rifampicin was not found, but investigations into that of *E. coli* found no concentration that prevented the selection of mutants when testing up to 4000 μg/ml (Xilin and Drlica, 2002). A higher concentration to the working concentration of 100 μg/ml was chosen, but it was not certain to what extent this could prevent the selection of mutant donors.

3.3.3 Preliminary results

After overnight incubation of transconjugants on double-selective plates in the first experiment, one colony was seen on one neat plate over all biological replicates. The plates were left to incubate for a further 72 hours, after which all three neat plates were covered in an uncountable smear of small colonies, with two (one of which was the colony from day one)

notably larger than the others. Many of the small colonies had a different morphology to those of both H218 and I967, with dark concave centres. No colonies were visible on the plates inoculated with 10^{-1} or 10^{-2} dilutions after four days, where a 10-fold difference in number of colonies between each successive dilution was expected. 10 colonies were carefully re-plated using sterile toothpicks onto LB agar containing 0.25 μg/ml doripenem and 400 μg/ml rifampicin: the two large colonies and eight randomly selected others, and their morphologies noted. After overnight incubation, only three of these had grown, of which the original morphologies were the two large colonies, and one small convex colony. These three were tested for presence of the pKpQIL backbone by colony PCR, and all presented a band of the expected size (Appendix B).

The curious pattern of growth across the dilutions and the variety of colonies present could have had several possible explanations. A high number of cells on the neat plates could have provided a barrier of dead cells between the antibiotic in the agar and the observed colonies, resulting in lower exposure to rifampicin and doripenem which should have killed donors and plasmid-free recipients respectively. Contamination was also considered as the source of these unexpected colonies.

Lastly, it was possible that 400μg/ml rifampicin may not have been enough to prevent spontaneous mutant donors from growing on the double selective plates, which could be contributing to the high numbers of observed colonies. However, no colonies grew on the mutant selection plates of H218 plated on 400μg/ml rifampicin even after four days. The mutation rate calculated from this method was below the limit of detection, and it therefore seemed unlikely that mutated donors could account for the huge number of colonies appearing on the neat plates.

3.3.4 Subsequent follow-up replicates

Repeated attempts of this conjugation were undertaken to investigate the above issues and to calculate conjugation frequencies for comparison with previous studies. Seven separate conjugation experiments gave consistent results: few colonies grew during the initial overnight growth, but many hundreds more small slow-growing colonies, some with characteristic dark concave centres, appeared after two or more days of incubation. The 10^{-1} dilution plates showed growth in some of the experiments, but only of the small, slow-growing clustered morphology, and far fewer than the expected 10-fold lower than the neat plates- though colonies could not be counted in either case due to excessive clustering of colonies making them impossible to distinguish. There was a consistent lack of growth on the 10^{-2} dilution plates.

When checked for mutants, H218 mutant selection plates grew at most one colony per neat plate, which was at the limit of detection for this assay. Calculated as the observation of a single colony divided by the average viable counts for each experiment, the average limit of detection for H218 ranged from $2.07\text{x}10^{-8}$ to $2.86\text{x}10^{-8}$ per donor CFU, and from $2.50\text{x}10^{-8}$ to $3.70\text{x}10^{-8}$ for I967. I967 mutant selection plates were consistently clear, indicating a mutation frequency below the limit of detection.

When colonies were PCR tested for the presence of pKpQIL-UK, the large, fast growing colonies consistently contained the plasmid, whereas presence in colonies of other morphologies was inconsistent. There was also inconsistent plasmid loss upon replica plating of colonies onto double-selective agar, for example in one experiment, the majority of colonies (eight in ten) on the 10^{-1} dilution plates tested positive for the plasmid, but with six out of seven colonies appearing as plasmid-negative upon replica plating on LB after three days of growth (Figure 3.5).

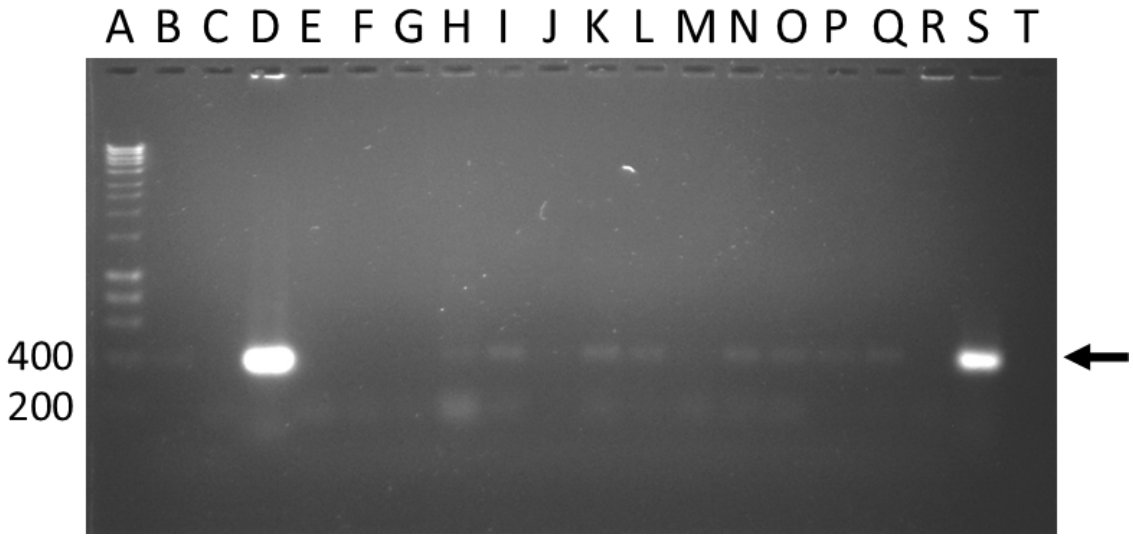

Figure 3.5: Colony PCR of putative transconjugants from a conjugation experiment between H218 and I967, both from the original double-selective plates and from replica double-selective plates, for the pKpQIL backbone. Replica plating of colonies was done using sterile toothpicks to transfer single colonies of a range of observed morphologies onto new LB plates.
Lanes A: 1kb hyperladder, B-G: colonies replica plated onto double-selective agar, H-Q: putative transconjugants taken straight from 10^{-1} dilution plates, R: putative contaminant replica plated onto LB agar without antibiotic, S: H218, T: PCR negative control (water). Appropriate hyperladder band sizes (in base pairs) are indicated on the left. Band of interest has a size of 383bp and is identified with an arrow.

In each of these experiments, attempts were made to troubleshoot the origin of and better understand these unexpected results. The remainder of this section describes and explains the approaches made, results observed and conclusions drawn as part of this investigation.

Contamination

To investigate the possibility of presence of a contaminant, Gram staining was performed on colonies of all three morphology types: large and fast-growing; small and slow-growing; and small slow-growing with dark concave centres. When viewed under the microscope, large colonies consistently presented as Gram-negative bacilli, whereas both smaller morphologies presented as a range of forms, with predominantly Gram-negative cocci. When streaked onto

antibiotic-free LB agar, these latter colonies did not appear dissimilar to the *K. pneumoniae* donor or *E. coli* recipient. Colony PCR testing of a colony from this plate revealed no plasmid (Figure 3.5).

These data were insufficient to rule out or confirm contamination as the source of these results, and so to locate any source of putative contaminant, suspensions from each intermediate step of the protocol were plated onto double selective plates. This consisted of: donor alone; recipient alone; donor and recipient in their final ratio; filter disk impregnated with 100 μl LB broth (that had been overnight on an agar plate as per the protocol); and LB broth alone. All plates were incubated for six days, and returned clear except from H218 alone, where irregularly sized and shaped colonies had grown. These morphologies were curiously inconsistent with both H218 colonies and with the colonies observed in the conjugation experiments. H218 mutant selection plates containing rifampicin once again returned clear in this experiment, suggesting a mutation frequency below $2.07\text{x}10^{-8}$, the limit of detection of H218 mutants for this experiment. Nevertheless, due to the presence of rifampicin in the double selective plates, there should have been no growth on these plates. As a result, it was concluded that the unexpected outcomes of the conjugation experiments were sourced from the H218 stock.

A new *K. pneumoniae* donor was chosen, H203, a ST468 strain which also contained pKpQIL-UK (Table 2.2), in an attempt to resolve this issue. However, three subsequent conjugation experiments using H203 as a donor resulted in the same range of colony morphologies, with the same characteristic smeary growth and deviation from the expected 10-fold difference in colony count between dilutions.

Donor mutations

Raising the rifampicin concentration to 500 μg/ml made negligible difference to the growth of H203 on the mutant selection plates. It was however noted that the the mutation rates

were being calculated from the cellular density at the beginning of the experiment, which was relatively low (in the order of 10^8 as calculated using viable counts). After overnight incubation on filters, the total number of donors would be expected to increase exponentially, increasing the pool of donors from which mutants could be selected. In an attempt to better quantify the extent to which mutant donors could be confounding the results, H203 was added alone onto filter disks on plain LB agar, at the same starting OD_{600} as the experimental mixture, and incubated overnight in order to approximate how many mutants may have been selected for at the end of the experiment.

After vortexing, re-plating on double selective plates and incubating, an average of 25 large colonies growing at the neat dilution after one day's incubation, which increased to 32 after seven days' growth. The mutation frequency could unfortunately not be calculated for this particular experiment due to an error in plating viable counts, however it was clear that rifampicin-resistant mutants were present in significant numbers after growth on filters. It therefore seemed likely that H203 mutants (mutant donors) were quickly appearing on double selective transconjugant plates and confounding the putative transconjugant counts.

The unexpected morphology as observed by Gram staining, slow growth and inconsistent plasmid carriage detected by PCR made the small, slow-growing and clustered colonies difficult to count or confirm. Nevertheless, since mutant donors seemed to account for the large, faster-growing colonies, and the possibility of contamination was unlikely, this pointed to the smaller colonies being putative transconjugants.

Ratio

Different donor:recipient ratios were tested to the 1:1 ratio used in the protocol (Section 2.2.5). Based on the optimised ratio of 8:1 used in Buckner et al. (2018b), where pKpQIL-UK was successfully conjugated between *K. pneumoniae* strains, ratios of 1:1, 4:1, 8:1 and 16:1 were compared. These ratios were tested once for each the H218 and H203 donors. All

ratios in both experiments produced the same consistent results after two days' incubation as described above: too many colonies to count on the neat plates, individual colonies of various morphologies along with smears of small colonies on the 10^{-1} dilution plates, and no growth on the 10^{-2} dilution plates.

Growth time

As a part of one of the experiments using H203, colonies growing on the double selective plates were counted each day for eight days to investigate the extent of the smaller colonies' apparent slow growth. These were measured from the 10^{-1} dilution plates, since colonies on the neat plates were impossible to count due to their proximity to each other. The numbers were estimates due to a high degree of clustering making individual colonies difficult to distinguish. The cumulative colony counts for this experiment, shown in Figure 3.6A, demonstrate that the majority of colonies appeared between days four and six, after which new colonies still appeared but at a slower rate. After seven days, 16 colonies were tested for presence of the pKpQIL backbone by colony PCR, with six showing faint bands of interest and the rest presenting as plasmid-negative (Figure 3.6B).

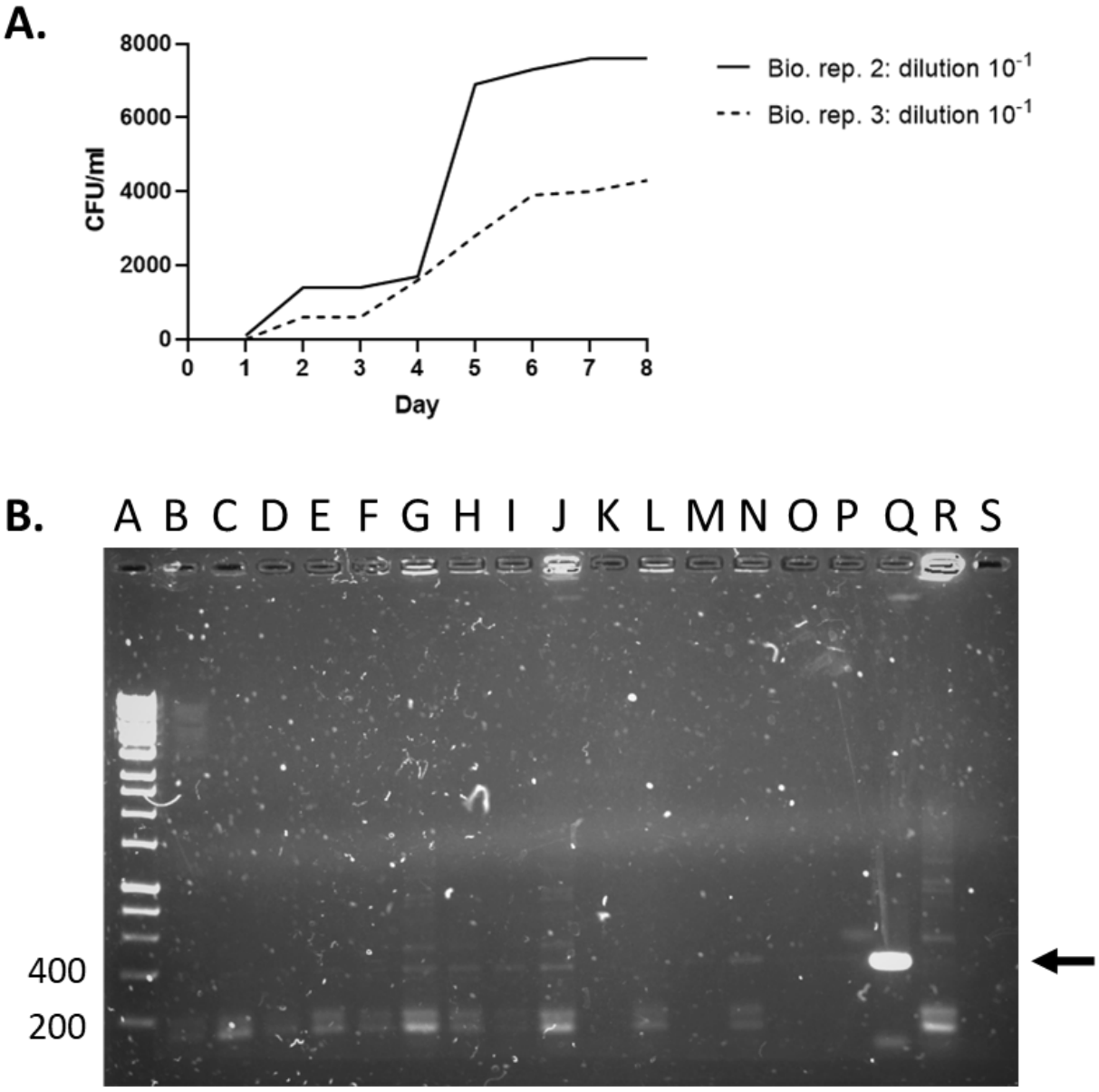

Figure 3.6: Cumulative colony counts over eight days, with a PCR test for plasmid-containing colonies on day seven. From a conjugation between H203 and I967.

A. Cumulative colony counts on double-selective plates. Counts were calculated as CFUs per ml from the resuspended filter, and counted on each of the eight days of incubation. Biological replicate 1 was omitted as an outlier due to >100-fold more colonies on the 10^{-1} dilution plate, rendering counts impossible.

B. Colony PCR for the pKpQIL backbone of 16 putative transconjugant colonies after seven days of growth on double-selective plates.

Lanes A: 1kb hyperladder, B-P: putative transconjugants, Q: H203, R: I967, S: PCR negative control (water). Appropriate hyperladder band sizes (in base pairs) are indicated on the left. Band of interest has a size of 383bp and is identified with an arrow.

Individual colonies were not PCR tested at different time points, since although this would have been ideal for investigating whether the low frequency of plasmid carriage was due to plasmid loss over time, the colonies were too small and clustered to avoid disrupting colony integrity with the sterile toothpicks, and be able to test the same colony again. However, this experiment demonstrated that there was no benefit to incubating the transconjugants for longer, as this did not improve the ease of counting and isolating plasmid-positive transconjugants.

bla$_{\text{KPC}}$ transposition

A final explanation explored was the potential for the carbapenem-resistance determinant, *bla*$_{\text{KPC-2}}$, to transpose. Tn*4401* is an active transposon, nested in an active Tn2-like element (Sheppard et al., 2016), and so it is possible that the *bla*$_{\text{KPC-2}}$ gene had integrated into the chromosome of transconjugants, resulting in rapid loss of the plasmid but retention of *bla*$_{\text{KPC-2}}$ and the carbapenem resistance phenotype. Colony PCR using primers specific to *bla*$_{\text{KPC-2}}$ (Table 2.3) was used in one of the conjugation experiments using the H203 donor, and the results compared with the PCR using the pKpQIL backbone primers. The band pattern patterns were revealed to be identical (Figure 3.7), demonstrating that presence of pKpQIL and *bla*$_{\text{KPC-2}}$ were tightly linked enough for *bla*$_{\text{KPC-2}}$ integration into the chromosome to be unlikely to have a confounding effect.

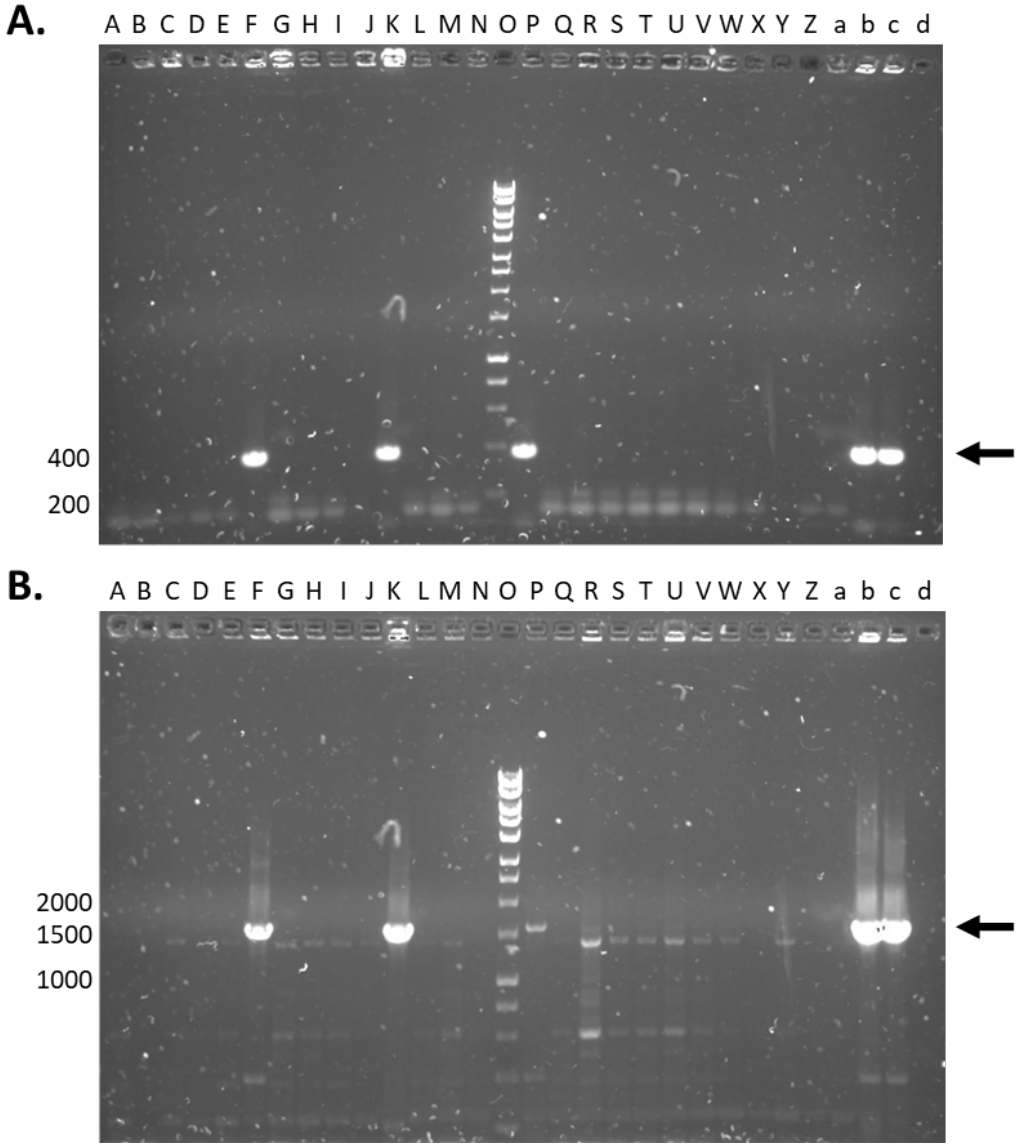

Figure 3.7: Colony PCR for the plasmid backbone (**A.**) and *bla*$_{\text{KPC-2}}$ gene (**B.**) of putative transconjugants from a conjugation experiment using the H203 donor and I967 recipient. Putative transconjugants were incubated for 7 days.
Lanes A-N: putative transconjugants, O: 1kb hyperladder, P: H203, Q: I967, R-c: amplicons from a different PCR, not relevant to this experiment, d: PCR negative control (water). Appropriate hyperladder band sizes (in base pairs) are indicated on the left.
A. Band of interest has a size of 383bp and is identified with an arrow.
B. Band of interest has a size of 1600bp and is identified with an arrow.

Chromogenic selection

Lastly, to aid in characterising the strains growing on the double selective plates, colonies from the experiments using H203 as a donor and I967 as a recipient were replica plated onto UTI chromogenic agar (Sigma-Aldrich) using sterile toothpicks. Colonies of *K. pneumoniae* H203 and *E. coli* I967 appeared dark blue and light purple respectively (not pictured), making them easy to distinguish. UTI agar could not be used for the double selective plating, due to the deep orange colour of rifampicin, but was instead used to replica plate randomly chosen colonies with sterile toothpicks. Replica plating of six random colonies onto UTI agar revealed that four of the six colonies growing on the double selective plates appeared to be *K. pneumoniae*, indicating that a significant proportion of colonies appearing on the double-selective plates were likely to be mutant donors. These blue colonies were consistently those that appeared larger and grew faster on the double selective plates. When checking the colonies from UTI agar for the pKpQIL backbone, colonies presenting as purple (indicating *E. coli*) appeared to have lost the plasmid, as prior to replica plating, the amplicon was present (Figure 3.8A), but was absent after growth on UTI agar (Figure 3.8B).

Finally, a purple UTI morphology appeared to correlate with a non-specific band pattern at <200bp present in I967, which was absent from the blue colonies and H203 (Figure 3.8).

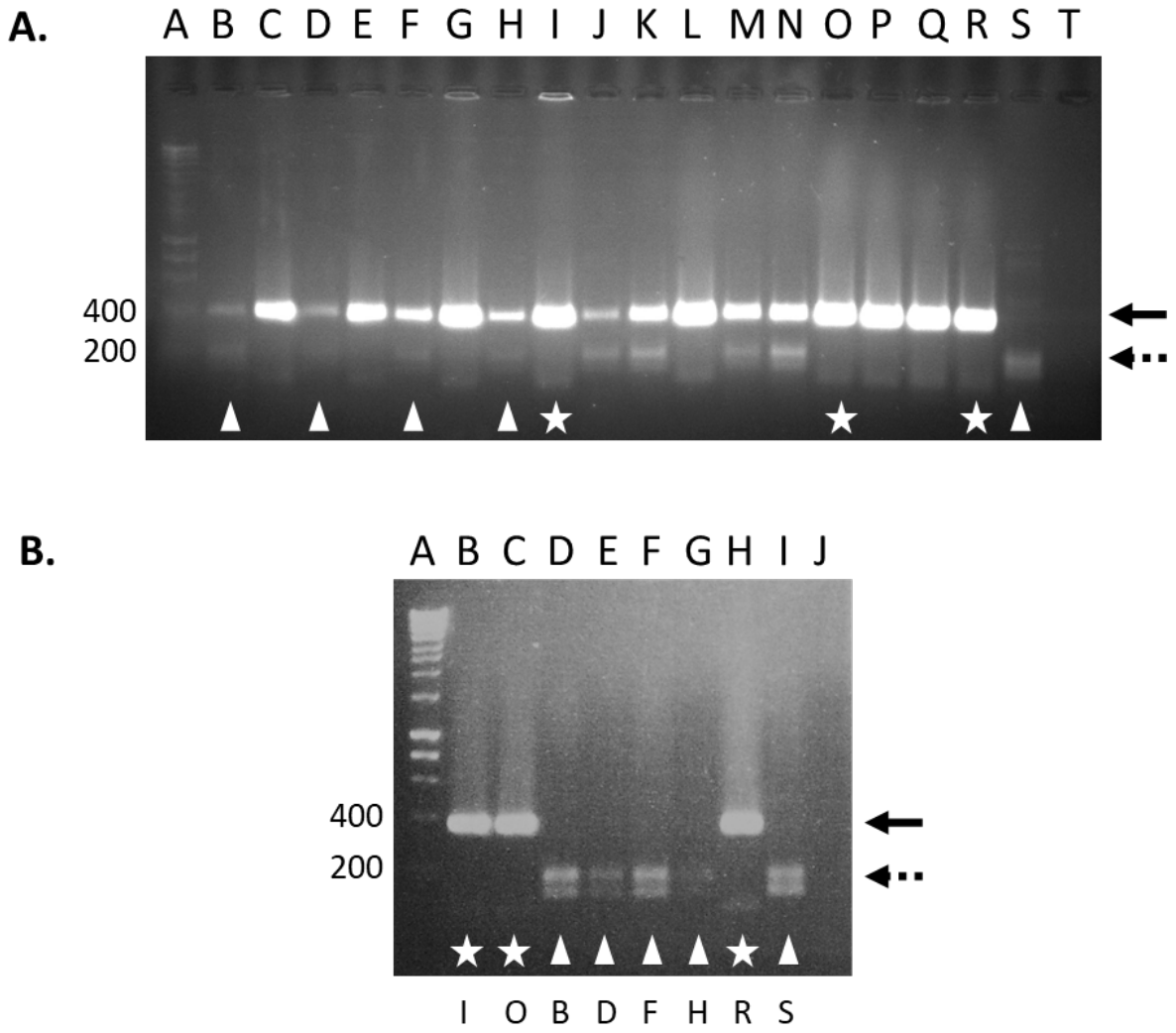

Figure 3.8: Colony PCR testing putative transconjugants from the first experimental repeat using the H203 donor, directly from the double-selective plates (0.25 μg/ml doripenem and 400 μg/ml rifampicin) (A) and from the UTI replica plates (B). Colonies presenting as purple on UTI agar (indicating *E. coli*) are indicated with a triangle, and colonies presenting as blue (indicating *K. pneumoniae*) with a star. Band of interest has a size of 383bp and is identified with a full arrow. Non-specific bands suspected to be unique to I967 are indicated with a dashed arrow.
A. Lanes A: 1kb hyperladder, B-Q: putative transconjugants, R: H203, S: I967, T: PCR negative control (water). Appropriate hyperladder band sizes (in base pairs) are indicated on the left.
B. Lanes A: 1kb hyperladder, B-G: putative transconjugants, H: H203, I: I967, J: PCR negative control (water). Appropriate hyperladder band sizes (in base pairs) are indicated on the left. The corresponding colonies from 1. are indicated underneath the symbols.

The above findings supported that the large colonies that grew as blue on UTI agar were spontaneous rifampicin-resistant mutants of H203. The smaller, clustered colonies were likely therefore putative transconjugants, as they grew as purple on UTI agar. However, these putative transconjugants appeared to lose the plasmid very quickly, both when replica plated onto non-selective agar, and when left for several days on double-selective agar as mentioned earlier. The reasons behind the different morphologies of small colonies (cream and convex as well as dark-centred and concave) and the altered Gram staining morphology remained unclear. It was plausible that the double selective conditions or acquisition of the plasmid caused the cells a significant amount of stress and metabolic changes, which could have accounted for morphology change. Westfall and Levin (2018) suggested several mechanisms by which central carbon metabolism in *E. coli* could alter the morphology of cells. These included a cAMP-mediated inhibition of transcription of *mreB*, a gene encoding an actin homologue partly responsible for cellular elongation, the depletion of which has been shown to result in spherically-shaped cells (Kruse et al., 2005). It has also been reported that carbapenems can select for *E. coli* mutated in the transpeptidase gene *mrdA*, and that some of these display more rounded morphologies (Lange et al., 2019). Lastly, Kitano and Tomasz (1979) observed that *E. coli* mutants would display characteristic ovoid morphologies in the presence of some β-lactam antibiotics such as mecillinam. There was insufficient time to investigate these colonies further, but in any case the purple colour of the colonies on UTI agar confirmed that these were likely not contaminants.

3.3.5 Further considerations

The results described in the previous section were concluded to be consistent. Conjugation frequency could not be calculated due to the slow growth of transconjugants and inconsistencies in plasmid carriage. These results were inconsistent with previous work using this plasmid with this protocol (Saw, 2015; Buckner et al., 2018b), where the above issues were

not present and did not confound the calculation of conjugation frequency.

Troubleshooting attempts for the problems in conjugating pKpQIL-UK into I967 were halted at this point, in the interest of time. However, several further investigations, outlined below, could have been made to pinpoint a potential source of these unexpected results.

Cryopreservation

A possible reason considered for these results was the negative effects of long-term cryopreservation: reports have been published of rare genetic changes acquired during long-term cold storage, presumably as a result of different kinds of shock and stress induced by the process (Prakash et al., 2013). Sequencing of the strains and plasmids to compare with reference sequences could be completed in the future in order to investigate any acquired genetic changes. However, this was not performed as part of this project due to time constraints.

Recipient strain

I967 was in this case not investigated or replaced, as alongside this project, a fellow lab member (O. Neo, PhD candidate in the Buckner Lab) successfully conjugated the *E. coli* plasmid pCT (Cottell et al., 2011) into I967 with a conjugation frequency of $4x10^{-6}$ per donor cell (unpublished data), thus determining that this stock of *E. coli* J53 was a suitable recipient for new plasmids. I967, as an *E. coli* member of the family *Enterobacteriaceae*, was expected to readily accept pKpQIL-UK, especially as Saw (2015) observed that pKpQIL-UK was able to conjugate into an *E. coli* NCTC10418 strain at a frequency of $1.4x10^{-5}$ per donor cell, a frequency comparable to the $1.57x10^{-5}$ observed by Buckner et al. (2018b) using a *K. pneumoniae* Ecl8 recipient.

Further investigations into the recipient strain could have included using a *K. pneumoniae* Ecl8 recipient, as had been done successfully by Buckner et al. (2018b), to check whether conjugations with this recipient returned results similar to that reported by Buckner et al.

(2018b), or to that reported in this project. Successful conjugations into Ecl8 would suggest that the problem lay with the I967 strain, and unsuccessful conjugations would point towards the plasmid or donor.

However at this time in the project, newer clinical isolates of *K. pneumoniae* expressing plasmid-encoded carbapenemases were obtained (further details in Section 3.4.1). Since repeated attempts at pKpQIL conjugation were unsuccessful, these new strain-plasmid combinations were tested. This enabled progress on addressing the hypotheses to be made, rather than spending more time addressing the above anomalies.

3.4 Experiments and Results: pCPE01_2

3.4.1 Investigating a new plasmid: *K. pneumoniae* CPE01 contig_2

The donor strain chosen to continue with this project was a carbapenem-resistant *K. pneumoniae* donor, expressing the $bla_{\text{NDM-5}}$ carbapenemase gene on the conjugative plasmid contig_2 (Figure 3.9), henceforth referred to as pCPE01_2. Strain and plasmid characterisation was performed by bioinformatic analysis by S.J. Element (PhD candidate, Buckner lab).

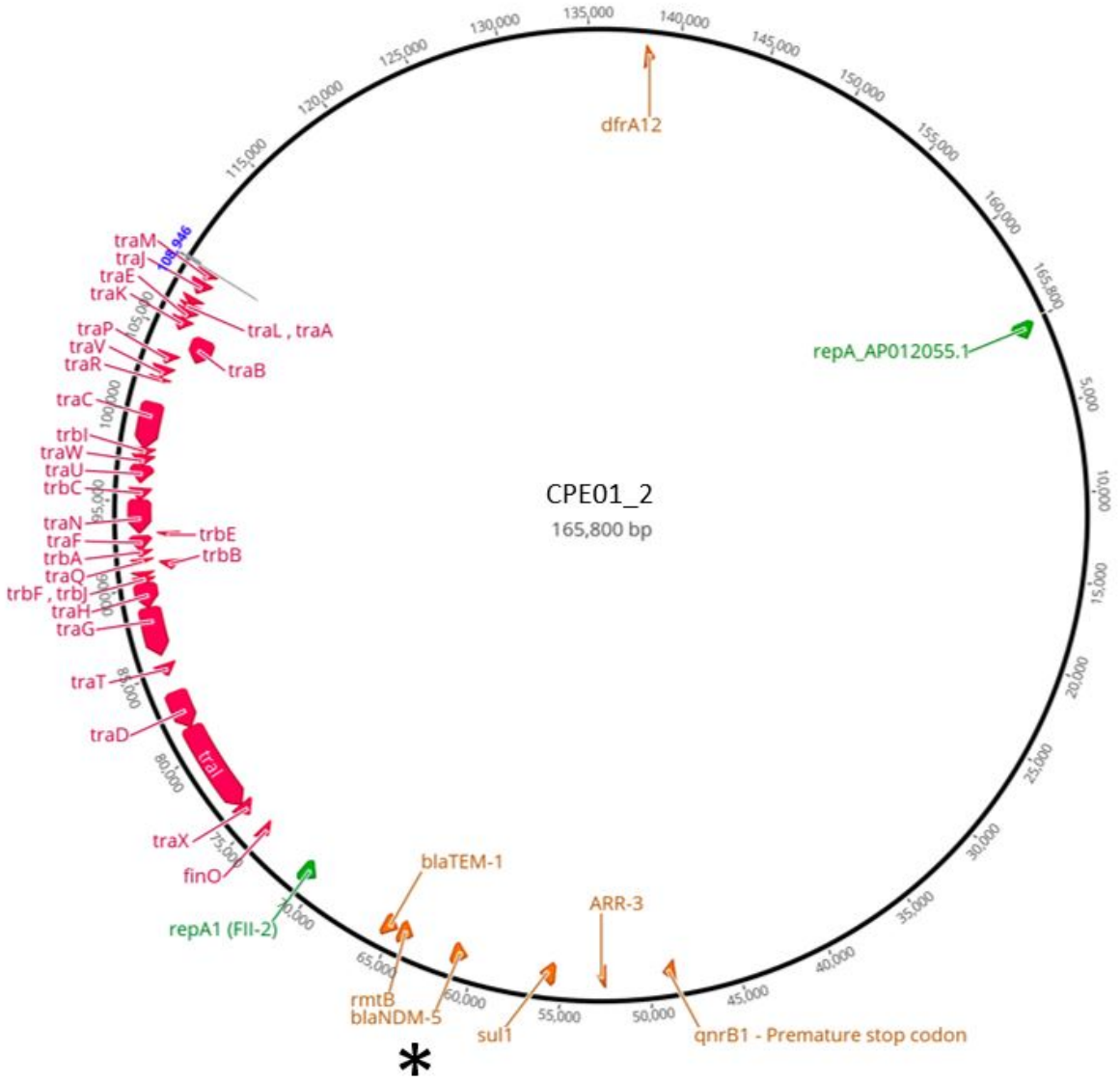

Figure 3.9: Annotation of plasmid pCPE01_2 of *K. pneumoniae* strain CPE01. The position of the carbapenemase-encoding gene $bla_{\text{NDM-5}}$ is identified with an asterisk. Figure adapted from and compiled by S.J. Element (PhD candidate, Buckner Lab).

The strain CPE01, identified as ST147 (S.J. Element, unpublished data), was one of a group of carbapenemase-producing *Enterobacteriaceae* isolated between March 2018 and March 2019 from the Queen Elizabeth Hospital Birmingham, and kindly provided by Drs M. Garvey and C. McMurray (Queen Elizabeth Hospital Birmingham). The source of this particular isolate was from a patient's ear. This strain was chosen as ongoing bioinformatic

analysis of the strains' plasmids revealed that pCPE01_2 was highly likely to be conjugative (S.J. Element, unpublished data). This analysis was based on results from Basic Local Alignment Search Tool (BLAST) searches against an experimentally-determined conjugation module from an *E. coli* K12 plasmid (GenBank reference sequence AP001918).

3.4.2 Initial characterisation of strains

Presence of the plasmid in the CPE01 strain was confirmed by colony PCR (Section 2.2.3) using primers specific to the *repA* gene in the plasmid backbone (Table 2.3; Figure 3.10).

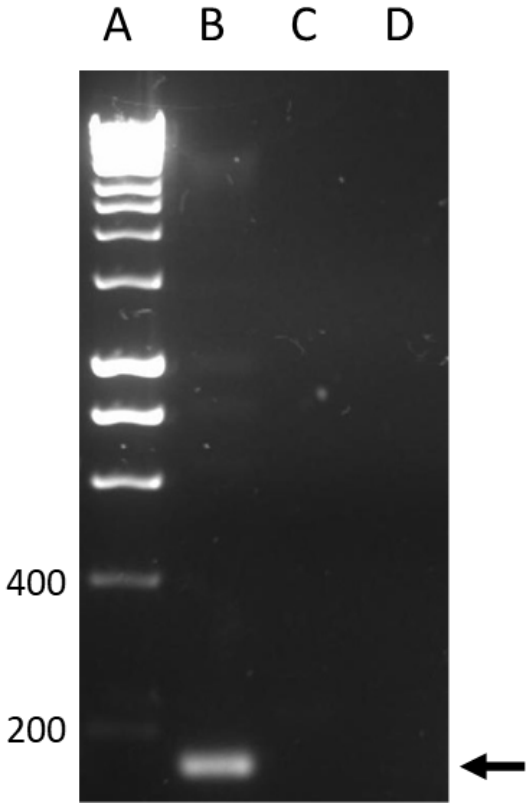

Figure 3.10: Colony PCR of CPE01 donor and Az^R J53 recipient for plasmid pCPE01_2, using primers specific to the plasmid backbone (Table 2.3).
Lanes A: 1kb hyperladder, B: CPE01, C: Az^R J53, D: PCR negative control (water). Appropriate hyperladder band sizes (in base pairs) are indicated on the left. Band of interest has a size of 161bp and is identified with an arrow.

Similarly to previous conjugation experiments, a sodium azide-resistant J53 *E. coli* recipient was used. Since CPE01 exhibited high levels of resistance to rifampicin (Table 3.3), I967 was deemed an inappropriate recipient for these experiments. Nevertheless, CPE01 was sensitive to sodium azide when plated on 100 μg/ml in agar. A sodium azide resistant J53 (Az^R J53) was kindly provided by Dr S. Dunn (PostDoctoral Research Associate in the lab of Professor A. McNally).

Table 3.3: MICs of CPE01 and Az^R J53. Antibiotic abbreviations are outlined in Table 2.1. Where biological replicates gave different values, the MIC is indicated as a range. *Range as accepted by EUCAST (2020b); N/A indicates that recommendations are not available for that antibiotic. **Experiments done by Nicholas Lim (placement student, Buckner Lab). - indicates that the MIC was not performed.

Strain	MIC (μg/ml) of antibiotic	
	RIF	DOR
I448	4	0.03125-0.0625
I448 range*	N/A	N/A
CPE01**	>512	>16
Az^R J53	-	0.015625 - 0.03125

3.4.3 Conjugating pCPE01_2 into Az^R J53: preliminary experiment

The conjugative ability of pCPE01_2 had been presumed using bioinformatic analysis, but had not been proven experimentally. A single preliminary conjugation in liquid (Section 2.2.6) experiment was set up between CPE01 and Az^R J53, using 1 μg/ml doripenem to select for CPE01 and the plasmid, and 100 μg/ml sodium azide (NaN_3) to select for Az^R

J53. Since this donor had not been used in previous conjugation studies, filter mating for the comparison of results was not used. Liquid mating was chosen instead, to be consistent with the original experimental design outlined in the hypotheses.

This conjugation was only performed once using this protocol because of time constraints (see COVID-19 Impact Statement). The results from this preliminary experiment were used to guide the experimental design for the rest of the conjugations using these strains, since this was not yet established. The results showed that putative transconjugants could be isolated using double selective plates, replica plated and grown on UTI agar containing 1 μg/ml doripenem, and pCPE01_2 plasmid carriage could be confirmed using PCR with primers targeting the plasmid backbone (Table 2.3). Putative transconjugants took two nights to grow, and some of the colonies were confirmed as mutant donors as they presented as blue when replica plated on UTI chromogenic agar. This confirmed that azide-resistant CPE01 mutants were likely to arise in this conjugation experiments. Similarly to rifampicin, resistance to azide can occur from single point mutations in the gene encoding its protein target, in this case the transmembrane protein transporter SecA (Oliver et al., 1990). CPE01 mutants resistant to the working concentration of sodium were therefore expected, but would be able to be differentiated from putative transconjugants by replica plating onto UTI agar containing doripenem.

3.4.4 Effect of co-culture with *B. fragilis* on bacterial growth

Using the anaerobic end-point growth assay method (Section 2.2.8), exponential phase cultures of CPE01 and Az^R J53 were incubated anaerobically in BHIS for four hours, with viable counts taken immediately before and after incubation. Three experimental replicates were performed for each strain in monoculture and co-culture with a 40h pelleted culture of *B. fragilis* (Section 2.2.9), for which OD_{600} and viable counts were measured before incubation. The average OD_{600} and density of *B. fragilis* ranged from 1.58-1.91 and $4x10^8$-$3.83x10^9$

CFU/ml respectively (discussed further in Section 3.5.1).

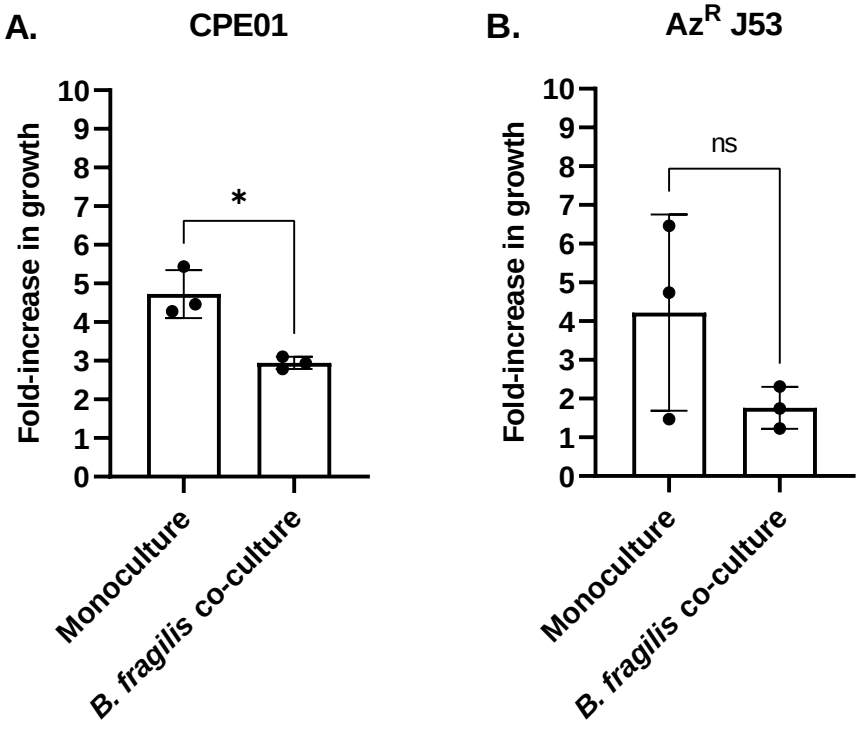

Figure 3.11: Growth assays of CPE01 (**A.**) and Az^R J53 (**B.**) in monoculture and in co-culture with *B. fragilis*. Fold-increase in growth was calculated using viable counts at zero and four hour timepoints. Each data point represents one experiment, each consisting of three biological replicates, unless specified otherwise. Error bars represent one standard deviation above and below the mean. * = P $\leq$ 0.05; ns = not significant, when analysed with an unpaired t-test.

Welch's t test was chosen to analyse the significance of effect size of co-culture on growth of CPE01 and Az^R J53 (Figures 3.12, 3.12 and 3.13), since this test considered and corrected for the variations in standard deviation. CPE01 growth was observed to be inhibited by co-culture with *B. fragilis* (P = 0.0317; Figure 3.11A).

When collecting the viable counts results for the growth assays of Az^R J53 (Figure 3.11B), several of the biological replicates appeared as though they may have been anomalies. One

appeared to show a reduction in growth, with a fold-increase of less than one, and two others had a fold-increase of ten-fold higher than all other biological replicates. These were not removed however, as due to the lack of further experimental replicates, it was not possible to perform a robust enough analysis for the identification of outliers such as Grubb's or the ROUT tests. These issues also highlight a limitation of taking single viable counts for each biological replicate, and this is further discussed in Section 3.5. Further experimental replicates would have ideally been performed to obtain more stringent data, however due to time constrains (See COVID-19 Impact Statement) these were not performed.

The inability to exclude these biological replicates resulted in a large range of values, though these data showed no significant difference in growth rate between the two conditions ($P = 0.2315$ using Welch's t-test). Despite the apparent lack of significant difference in growth rate of Az^R J53 between monoculture and co-culture, it was taken into account for future conclusions that these data were preliminary.

3.4.5 Effect of co-culture with *B. fragilis* on plasmid conjugation

The effect of co-culture with *B. fragilis* on conjugation of pCPE01_2 under the same conditions were tested (Section 2.2.9). The growth of the donor and recipient, as well as the conjugation and mutation frequencies were measured, with three experimental replicates performed for each conditions (with and without *B. fragilis* co-culture).

As had been previously observed in conjugations between *K. pneumoniae* and *E. coli* (Section 3.3), a range of distinct morphologies was observed: large, faster growing colonies that predominantly presented as blue on UTI agar (thus confirmed as mutant donors), smaller slower growing colonies that predominantly presented as purple (thus confirmed as *E. coli*), and small smears of tightly clustered colonies that were difficult to count and, when replica plated onto UTI agar, often presented both blue and purple colours. All tested colonies and smears contained the plasmid pCPE01_2, as confirmed by PCR. When choosing the colonies

to replica plate and PCR test, a full range of morphologies was tested. Unless proven otherwise by UTI results, small colonies were assumed to be transconjugants, and larger colonies to be CPE01. Smears were tested on UTI agar but not included in the counts, due to the difficulty in distinguishing individual colonies.

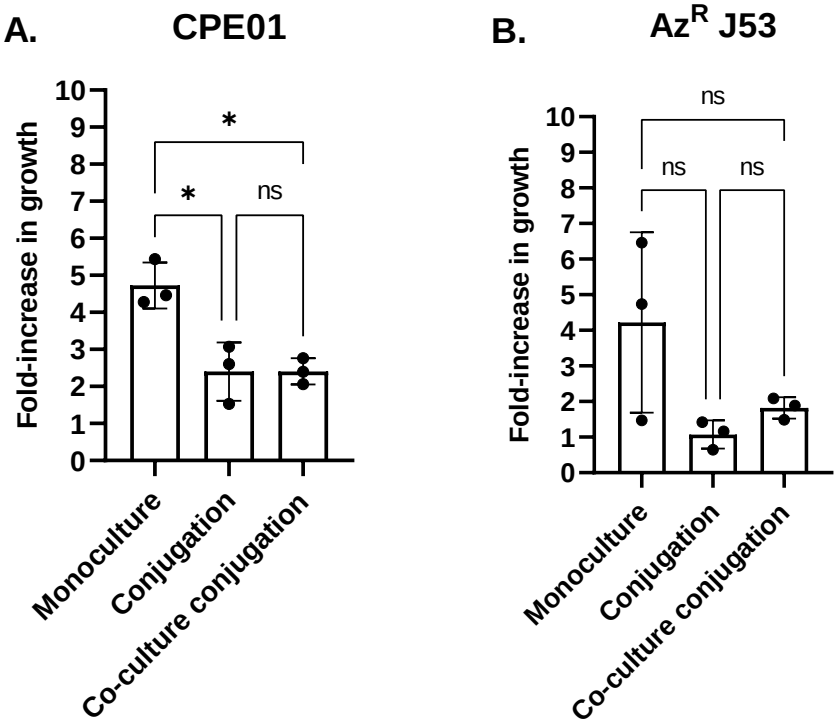

Figure 3.12: Growth assays of CPE01 (**A.**) and Az^R J53 (**B.**) in conjugations with and without *B fragilis* co-culture. Fold-increase in growth was calculated using viable counts at zero and four hour timepoints. Growth of each strain in monoculture from Figure 3.11 included for reference. Each data point represents one experiment, each consisting of three biological replicates, unless specified otherwise. Error bars represent one standard deviation above and below the mean. * = P $\leq$ 0.05; ns = not significant, when analysed with Dunnett's T3 multiple comparisons test.

Analysis was done using Dunnett's T3 multiple comparison test, as this variation of an ANOVA test considers variations in standard deviations. Analysis showed that co-culture with *B. fragilis* had no effect on the growth of either strain in the conjugation experiments (CPE01 P > 0.9999; Az^R J53 P = 0.1448; Figure 3.12). Figure 3.12 shows however, that

presence of Az^R J53 significantly reduced the growth rate of CPE01 by almost half when grown together (P = 0.0403).

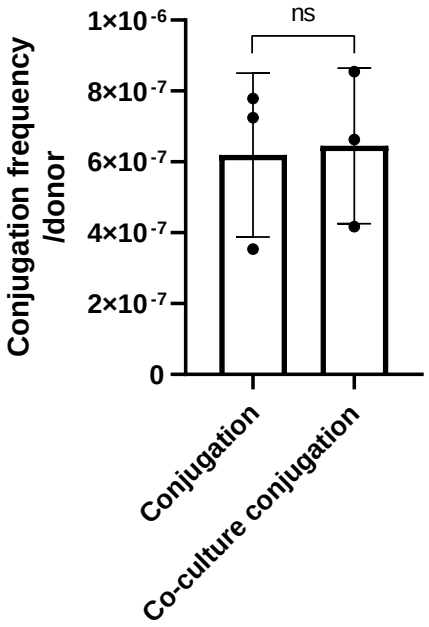

Figure 3.13: Conjugation frequency per donor of pCPE01_2 between CPE01 and Az^R J53 with and without co-culture with *B. fragilis*. Each data point represents one experiment, each consisting of three biological replicates, unless specified otherwise. Error bars represent one standard deviation above and below the mean. ns = not significant, when analysed with Welch's t-test.

Conjugations performed in the presence of *B. fragilis* showed no difference in conjugation frequency to those without (Figure 3.13; P = 0.8950 using Welch's t-test).

Two biological replicates- one from an experiment in each condition- were omitted due to discrepancies in UTI results. Unless all tested colonies of the small morphology presented as purple (signifying *E. coli*), the final number of transconjugants per plate was not confirmed. All putative transconjugants were confirmed by PCR.

No Az^R J53 colonies grew on doripenem-containing mutant selection plates, indicating that the mutation rate for this strain was consistently below the limit of detection. However CPE01, when plated neat onto 100 μg/ml sodium azide, grew between zero and 11 colonies

across all biological replicates. The average mutation frequency for each experiment (assuming a value of zero for those below the limit of detection) ranged between $6.6\text{x}10^{-9}$ and $2.27\text{x}10^{-7}$ per CFU of CPE01. Due to the confirmation of *E. coli* transconjugants using UTI agar, these mutations were not considered to have confounded the transconjugant counts, and colonies confirmed as mutant donors from UTI replica plating were excluded from the putative transconjugant counts. In conclusion, the conjugation frequencies resulting from these experiments were calculated with the confidence there was a negligible confounding effect from colonies of mutants.

3.5 Discussion and future work

Unfortunately, the first hypothesis made in Section 3.1.6 was not fully investigated due to difficulties in generating a clinically relevant donor strain carrying the plasmid pKpQIL-*gfp-aph* (Section 3.2). Nevertheless, changes were made to the experimental design to investigate the two latter hypotheses.

Statistical analysis of the results as shown suggested to reject the two latter hypotheses made in Section 3.1.6: that co-culture with *B. fragilis* did not affect the conjugation frequency of pCPE01_2 between CPE01 and Az^R J53 (Figure 3.13), and that co-culture with *B. fragilis* did not affect the growth rate of CPE01 and Az^R J53 (Figures 3.11 and 3.12). However, due to time constraints (see COVID-19 Impact Statement) and the inability to have repeated or optimised certain experiments, the stringency of these results was compromised. The following changes considered would have been made to these experiments, had time permitted.

3.5.1 Optimising the experimental design

A limitation of the experimental design, for the growth of both CPE01 and Az^R J53 with and without *B. fragilis* co-culture, which likely contributed to the wide range of growth results

for Az^R J53 was that only one set of viable counts was taken at each time point for each biological replicate. As a result, some large variation in counts was observed whereby counts for a select few biological replicates of Az^R J53 implied that the number of viable CFUs in the experiment had decreased over the four hours. The reasons for this were unknown, and more experimental replicates would have been necessary to confirm these observations as anomalous. As a result, there was a large standard deviation for the data points of Az^R J53 growth (Figure 3.11), which may have masked any potential effects of co-culture on Az^R J53 growth. Finally, it was difficult to obtain the true ingoing and outgoing donor:recipient ratios due to the unreliability of single viable counts. To circumvent these issues, three sets of viable counts could have been done for each biological replicate, as recommended by Rodriguez-Grande and Fernandez-Lopez (2020). This would have inevitably lengthened the viable counts plating step, causing the cells to spend significantly longer at room temperature, where they could still replicate and result in artificially high viable counts. To avoid this, the dilutions of each replicate could have been kept on ice throughout the plating process to prevent this further replication from confounding the results.

The final densities of *B. fragilis* over all co-culture experiments were within a range of $1x10^8$ to $2.1x10^9$, which was consistently lower than those used by J. D. Anderson (1975), who did not specify how the desired densities for co-culture were achieved. For this project, OD_{600} was measured prior to each experiment and compared with the viable counts (Figure 3.14), of which a simple linear regression analysis revealed a direct correlation ($R^2 = 0.6587$) with a significantly non-zero slope ($P < 0.0001$). This would have ideally been done prior to performing the co-culture and conjugation experiments to calculate the target OD_{600} for a particular CFU/ml, but due to a shortage of time, this validation was unable to take place.

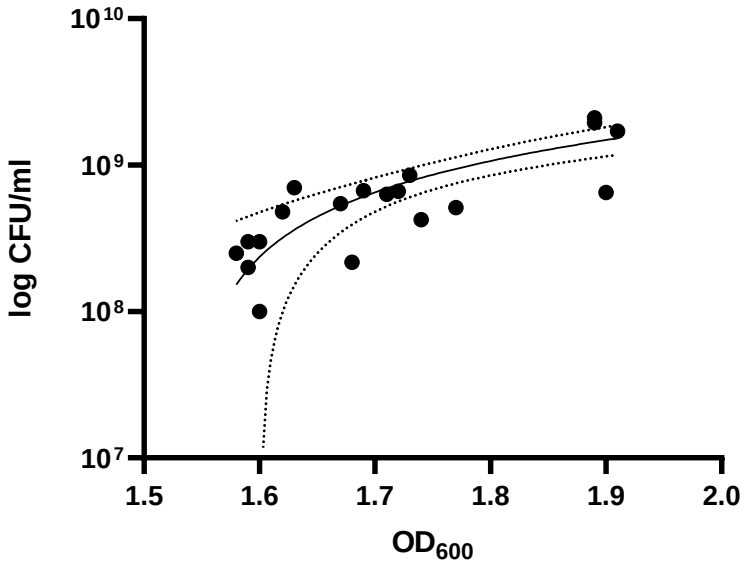

Figure 3.14: Preliminary relationship between *B. fragilis* OD_{600} and density of viable cells (CFU/ml). Each plotted point is a single biological replicate of a 40 hour culture of *B. fragilis* used in a co-culture experiment. Filled line represents the fitted line of regression (R^2 = 0.6587), with the dashed lines as 95% confidence intervals.

The relationship observed in Figure 3.14 indicated that the OD_{600} of *B. fragilis* was a reasonably good predictor of CFU/ml. Subsequently, a target OD_{600} for a target CFU/ml value could have been established experimentally by testing the OD_{600} and CFU/ml of various concentrations of 40 hour culture, such as resuspension in 20%, 10% and 5% volume after centrifuging. The target OD_{600} for Anderson's CFU/ml ranges of 3-5x10^9 and 2x10^{10} could have been established using linear regression, as demonstrated in Figure 3.14.

Determining a near-physiological target density would be difficult, however. Several studies have reported on the *in situ* density of the species *B. fragilis* in the human gut microbiome, though are difficult to compare due to different methods used. Zitomersky et al. (2011) found a density of culturable members of the order *Bacteroidales* in the range of 5x10^8 and 8x10^8 per gram of wet faeces, alluding to the density of *B. fragilis* being lower than this, and Moore and Holdeman (1974) observed a *B. fragilis* density of 2.98x10^9 per gram of dry faeces. The

densities used by J. D. Anderson (1975) were likely therefore higher than would be physiologically realistic, though the difference could not be quantified since the volume of 1 ml of media does not equate to one gram of faeces, wet or dry. Since the investigation of this project focused on the effect of individual strains on conjugation rather than on the effect of the density of these strains, further experiments would continue to use 40 hour stationary phase cultures.

Finally, additional equipment would be used to optimise these experiments. Strain handling and incubation would ideally have taken place inside of a temperature-controlled anaerobic cabinet at 37°C. Smaller items of equipment such as a microcentrifuge and vortex could have been placed within the cabinet, so that most of the strain preparation could take place in anaerobic conditions. Only samples to be analysed for OD_{600} would need to be removed from the cabinet. Incubation of co-cultures would still be done in universal tubes due to the need for vortexing after four hours. In addition to the anaerobic cabinet, a plate reader with the ability to maintain an anaerobic environment would have been beneficial in supplementing the growth data by producing growth kinetics curves for each strain. In this way, the donor and recipient OD_{600} could be separately monitored continuously over time to establish in more detail how well the strains grow over a four hour incubation period, and better understand why the strains were observed to grow at different rates under the experimental conditions.

3.5.2 Further investigations

L. casei strain Shirota

Following the optimisation of the experimental design for testing the effect of *B. fragilis* co-culture on the growth of and conjugation between CPE01 and Az^R J53, this project aimed to repeat the experiments with *L. casei* strain Shirota (Douillard et al., 2013). *L. casei*, a

probiotic, was hypothesised to have a significant effect on the growth of the strains. Although these combinations of strains had not yet been tested in the literature, this hypothesis was based on the observations in many studies of growth inhibition of *Enterobacteriaceae* by Lactobacilli, a subset of which are discussed here (Ogawa et al., 2001; Fayol-Messaoudi et al., 2005; C.-C. Chen et al., 2019).

The growth inhibition of *Enterobacteriaceae* by Lactobacilli is generally accepted to come as a result of the lowering of the environmental pH by the secretion of SCFAs such as lactic acid (Sinha, 1986; Alakomi et al., 2000). Lactic acid in its undissociated form can diffuse across the membranes of Gram-negative bacteria (Eklund, 1983), resulting in acidification of the cytosol, dissipation of the membrane potential and subsequent failure of membrane-based processes. Alakomi et al. (2000) also reported an increase in membrane permeablisation of *E. coli* and *S. enterica* in the presence of lactic acid, more so than hydrochloric acid at the same pH. C.-C. Chen et al. (2019) reported that the inhibitory effect of cell-free supernatant (CFS) of various Lactobacilli on a range of CRE disappeared when neutralised to pH 7.0 using sodium hydroxide, suggesting that presence of these acids was sufficient for growth inhibition. However, other investigations have revealed uncharacterised pH-independent factors associated with Lactobacilli. For instance, Fayol-Messaoudi et al. (2005) noticed a significant decrease in the inhibitory activity of CFS of various Lactobacilli (including *L. casei* strain Shirota) on *S. enterica* after one day of CFS storage at 4°C, indicating the presence of an unstable inhibitory factor in the CFS.

Much of the research into the inhibitory effects of Lactobacilli on opportunistic pathogens has focused on these secreted factors, using CFS from centrifuged monocultures, which could not be fully relied on for hypothesis design for this co-culture project using pelleted cells as these are different materials. Ogawa et al. (2001) used a centrifuged pellet of *L. casei* strain Shirota (among other species of *Lactobacillus*) at a final density of 10^9 CFU/ml to set up a co-culture with *E. coli* O157:H7, a shiga-like toxin-producing foodborne pathogen. The authors

monitored the CFU/ml of *E. coli*, pH, and concentration of both total and undissociated lactic acid in the media at two-hour intervals for 14 hours. After four hours, the time point of interest for this project, concentration of undissociated lactic acid in the *L. casei* co-culture had risen from 0 to just over 60 mM. Viable counts of *E. coli* had fallen by less than 10-fold over four hours, though growth inhibition appeared to increase over time with a $>10^5$-fold decrease in viable counts after 10 hours. pH decreased dramatically from between 6-6.5 to 3.5-4 at two hours, then stabilising around pH 3.5 over the remainder of the experiment.

This study by Ogawa et al. (2001) demonstrated how quickly the low pH conditions of CFS could be established using pelleted culture, which had important implications for the design of this project. Despite the sharp increase in concentration of undissociated lactic acid and the decrease in pH in just four hours, *E. coli* viable counts were relatively stable. It was clear however, that the *E. coli* were not growing well in these conditions, as there was no recorded increase in CFU/ml, even initially. Based on these observations, it was hypothesised that *L. casei* would have a significant effect on the growth of CPE01 and Az^R J53, and that this would be important to characterise in the case that co-culture with *L. casei* resulted in a significant decrease in conjugation frequency. This was also hypothesised to be the case, based on observations by Headd and S. A. Bradford (2020) that *E. coli* in stationary phase conjugated an IncF plasmid significantly less frequently than when in exponential phase.

The viability of *L. casei* in BHIS was checked, by incubating three biological replicate colonies anaerobically for 40h. OD_{600} was recorded, with an average of 1.29 over the three replicates. This indicated good growth under these conditions, however there was insufficient time to perform viable counts or to repeat this.

Future directions

Optimisation of the anaerobic growth assay and co-culture protocols as discussed in Section 3.5.1 would result in a simple but robust model of conjugation of AMR plasmids in the gut

microbiome, whereby conjugation of an AMR plasmid between a clinically relevant pathogen and *E. coli* recipient could be easily measured. This *in vitro* model could continue to be used to investigate further aspects of the microbiome on the conjugation of this AMR plasmid. By just ensuring that each component strain was concentrated or diluted to the desired final density, more strains of the human microbiota, combinations of strains, killed cells, monoculture CFS or whole-microbiome CFS could be investigated using this system.

Additionally, the investigation into each strain could be taken further. For example, the preliminary results from this project suggest that *B. fragilis* may have little effect on the growth and conjugation of pCPE01_2, but plasmid persistence and evolution could also be assessed. There is evidence that AMR plasmid persistence in the absence of antibiotic pressure can be higher in *in vivo* mouse gut conditions than *in vitro* (Gumpert et al., 2017). The mechanisms behind this phenomenon have not yet been elucidated however, and little to no further research has been published to date. The effect of inter-strain competition on plasmid persistence could be investigated as a part of this, using simple passaging experiments in the same co-culture conditions as used in this project. Colonies of transconjugants could be grown in broth containing doripenem and sodium azide, then washed and transferred to fresh antibiotic-free BHIS broth, with or without co-culture. At selected intervals, aliquots of this liquid culture could be made, diluted and plated out onto both double selective agar and agar containing just sodium azide, to monitor both the overall population of Az^R J53, and the proportion still containing the doripenem resistance-encoding plasmid.

A key limitation of this model is that it is highly reductionist, and although care was taken in the experimental design to mimic aspects of the gut microbiome environment (e.g. anaerobic conditions, temperature), these were far from the complexity of conditions in the human gut. This inevitably limits the translatability of the results acquired using such experiments. These conditions and the use of established *in vitro* models to incorporate them are described in detail in Section 4.3. Nevertheless, the robustness of this reductionist model provides a

solid foundation of understanding of the behaviour of these strains and their interactions with one another, inviting and supporting further investigation into this system in future.

4. Methods and models for investigating conjugation

4.1 Introduction

Chapter 3 investigated the impact of a factor of interest, bacterial co-culture, on the rate of conjugation of an AMR plasmid between members of the human gut microbiome. A key limitation identified in the discussion was the reductionist nature of such *in vitro* experiments, as they cannot mimic the highly complex and dynamic nature of the gut microbiome, compromising the translatability of the results from such experiments. This following chapter aims to address this particular limitation, by exploring published alternative *in vitro* experimental models featuring higher degrees of complexity, which could be considered for use in future observations and experiments investigating conjugation of AMR plasmids. Instances of the use of *in vitro* models of the gut to investigate rates of conjugation were found to be few, but the potential for such models to be more widely incorporated into this field of research is discussed.

In addition to this literature review, the experimental work detailed in this chapter presents an example of such an investigation which could be replicated in the setting of an *in vitro* model. This work contributed to an ongoing investigation into the discovery of potential new anti-plasmid compounds, here determining the effect of dosage of natural extracts on conjugation frequency.

4.1.1 Investigating potential anti-plasmid extracts

In Section 1.2.2, various methods of targeting plasmids and their conjugation *in vivo* were discussed, in the context of developing new therapies to reduce the conjugation of AMR plasmids and the spread of ARGs. These included administration of plasmid-curing or conjugation-inhibiting compounds, exploiting plasmid incompatibility, phage and CRISPR/Cas systems, as reviewed by Buckner et al. (2018a). As part of an ongoing investigation into the anti-plasmid properties of a range of extracts from botanical sources, this project aimed to characterise the effects *in vitro* of two particular natural extracts: turmeric and black pepper. Pure extracts were kindly provided by Prof. S. Gibbons, University College London, and diluted in DMSO to make stock solutions.

In previous preliminary experiments using *E. coli* ST131 and *K. pneumoniae* Ecl8 in the dual-fluorescence system and experimental setup described in Sections 3.1.3 and 2.2.7, presence in incubation media of both extracts at 0.25 mg/ml had been observed to decrease the number of observed transconjugant bacteria by >50% with respect to 0 mg/ml ($P < 0.01$). These decreases were observed in both *E. coli*/pCT and *K. pneumoniae*/pKpQIL systems (J. Rodriguez, unpublished data).

These preliminary experiments appeared promising in the search for compounds with inhibitory effects on plasmid conjugation. Subsequently, further experiments were performed on some of the constituent compounds found in these extracts. Preliminary results, as well as extract background, are detailed below.

Turmeric

Turmeric, the common name for the root of the plant *Curcuma longa*, has been used both as an aromatic spice and medicinal agent for centuries (Meng et al., 2018). It is well known for its use in traditional medicine, in treating a wide range of conditions including coughs, diabetic

wounds, hepatic and cardiovascular disorders. More recently, turmeric and its components have been of interest in research into novel anti-cancer agents (Meng et al., 2018).

Over 235 component phytochemicals have been identified in turmeric (Li, 2011). Of these the curcuminoids, predominantly curcumin which makes up 3% of pure turmeric powder by weight (Tayyem et al., 2006), have been the most extensively studied, and have shown significant efficacy in clinical studies investigating their anti-inflammatory, antioxidant and anti-cancer properties (Meng et al., 2018). However, many of the non-curcuminoid phytochemicals in turmeric have also demonstrated promising anti-cancer activity in human cancer cell lines (A. Nair et al., 2019). Whether these compounds act additively or synergistically, or even negatively, in whole turmeric extract is unknown.

Despite its promising therapeutic properties, curcumin has very limited bioavailability when ingested, which has been repeatedly demonstrated by little to no detection in blood plasma in human participants (Shoba et al., 1998; Ireson et al., 2002; Garcea et al., 2005). It has also been demonstrated to be metabolised within the gut, primarily into curcumin sulfate and curcumin glucuronide, found by *in vitro* incubation with cytosol and microsomes originating from intestinal tissue (Ireson et al., 2002). Garcea et al. (2005) investigated the levels of curcumin and its metabolites in colorectal tissue biopsies and blood plasma in colorectal cancer patients, in response to various oral doses of curcumin. The highest dose, 3.6g daily for 7 days, resulted in curcumin levels in non-malignant tissue of 12.7 $\pm$ 5.7 nmol/g (n = 4), with plasma levels below 3 nmol/L (detected by mass spectrometry). These data supported the general observation that orally administered curcumin has low systemic availability, but remains locally in the gut. Curcumin sulfates and glucuronides were also present in patients on higher doses, but with low prevalence of approximately 1 pmol/g (HPLC), suggesting that although curcumin metabolism occurs in the intestine, the rates of this are relatively low. In the context of targeting AMR plasmids in the human gut, these findings are promising, as high concentrations of curcumin can be maintained without significant depletion by absorp-

tion through the intestinal wall.

Several studies have demonstrated some antimicrobial activity in curcumin. Tyagi et al. (2015) performed killing assays on a range of Gram-positive and Gram-negative bacteria including *E. coli*, and found that *E. coli* reduced in viability by 40% after 120 minutes of incubation in 25 μM (0.00921 mg/ml) curcumin, and were undetectable at 100 μM (0.03684 mg/ml). The mechanism of action was thought to be membrane permeablisation, due to significantly increased propium iodide uptake in an assay. Marathe et al. (2016) demonstrated damage of and binding to the flagella in *S. enterica*: flagella were observed to shorten and decrease in number with no change in gene or protein expression. A fluorescence binding assay demonstrated binding of curcumin to the flagella (Marathe et al., 2016).

Little to no research has been published on the effects of whole turmeric extract or curcumin on the transfer of plasmid DNA. However, Ahsan and Hadi (1998) demonstrated that in the presence of copper(II), curcumin cleaved supercoiled pBR322 DNA into open circular DNA by generating reactive oxygen species (ROS), and therefore exhibiting pro-oxidant activity. Since DNA damage is a mechanism used by many anti-plasmid compounds (Buckner et al., 2018a), this activity may rationalise the testing of turmeric extract for anti-plasmid activity.

Taken together, the preliminary data demonstrating that turmeric extract decreased transconjugant counts in a dual-fluorescence assay (J. Rodriguez, unpublished data), and the observations that curcumin concentrates in the intestinal tract with poor absorbance and can induce DNA damage, make turmeric an attractive agent for plasmid targeting in the gut microbiome. Evidence of the antimicrobial activity of curcumin would need to be considered in such investigations, as well as the possibility of other active phytochemicals in whole turmeric extract that may exert additive or synergistic effects.

Black pepper

Black pepper, the dried unripened fruit of the *Piper nigrum* plant, is also a common culinary spice with a long history of use in traditional medicine (Butt et al., 2013). Similarly to turmeric, it has a complex phytochemical composition, of which one predominant compound has been extensively studied: the alkaloid piperine. Piperine constitutes approximately 2% of black pepper (Yuanzhe Wang et al., 2020), but this is variable, as ranges of values up to 9% have been reported (Gorgani et al., 2017). In recent investigations into the health benefits of piperine, this compound has demonstrated anti-inflammatory, anti-cancer and antioxidant properties (Y. Liu et al., 2010; Zarai et al., 2013; Gorgani et al., 2017). It has also been reported to have some antimicrobial activity, with MICs of 625 μg/ml of purified piperine found for *E. coli* and *K. pneumoniae* using an agar diffusion assay (Zarai et al., 2013).

Piperine has much greater bioavailability than curcumin, with about 63% absorption measured in rat intestines *in vitro* and no evidence of metabolic changes to the compound in this process (Suresh and Srinivasan, 2007). It has also been found to increase the bioavailability of other nutrients and compounds, including vitamins such as β-carotene (Badmaev et al., 1999), minerals such as iron (Fernández-Lázaro et al., 2020), certain orally-administered drugs (Han, 2011) and even curcumin (Shoba et al., 1998). Piperine's properties as a bioavailability enhancer has led it to be patented and commercialised as the supplement BioPerine® (Badmaev et al., 1999; Fernández-Lázaro et al., 2020). Finally, it likely contributes to black pepper's use in traditional medicine as a treatment in gastrointestinal disorders (Butt et al., 2013), for example an investigation into rodent models of constipation and diarrhoea found that both piperine and whole black pepper extract had a positive effect on both gastrointestinal conditions (Mehmood and Gilani, 2010).

Again as with turmeric, little to no research has been published investigating the effects of black pepper on the transmission of bacterial plasmids. However, ethanolic extraction of

whole black pepper has been demonstrated to exhibit DNA-damaging activity through the generation of ROS (de Souza Grinevicius et al., 2016). This investigation was performed with human breast and colon carcinoma cells in the context of cancer treatment research, but this activity could present a mechanism of action for any effect of black pepper extract on bacterial conjugation. With preliminary data suggesting that whole black pepper extract has anti-plasmid activity (J. Rodriguez, unpublished data), it is worth investigating further. It would be important to take into consideration the complex phytochemical composition of the whole extract, and that components may exert additive or synergistic effects. As with turmeric, potential antimicrobial activity of components of the extract would also need to be considered in such an investigation.

4.1.2 Exploring more complex *in vitro* models

Buckner et al. (2018a) stated that very little *in vivo* research has been undertaken in the field of plasmid curing, and that this was urgently needed. More recently, anti-plasmid work has expanded to incorporate more *in vivo* approaches (Bharathan et al., 2019; Lazdins et al., 2020), as explored in Section 1.2.2, but there is indeed still an urgent need for anti-plasmid strategies to be tested in more complex models to explore their viability as future treatment options. Especially in the context of the human gut microbiome, complex and dynamic *in vivo* environments differ greatly from reductionist *in vitro* laboratory experiments, compromising the translatability of results achieved from the latter. Progress in developing novel anti-plasmid strategies can only be made by testing in experimental contexts that better mirror how they would interact with the host and microbiome *in situ*.

In vitro models of the human intestine have been increasingly developed over the past few decades, and provide an alternative to *in vivo* approaches. A critical comparison of these approaches is elaborated on in Section 4.3.3. In brief, a key rationale for the use of *in vitro* models is that they are attractive for both the observation and manipulation of plasmid

dynamics, since they are easier to both control and access than *in vivo* systems. The literature review incorporated into this chapter explores a range of existing models with the potential for use in investigating plasmid dynamics, as well as a review of how plasmid dynamics can be observed *in situ* in the human gut microbiome.

4.1.3 Hypotheses

The aims of this chapter were to contribute to ongoing anti-plasmid compound discovery work, and to explore available intestinal models that could potentially be incorporated into this work to increase its translatability. This chapter addresses research question 2 (Section 1.5.2).

The specific hypotheses devised in this chapter were as follows:

- That incubation with turmeric and black pepper extracts reduces the conjugation of pCT and pKpQIL in a dose-dependent manner.
- That any observed effects do not result from compromised cell growth or viability in the presence of these extracts.
- That these dual-fluorescence experiments can be replicated in an *in vitro* model of the human gut, by modifying the incubation step of the experimental design, to provide more translatable data on the impact of natural extracts on bacterial conjugation in the human gut microbiome.

4.2 Results: natural extract experiments

4.2.1 Initial characterisation of strains

In order to use the dual-fluorescence system, two bacterial conjugation models were used, both using the GFP-mCherry combination described in Section 3.1.3. The previously described *K. pneumoniae* H235 containing plasmid pKpQIL-*gpf-aph* was paired with H234, a plasmid-free *K. pneumoniae* chromosomally tagged with *mcherry*, otherwise isogenic with H235. Similarly, an *E. coli* ST131 dual-fluorescence system was used: I1068 containing a *gfp-aph*-tagged pCT plasmid was paired with the plasmid-free I1069 encoding a chromosomal *mcherry* (Table 2.2).

The four strains' identities were confirmed, using colony PCR and plasmid backbone-specific primers (Table 2.3) to check for presence of pKpQIL and pCT in the correct strains (Figure 4.1).

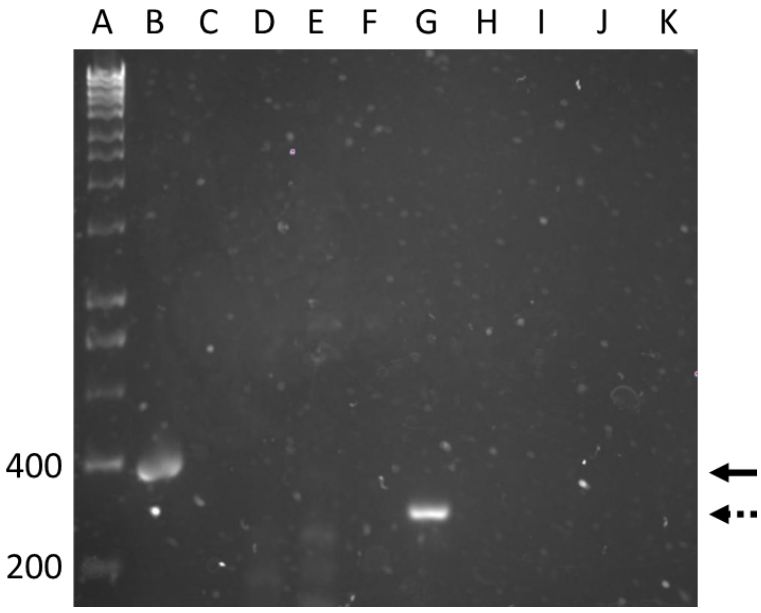

Figure 4.1: Colony PCR of H235 (*K. pneumoniae* Ecl8 with plasmid pKpQIL-*gfp-aph*)and H234 (*K. pneumoniae* Ecl8 with chromosomal *mcherry*) for pKpQIL, and of I1068 (*E. coli* ST131 with plasmid pCT-*gfp-aph*) and I1069 (*E. coli* ST131 with chromosomal *mcherry*) for pCT.
Lanes A: 1kb hyperladder, B: H235, C: H234, D: I1068, E: I1069, F: PCR negative control (water), G: I1068, H: I1069, I: H235, J: H234, K: PCR negative control (water). Samples in lanes B-F were tested using pKpQIL-specific primers, and G-K with pCT-specific primers (Table 2.3). Appropriate hyperladder band sizes (in base pairs) are indicated on the left. pKpQIL band of interest has a size of 383bp and is identified with a solid arrow. pCT band of interest is 290bp and is identified with a dashed arrow.

4.2.2 Growth and viability

In order to rule out any potentially confounding bactericidal or bacteriostatic effects of the extracts that could reduce apparent conjugation frequency by compromising bacterial growth or viability, MIC testing (Section 2.2.4) and growth kinetic analyses (Section 2.2.8) were planned.

The effect on bacterial viability of turmeric and black pepper extract concentrations of up to 1024μg/ml were tested by broth microdilution MIC, along with the equivalent concentrations of DMSO solvent as a control. It was noted that, at concentrations of 512μg/ml

and above, both extracts precipitated and rendered the wells cloudy. Despite this, growth was clearly observed at the bottom of each well, giving all four strains MIC values of >1024μg/ml for both extracts.

4.2.3 Plasmid conjugation

The primary objective of this investigation was to characterise any dose-dependent effect that presence of these extracts in incubation medium may have on plasmid conjugation, to assess their potential as anti-conjugation agents. Welch's t test was chosen to analyse the significance of effect size in all cases, as this test considered variation in both standard deviation and sample size. Each condition was compared to the LB control, with no extract present. All conditions were repeated using the concentration equivalent of DMSO to identify any potential confounding effect of the solvent (Appendix D).

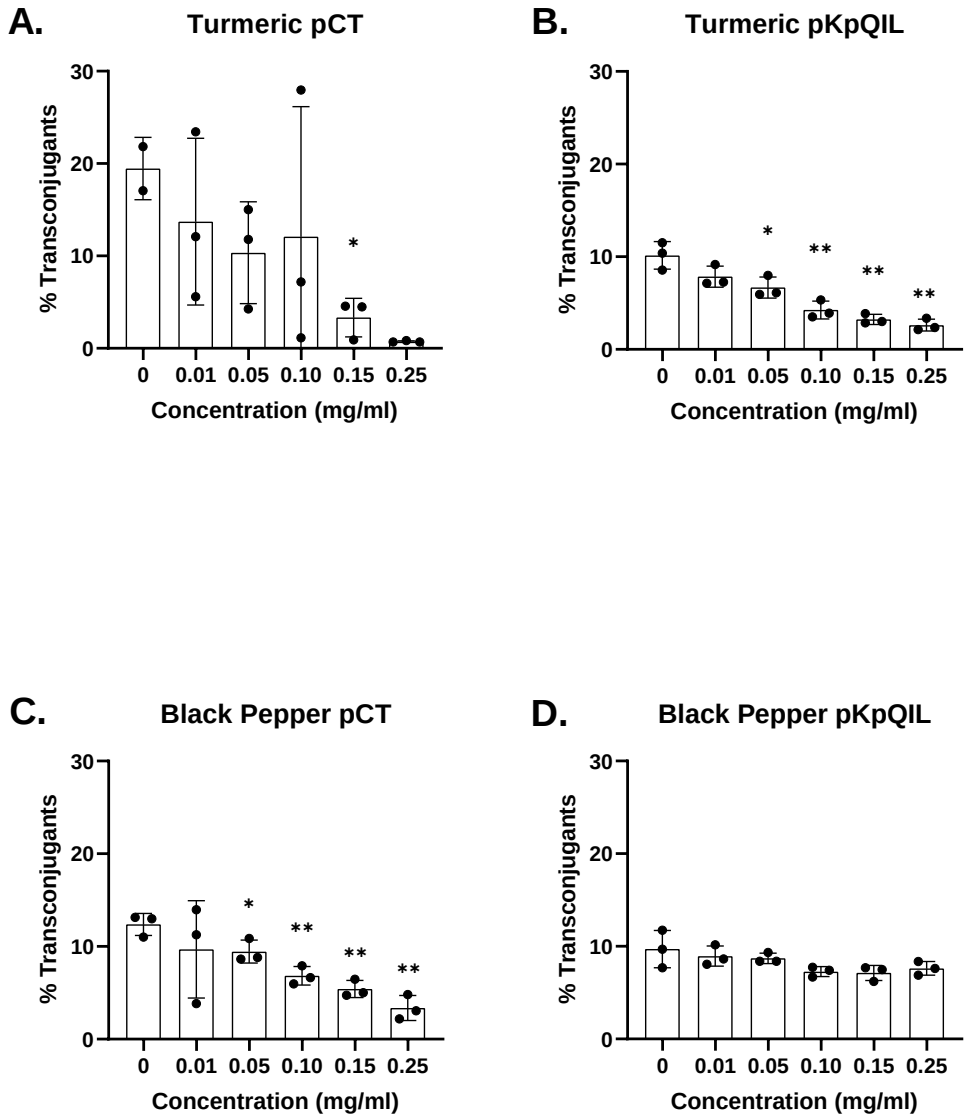

Figure 4.2: Effect of increasing concentrations of turmeric and black pepper on conjugation of pCT and pKpQIL. **A.** Turmeric extract tested on pCT. **B.** Turmeric extract tested on pKpQIL. **C.** Black pepper extract tested on pCT. **D.** Black pepper extract tested on pKpQIL. Each data point represents one experiment with four biological repeats. Error bars represent one standard deviation above and below the mean. * = $P \leq 0.05$; ** = $P \leq 0.01$, when the difference to the control (0 mg/ml) was calculated with Welch's t-test.

Turmeric extract exerted a significant effect on the conjugation frequency of both plasmids (Figures 4.2A; 4.2B). There was a greater effect size on pCT than pKpQIL: the per-

centage of gated events that were consistent with transconjugants dropped from 19.46% at 0 mg/ml to 0.73% at 0.25 mg/ml for pCT (Figure 4.2A), and from 10.15% at 0 mg/ml to 2.62% at 0.25 mg/ml (Figure 4.2B). Despite a greater effect size, the effect of 0.25 mg/ml turmeric on pCT was statistically insignificant (P = 0.081) whereas pKpQIL was (P = 0.0058) for this concentration. This was likely due to having only two data points for the pCT control, as well as the higher standard deviations across all concentrations tested on this plasmid, and these features being accounted for by Welch's t test. Additionally, the DMSO solvent may have had a confounding effect on 0.25 mg/ml turmeric, as the DMSO equivalent alone significantly reduced conjugation (P = 0.0391; Figure D.1B, Appendix D). Otherwise, the effect of turmeric extract on pKpQIL appeared to be dose-dependent, as the effect size increased with concentration. This relationship was less evident with pCT. Given the high standard deviations observed in Figure 4.2A, it is possible that some of the data points from the turmeric pCT experiments were outliers. However not enough experimental replicates were performed to confirm this using Grubb's or ROUT tests. Further experiments testing the effect of turmeric extract on pCT conjugation would need to be performed to identify outliers, if any.

Black pepper extract appeared to affect the conjugation of pCT in a dose-dependent manner (Figure 4.2C), with effect size increasing with concentration of extract and statistical significance of the effect size for all concentrations above 0.05 mg/ml. Contrastingly, there appeared to be no significant effect on the conjugation of pKpQIL at any concentration (Figure 4.2D).

DMSO alone (Appendix D) appeared to have no significant effect on the conjugation of pCT, but a slight decrease in conjugation of pKpQIL was observed with increasing concentrations (Figures D.1B and D). These decreases were largely insignificant, with the exception of the DMSO equivalent of 0.25 mg/ml turmeric extract.

4.2.4 Fluorescence interference

Data corresponding to the number of non-fluorescent events were also collected, to identify any potential changes in background noise. These data indicated the percentage of the 10,000 collected events that were not considered by flow cytometry to contain GFP or mCherry, and that therefore constituted noise.

Turmeric extract had a dose-dependent effect on the percentage of non-fluorescent events captured in experiments performed with both plasmids (Figures 4.3A; 4.3B), indicated by the increase in effect size with concentration. The non-fluorescence increased at a similar rate for both sets of experiments, reaching 69.06% (pCT) and 62.68% (pKpQIL) at 0.25 mg/ml turmeric extract. Similarly to Figure 4.2A, the significance of the differences in non-fluorescence shown in Figure 4.3A are relatively low, likely due to the inconsistent sample sizes and high standard deviations.

Black pepper also appeared to have a dose-dependent effect on the percentage of gated non-fluorescence, but this effect was only observed in pCT conjugation experiments (Figure 4.3C). There was no difference the detection of non-fluorescent events in pKpQIL conjugation experiments (Figure 4.3D).

Turmeric extract had a similar effect size on non-fluorescence in both experiments, but black pepper did not. This result was interesting as it implied that there may be a biological determinant contributing to non-fluorescence in the presence of black pepper extract. Possible pCT plasmid loss from the I1068 donor strain could have resulted in an increase in perceived noise that may have been plasmid-free I1068 cells. If this was the case, it could have been the result of either lower plasmid stability of pCT compared with pKpQIL in the presence of black pepper extract, or that the incubation time for pCT experiments was longer (24 hours for pCT; 6 hours for pKpQIL) allowing for more time for plasmid loss. To test this, I1068 could be passaged in LB broth alone and with working concentrations of extracts to assess

the relative persistence of pCT and pKpQIL in these different conditions. This would also be performed using flow cytometry, using a similar setup to the plasmid transmission assay but instead quantifying total fluorescent events at defined time points. If the percentage of fluorescence events collected from a culture of I1068 was observed to decrease over 24 hours, this would suggest plasmid loss within this time window.

DMSO alone (Appendix D) did not have a significant overall confounding effect on non-fluorescent events. A single significant condition was observed, with DMSO at the equivalent concentration of 0.05 mg/ml black pepper reducing the percentage of non-fluorescent events (Figure D.2C), though since this was a decrease, it was not considered a confounding factor in the significant increases observed in Figure 4.3C.

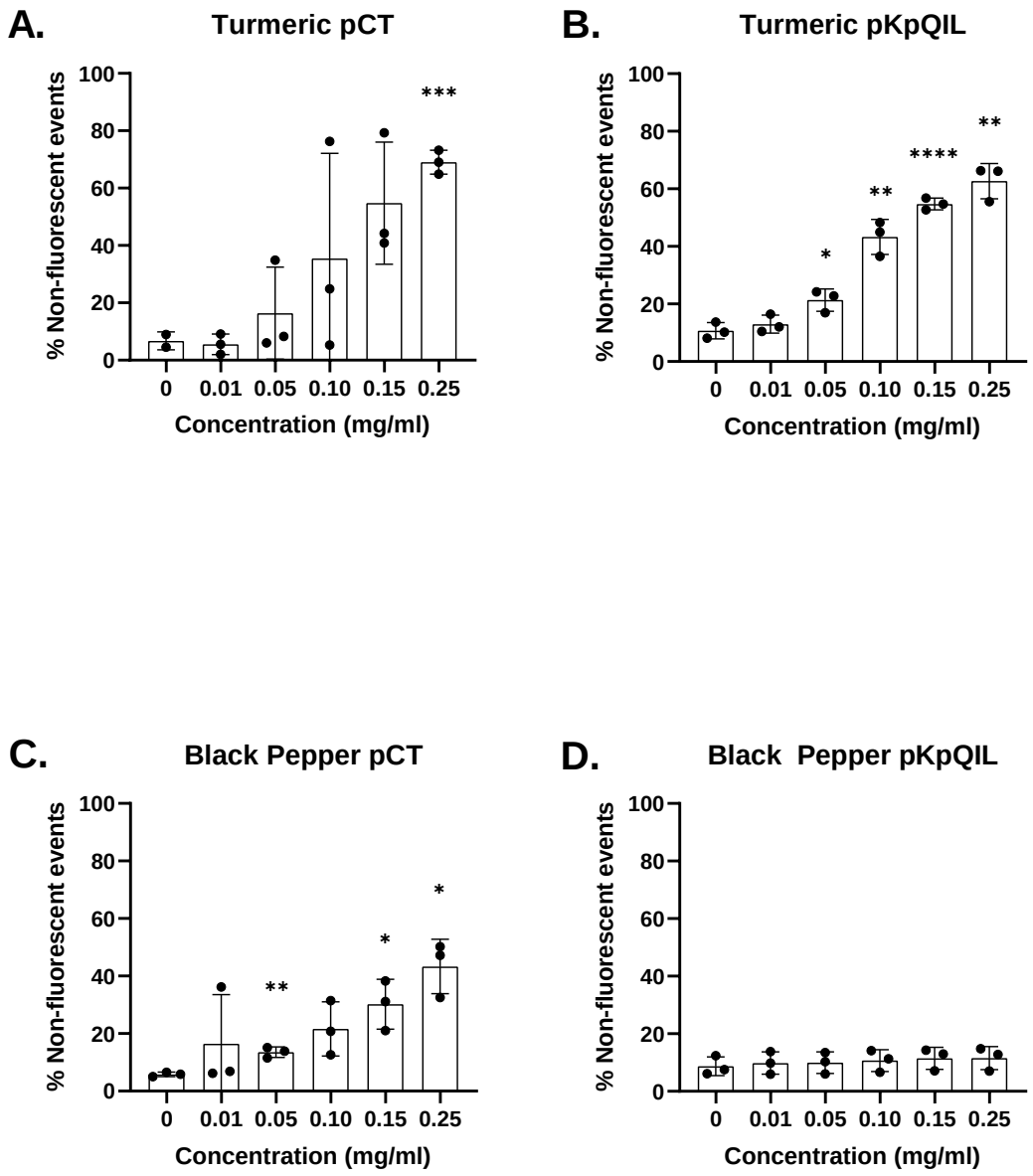

Figure 4.3: Effect of increasing concentrations of turmeric and black pepper on non-fluorescent events detected by flow cytometry. **A.** Turmeric extract tested on pCT. **B.** Turmeric extract tested on pKpQIL. **C.** Black pepper extract tested on pCT. **D.** Black pepper extract tested on pKpQIL. Each data point represents one experiment with four biological repeats. Error bars represent one standard deviation above and below the mean. * = $P \leq 0.05$; ** = $P \leq 0.01$; *** = $P \leq 0.001$; **** = $P \leq 0.0001$, when the difference to the control (0 mg/ml) was calculated with Welch's t-test.

Of the 10,000 events collected in each control experiment (0 mg/ml extract), a low but

consistent number of these were observed to be non-fluorescent, indicated by the non-zero percentage of non-fluorescent events in the absence of extract (Figure 4.3). This level at 0 mg/ml was interpreted to be the background noise of the assay. However, significant increases in non-fluorescent events correlating with extract concentration in all experiments except black pepper with pKpQIL were observed, which could compromise the sensitivity of the assay at higher extract concentrations. Here, transconjugants would have been detected from a much smaller number of total fluorescent events than at lower concentrations.

Additional controls were added to the experimental design in light of this: the donor alone and recipient alone were incubated with 0.25 mg/ml extract to investigate the impact of the extract on the emission of each fluorophore (Figure 4.4). Due to restricted lab time (see COVID-19 Impact Statement), these additional controls were only included in the experiments using pKpQIL.

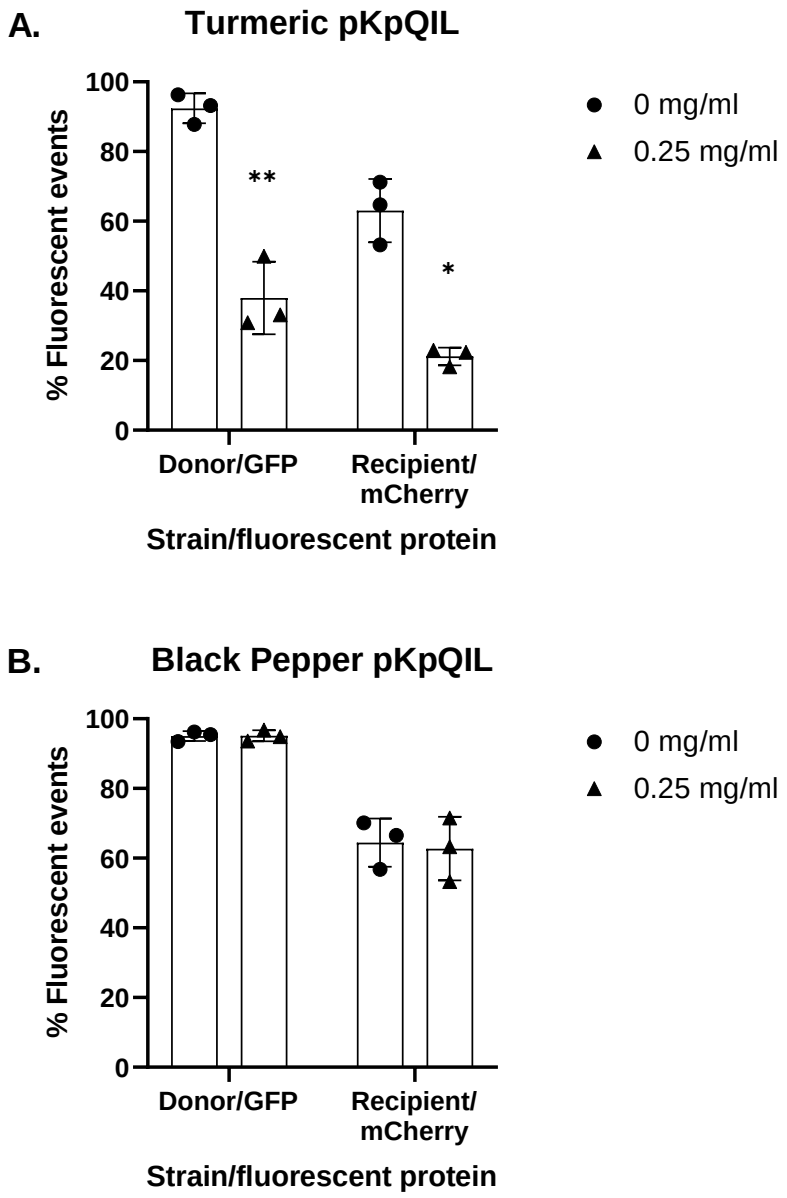

Figure 4.4: Effect of 0.25mg/ml extract on fluorescence detection in the pKpQIL experiment. Donors (circular data points) were tested for the GFP fluorescence profile, and recipients (triangular data points) were tested for the mCherry fluorescence profile. Each data point represents one experiment with four biological repeats. Error bars represent one standard deviation above and below the mean. * = $P \leq 0.05$; ** = $P \leq 0.01$, when the difference to the control (0 mg/ml) was calculated with Welch's t-test.

Presence of 0.25 mg/ml turmeric extract in the incubation medium significantly decreased

the detection of both GFP (P = 0.0056) and mCherry (P = 0.011) in the dual-fluorescence assay (Figure 4.4A). On the contrary, the same concentration of black pepper extract had no effect on the detection of either GFP (P = 0.95) or mCherry (P = 0.80) (Figure 4.4B).

Curcumin, a key component of turmeric, is a known fluorophore, and so autofluorescence of the curcumin in turmeric extract may have caused fluorescence interference, resulting in the increases in non-fluorescent events observed in Figure 4.3 and the decreases in total fluorescent events observed in Figure 4.4.

Two possible mechanisms could explain the fluorescence interference: either curcumin could be absorbing some of the excitation radiation, preventing the optimum amount from being absorbed by the GFP and mCherry fluorophores, or curcumin could be absorbing some of the emission radiation, interfering with emission detection. These possibilities were explored using published work on the autofluorescence of curcumin. However, studies investigating this have generally used excitation wavelengths in the range of 300 - 450 nm (Kurien et al., 2012; Wu et al., 2018; Ali et al., 2019). This range was below the excitation and emission wavelengths from this project (Section 2.2.7): excitation wavelengths were 488 nm, corresponding to the excitation peaks of GFP at 488 nm (Tsien, 1998), and 561 nm efficiently exciting mCherry near its peak of 587 nm (Shaner et al., 2004). The relevant emission peaks were at 509 nm for GFP and 610 nm for mCherry. Without generating excitation and emission spectra for curcumin or turmeric extract at these wavelengths, a mechanism of interference could not be determined.

4.2.5 Further considerations regarding completion of the dataset

The data in Figure 4.2 are preliminary and incomplete, as can be observed by insufficient control data to support the turmeric pCT experiment. The values from the first repeat of turmeric pCT were inconsistent with the results from the other two repeats, but could not be statistically confirmed as outliers due to the low number of experimental repeats. Further repeats

of testing turmeric on pCT would be necessary to increase the stringency of the data and the validity of the observations from the above section. Due to restricted laboratory access (see COVID-19 Impact Statement), there was insufficient time to complete these repeats.

Additionally, though any confounding bactericidal effects of the extracts were ruled out by broth MIC testing, it could not be determined whether the extracts had any bacteriostatic effects compromising cell growth. Growth kinetic analyses would still need to be performed to rule out any dose-dependent effect on cell growth at the working concentrations of both extracts.

Finally, data regarding fluorescence interference was not collected for the pCT experiments, as this was a parameter investigated in later experiments. Ideally the pCT experiments would have been repeated to collect these data, but this did not occur due to insufficient time.

4.3 Experimental models literature review

Despite *in vitro* approaches being reductionist and *in vivo* studies limited by confounding variables, both approaches bring valuable insight into the dynamics of AMR plasmids in the gut microbiome. A "middle ground" model, complex enough to generate translatable data while still maintaining a controlled environment, could provide an achievable compromise.

In this review, two main areas are discussed: directly studying the human gut *in situ* to identify accounts of conjugation within the gut, and the use of *in vitro* gut models of various complexities to study the same phenomenon. The two approaches are compared, with reference to animal-based *in vivo* models. Past and present approaches to studying plasmid dynamics in the gut microbiome are discussed, as well as the potential of current and developing experimental methods and models for bringing novel insight to this field. Understanding if and how the microbiome affects rates of conjugation between symbiotic bacteria could present novel bacterial or human targets for future efforts to reduce ARG

prevalence and the emergence of new AMR strains in these environments. In addition, the development of *in vitro* models could simplify research into novel antibacterial therapies targeting the GI tract.

4.3.1 Studying the human gut

Due to its spatially diverse microbiological niches, complex array of symbionts and the impact of host factors such as the immune system, the human GI tract is notoriously difficult to reproduce experimentally. As a result, the value of *in situ* experiments and observations are difficult to rival with models. Early experiments involving oral administration of donor and recipient *E. coli* to human volunteers demonstrated detectable levels of transmission of AMR phenotypes, though accompanied by very little colonisation (H. W. Smith, 1969; E. S. Anderson, 1975). More recent studies have also demonstrated transfer of AMR genes in the intestines of human volunteers, including sulphonamide resistance between human-derived *E. coli* strains (Trobos et al., 2008), and vancomycin resistance between animal- and human-derived *E. faecium* (Lester et al., 2006). These have since generally given way to animal and laboratory models due to the ethical risks of colonising subjects with AMR strains, compromising their health and the effectiveness of future treatment.

4.3.2 Observational studies

Despite a lack of recent direct experiments on the human gut, observational studies can utilise faecal samples or rectal swabs, most frequently from hospitalised patients where faecal screening is often routine (Goren et al., 2010; Galani et al., 2013; Prevel et al., 2019), to investigate the abundance and epidemiology of AMR bacteria without the ethical challenges of experimental approaches. Accounts of nosocomial outbreaks of AMR pathogens are abundant in the literature, with identified plasmid-borne ARGs often characterised *in silico* and *in vitro*. In many cases, the potential for dissemination is assumed, given the ability

of the plasmid vector to conjugate in subsequent *in vitro* experiments (Leavitt et al., 2010b; Aghamohammad et al., 2019; Bocanegra-Ibarias et al., 2019).

More direct evidence of conjugation events can come from multiple samples taken from the same patient or hospital, either within nosocomial outbreaks (Galani et al., 2013; Göttig et al., 2015) or in non-outbreak contexts (Balis et al., 1996; Karami et al., 2007; Goren et al., 2010; Rashid and Rahman, 2015). These conclusions can be drawn from the isolation of separate strains carrying the same plasmid either simultaneously (Balis et al., 1996; Rashid and Rahman, 2015), or sequentially, where a plasmid can be hypothesised to have transferred between two sampling dates (Karami et al., 2007; Goren et al., 2010; Galani et al., 2013; Göttig et al., 2015).

Case studies

Balis et al. (1996) studied nine patients from which ampicillin-resistant *Salmonella enteritidis* were isolated, as well as ampicillin-resistant *E. coli* identified as belonging to the normal gut flora. R plasmids with identical restriction patterns and conferring the same resistance phenotypes were found in both *S. enteritidis* and *E. coli* in two of these nine patients, implying a recent transmission event.

Karami et al. (2007) tested faecal samples from an infant from birth to 12 months of age, as part of a study investigating the role of intestinal colonisation on allergy development. Prior to ampicillin treatment, two distinct *E. coli* strains were consistently identified, one of which was ampicillin resistant. Following ampicillin treatment for a UTI, the second strain became ampicillin resistant, correlating with the acquisition of a $bla_{\text{TEM-1b}}$-containing plasmid confirmed to be the same as that present in the first strain, by PCR, sequencing and RFLP analysis.

Goren et al. (2010) followed the case of a single patient in Israel, with rectal swab screening initially detecting no CRE isolates, but a week later isolating a KPC-3-positive *K. pneu-*

moniae ST258 strain. KPC-3-positive *E. coli* were isolated from a cholecystectomy a month later. Retrospective analysis of the first swab detected a near-identical strain of *E. coli* that was KPC-negative, suggesting that the KPC-3 gene was transferred from the *K. pneumoniae* ST258 strain, which was likely hospital-acquired. Plasmid analysis of the KPC-3-positive strains identified a common plasmid of identical size, with PCR and sequencing analysis identifying identical KPC-3 transposon genetic markers between them, and RFLP analysis showing a 98% band pattern similarity. This plasmid correlated in size and shared KPC-3 transposon elements with pKpQIL, a known conjugative plasmid identified in previous outbreaks of *K. pneumoniae* ST258 in the same Israeli hospital (Leavitt et al., 2010b).

Similarly, Galani et al. (2013) initially isolated a carbapenem-susceptible *Enterobacter aerogenes* strain, followed by a KPC-2-positive *K. pneumoniae* seven days later, both from rectal surveillance cultures. Three months later, a KPC-2-positive *E. aerogenes* was isolated, which was otherwise isogenic with the initial isolate. S_1 nuclease restriction profiling demonstrated that the KPC-2-positive isolate contained a 70kb plasmid in common with the *K. pneumoniae* isolate, and PCR confirmed a common set of resistance genes absent from the initial *E. aerogenes* isolate.

Göttig et al. (2015) also focused on a single patient, sequentially isolating OXA-48-positive *K. pneumoniae*, OXA-48-negative *E. coli* and lastly OXA-48-positive *E. coli* strains. PCR and MLST analysis revealed that the *E. coli* strains had >99.7% genetic similarity, primer walking confirmed identical genetic contexts of the $bla_{\text{OXA-48}}$ gene within the positive strains and PFGE identified a 60kb plasmid in subsequent *in vitro* conjugation experiments.

Rashid and Rahman (2015) simultaneously isolated *E. coli* and *Shigella sonnei* strains, both multi-drug resistant with very simmilar resistance profiles, from a single patient hospitalised with shigellosis. Both strains were identified as ESBL-positive by double disk synergy testing, and gel separation following plasmid extraction confirmed the presence of a common 50 MDa plasmid which conjugated, along with the ESBL phenotype, when tested *in vitro*.

In vitro conjugation experiments using *E. coli* laboratory recipients (K12, J53 or DH5α) were used in the above studies to test the potential of these plasmids to spread horizontally, with the exception of Goren et al. (2010), where the susceptible *E. coli* isolate was used. Successful conjugation of putative conjugative plasmids was taken as supporting evidence for the occurrence of conjugation in the gut. In some cases however, *in vitro* conjugation was unsuccessful (Goren et al., 2010; Galani et al., 2013). A suggested explanation was the possibility of indirect conjugation through an intermediate strain (Galani et al., 2013), though natural transformation of plasmid DNA in the gut microbiome is theoretically also possible but has not been characterised (McInnes et al., 2020). It is also evident that using different strains and *in vitro* conditions does not exactly replicate the putative *in situ* event, though interestingly Goren et al. (2010), using their isolate as a recipient for a pKpQIL-like plasmid, were unable to observe any conjugation *in vitro*.

The apparent sampling bias favouring case studies of *in vivo* conjugation in *Enterobacteriaceae*, especially CRE, is likely a tribute to a combination of factors that make these events more likely to be identified. This could include hospitals routinely screening for carbapenem resistant organisms (Goren et al., 2010; Galani et al., 2013) due to their health threat and critical priority classification (Logan and Weinstein, 2017; Tacconelli et al., 2018), and the propensity of *Enterobacteriaceae* to carry clinically relevant AMR plasmids (Carattoli, 2009), reside as opportunistic pathogens in the gut (van Schaik, 2015; Price et al., 2017) and cause nosocomial infections (Vincent, 2003).

Methods

The most pragmatic sampling method, faecal collection, subjects samples to a certain bias whereby the composition is representative of only the endpoint microbiota. Metagenomic analyses comparing different niches along the GI tract, such as the mucosa, digesta or faeces, are inconsistent in their observations of which phyla dominate which niches, but conclusions

are synonymous: microbiota associated with different niches are phylogenetically distinct (Nava et al., 2011; Rangel et al., 2015; Ringel et al., 2015), suggesting that faeces are a poor proxy for microbiome representation. Additionally, there is no standard protocol for the handling of faecal samples, with a trade-off between homogenising to reduce variation and preserving sample community structure (Tang et al., 2020). Most alternative methods, e.g. biopsies and other surgical approaches, are invasive and their suitability for gut microbiota analysis of healthy participants disputed (Tang et al., 2020). Nevertheless, biopsies are used in studies relating to the microbiome of humans (Ringel et al., 2015; Tap et al., 2017) and of murine models (Nava et al., 2011). More widely, however, experimental and observational studies on bacterial conjugation in the human gut still tend to use faeces or rectal swabs as a proxy for the microbiota (H. W. Smith, 1969; E. S. Anderson, 1975; Lester et al., 2006; Trobos et al., 2008; Göttig et al., 2015; McInnes et al., 2020).

The rapid development of novel bioinformatic approaches in recent years has improved the quality of culture-independent data available from microbiome samples. Methods for detecting HGT events in metagenomes are reviewed in Douglas and Langille (2019), with their specific applications in the gut microbiome reviewed by McInnes et al. (2020). Many of these methods specialise in detecting abundance of ARGs, as well as genomic signatures of HGT. Of particular interest are methods which link ARGs to their plasmid and microbial hosts such as epicPCR or 3C, which vastly improve insight into the genomic contexts of individual ARGs, with the potential for assessing transmissibility and monitoring transmission events (McInnes et al., 2020; Yaffe and Relman, 2020).

Concluding remarks

Investigating conjugation in the human gut by direct observation is by far the best approach for understanding how bacteria behave *in situ*, identifying which plasmids are of immediate threat to human health and providing valuable epidemiological insight into their dissemina-

tion. Inevitably, however, observation does not present the full picture. Key limitations of this research approach include the lack of ability to ethically control most variables, requiring researchers to wait for these stochastic events to be uncovered by screening, as well as encountering limited access to the various internal environments. These limitations are overcome in the most part by the use of experimental *in vivo* animal and *in vitro* models of the gut.

4.3.3 *In vitro* models

Introduction and rationale

Replace; reduce; refine: the "3Rs" of a humane approach to using animals in science (Russell and Burch, 1959) are still widely referenced in contexts from research to policy (Tannenbaum and Bennett, 2015). Use of animals has long been defended in biomedical research, from screening for adverse drug reactions to modelling human disease, due to the similarities in genetics and physiology we share with commonly used animal models such as mice. National and international policy based around the 3Rs heavily restricts the use of animals in research and actively promotes research into alternative methods, including by providing financial support (Cronin, 2017).

In vitro models have the inherent advantage of having far more controllable parameters compared with the *in vivo*, though the vast reduction in complexity compared with *in situ* environments has its drawbacks in the translatability of results. Internal components are much easier to access, monitor and sample. Ultimately, the difficulty of developing insentient alternatives to animal research depends on the necessary complexity of the model for the purposes of a particular investigation.

Key features

In the context of the gut microbiome, simple models using co-culture with microbial communities in multi-vessel culture systems have been used since the 1980s (Veilleux and Rowland, 1981). Recreating the much more complex parameters of a real gut such as host cells and their regeneration, tissue structure, mechanotransduction, peristaltic flow, metabolite gradients and biochemical host-microbe cross-talk is more difficult, and covered in detail in reviews by Costa and Ahluwalia (2019) and Yuli Wang et al. (2018). These reviews are primarily focused on recreating the environmental niche for host gut cells to study factors of host health, such as inflammation, probiotics or nutrition bioavailability. To study the microbiome itself, features such as mechanotransduction, stem cell differentiation control and the ability to monitor host cells are less central, highlighting how models differ based on research context. Several of these models are reviewed by Venema and van den Abbeele (2013) and so their technical details are not reviewed here, though their applications for use in conjugation experiments are discussed.

Generally, these models are single- or multi-compartmental with vessels simulating environments of the GI tract, either using chemostat or batch fermentation methods. Batch fermentation models are the simplest, cheapest and most frequently used, however are far from physiological (Venema and van den Abbeele, 2013) and only suitable for experiments lasting up to about 24h due to accumulation of inhibitory metabolites and depletion of substrates. This can be prevented by using chemostat bioreactor models, some of which have been successfully used to study AMR plasmid transmission in the human gut (Haug et al., 2011; Smet et al., 2011; Lambrecht et al., 2019), or other gut environments such as the chicken caecum (Card et al., 2017). Common control variables in both single- and multi-vessel chemostat models include pH, anaerobic conditions, agitation, and presence of a stabilised microbial slurry. Validation studies investigating the stability of metabolic profiles

and community composition have been performed for and support the models discussed below, with many using a high-throughput phylogenetic microarray, the Human Intestinal Tract Chip (HITChip; van de Wiele et al., 2015; Zihler Berner et al., 2013; Rajilić-Stojanović et al., 2010).

Established models

Currently the only single model spanning the entire human GI tract (van de Wiele et al., 2015) is the Simulator of the Human Intestinal Microbial Ecosystem (SHIME®; ProDigest, Belgium), consisting of five vessels of which the latter three represent colonic environments. It is the most modern of a series of bioreactor models, originating from a three-stage colonic simulator system developed by a group at the University of Reading in the 1980s (Gibson et al., 1988). SHIME® has been further developed to add regularly replaced artificial mucosal components to the vessel walls, stimulating a naturally renewing mucus layer in the M-SHIME system (van de Wiele et al., 2015). Mucus has been identified as an important microbial mediator of growth and access to host cells (van den Abbeele et al., 2009), with bacterial populations localised to mucin surfaces shown to be phylogenetically and metabolically distinct from those grown planktonically (Macfarlane et al., 2005). Using the M-SHIME gut to study conjugation of plasmid p5876 from a broiler chicken-derived *E. coli* strain, Lambrecht et al. (2019) isolated approximately 30 times more transconjugants from the mucin microcosms compared to the lumen. This study also demonstrated proof of concept of exposure to food-derived strains risking AMR transfer to the human gut microbiota, with earlier experiments using a different broiler chicken-derived *E. coli* donor in a different, one-vessel fermentation model also producing AMR transconjugants of human origin (Smet et al., 2011).

Alternatively to mucin microcosms, a colonic fermentation model developed by the Lacroix group (Cinquin et al., 2004), later developed into the PolyFermS model (Zihler Berner et al.,

2013), uses polysaccharide gel beads to immobilise part of the microbiota used in its ves-
2185 sels, increasing microbial density to physiological levels. The group have used the model to investigate conjugation in the gut, determining that an *E faecium* donor can transfer a multi-drug resistant plasmid pRE25 to members of the commensal microbiota, as demonstrated by isolation of an *Enterococcus avium* transconjugant (Haug et al., 2011).

Other established models exist with the potential of contributing to our understanding
2190 of AMR transmission in the GI tract. The TNO *in vitro* model of the colon, TIM-2 (TNO, The Netherlands), designed by Minekus et al. (1999), consists of four compartments and incorporates peristalsis and a unique dialysate system to prevent accumulation of microbial metabolites, keeping them at physiological concentration and the microbiota at physiological density (Venema, 2015).

2195 Colonic simulation models such as TIM-2 are often used in conjunction with upper GI models, such as TIM-1 (TNO, The Netherlands) or The Smallest Intestine (TSI; Cieplak et al., 2018). Recreating the stresses of earlier digestive processes better emulates the state of bacteria and compounds entering the colon and increases the translatability of results, a notable advantage of SHIME® systems. TIM-1 has been used to complement TIM-2 (Keller
2200 et al., 2019) as well as other colonic models in a range of contexts, such as the single-vessel Artificial Colon (ARCOL; Applikon, The Netherlands) (Blanquet-Diot et al., 2012). Despite not having yet been used to study conjugation directly, combinations of upper and lower GI tract models could be used to address questions relating to AMR transmission.

Model standardisation

2205 Different setups and lack of direct comparison between models mean that there is no current standard of *in vitro* model for any context. For one, there is no consensus on ideal sources of the microbiota component, with some sampling from a single donor (Lambrecht et al., 2019), though pooling samples from multiple donors has been shown to decrease inter-

individual variability (Aguirre et al., 2014). Community stability is difficult to ensure, though has been observed in several models and their validation studies (Rajilić-Stojanović et al., 2010; Zihler Berner et al., 2013; van de Wiele et al., 2015; L. Liu et al., 2018). Reproducability within a model is a key design concern made difficult by the notoriously complex and variable nature of both the microbiota and of host factors, but can be approached with reductionist simplifications of both of these components, reviewed in detail by Elzinga et al. (2019). Elzinga and colleagues discuss the established Altered Schaedler Flora (Dewhirst et al., 1999), OligoMM^{12} (Brugiroux et al., 2016), SIHUMIx (Becker et al., 2011; Krause et al., 2020) and other communities and their applications, though highlight their predominant use in colonising animal models, with little but increasing application in *in vitro* systems.

Incorporating host factors

Routinely overlooked in *in vitro* models due to the complexity of their incorporation are factors such as host-microbe cross-talk and immune modulation, which create a pressured and constantly changing environment for microbes. Host-derived factors such as cells, bile salts, antimicrobial peptides and inflammatory mediators are sources of stress for bacteria, and can induce pathways such as the SOS response to increase rates of HGT, as can biofilm-promoting mucoid structures (Zeng and Lin, 2017). Stecher et al. (2012) observed a rapid "bloom" of *Salmonella* and *E. coli* following pathogen-induced inflammation in a mouse model, vastly increasing conjugation efficiency of an IncI1 plasmid. Alternatively, host-derived factors have also been observed to directly inhibit conjugation, with Machado and Sommer (2014) identifying a host cell-secreted peptide-based factor that inhibited conjugation of an ESBL plasmid between *E. coli* clinical isolates in co-culture with Caco-2 cells for two hours. The interplay between host and microbial elements of the microbiome is highly complex, and the relative effects on bacterial conjugation remain poorly understood.

The adenocarcinomal epithelial cell lines Caco-2 and HT29 are typically used in host-

microbiome studies, however co-cultures of cell lines with microbial populations are difficult to maintain in the long term. This is thought to be due to microbial cytotoxicity (van den Abbeele et al., 2009), as well as the complications of maintaining an anaerobic environment for the microbiota versus an aerobic environment to support the epithelial tissue. Ulluwishewa et al. (2015) demonstrated a significant loss in viability of Caco-2 cells co-cultured anaerobically for 12 hours with the obligate anaerobe *Faecalibacterium prausnitzii*.

Intestinal epithelial organoids, which have otherwise emerged as promising models due to their physiological structure, mimicking important features such as microbial product gradients (Yuli Wang et al., 2018; Costa and Ahluwalia, 2019), encounter similar issues relating to oxygen availability. Leslie et al. (2015) successfully cultured *C difficile* in an intestinal organoid model but detected up to 15% oxygen concentrations in the lumen, at which many anaerobic strains would be unable to persist.

Microfluidic, or "organ-on-a-chip" models address the limitations of microbial toxicity and oxygen availability, by physically separating the cultures whilst allowing metabolite exchange and bacterial adhesion via semi-permeable membranous structures. Systems such as the Host-Microbiome Interaction (HMI^{TM}; Marzorati et al., 2014) and Host-Microbial Crosstalk (HuMiX; Shah et al., 2016) modules have been shown to significantly increase viability of Caco-2 cells in co-culture with microbial communities compared with direct contact and more reductionist Transwell® membrane-separated models respectively. Though both developed with a focus on the host aspects, these methods providing longer viability of host cells in co-culture present new possibilities in investigating the microbiota *in vitro*.

Concluding remarks

The evident consensus on *in vitro* models is that they will always be oversimplifications of the systems they represent. Inclusion of fastidious details such as host cell co-culture and structure brings a model closer to the real gut environment, but for each particular context

there is a trade-off between recreating that environment as accurately as possible, and keeping a model down to its most relevant essentials to keep costs, analysis and maintenance at realistic levels. However, through the development of *in vitro* models of better and better accuracy, the relative need for and translatability of animal models is decreasing. Since *in vivo* models such as the murine gut are widely accepted to have translatability limitations due to physiological discrepancies (Nguyen et al., 2015), highly specialised human-based *in vitro* models have the potential to reduce or even replace animal models in many contexts.

At the time of writing this review, little has been published on the use of *in vitro* models such as those described above to study plasmid dynamics. Published studies have clearly demonstrated conjugation of AMR plasmids to microbiota members *in vitro* (Haug et al., 2011; Smet et al., 2011; Machado and Sommer, 2014; Lambrecht et al., 2019), both with (Smet et al., 2011) and without (Haug et al., 2011; Machado and Sommer, 2014; Lambrecht et al., 2019) antibiotic administration. Host-derived factors that could impact the rate of conjugation have also been uncovered (Machado and Sommer, 2014), prompting further investigation into the role of the human GI environment in bacterial conjugation. Despite a lack of experimental assessment on these models' comparative ability to provide insight into AMR transfer, their success in related fields show their vast potential in AMR research.

4.4 Discussion and future work

Despite the limitations of the dataset (Section 4.2.5), the data discussed in Section 4.2.3 suggest that turmeric extract reduces the conjugation of both plasmids pCT and pKpQIL in a dose-dependent manner, and that black pepper extract also does so to pCT, but not pKpQIL. However, due to potentially confounding effects from fluorescence interference within the assay (Section 4.2.4), these data could not be used with confidence to confirm the hypothesis that these extracts have a dose-dependent inhibitory effect on conjugation.

Additionally, as discussed in Section 4.2.5, the growth of the strains in the presence of these extracts was not assessed, and so any confounding effect on growth was not characterised. However, it was concluded that the reductions in conjugation observed were not as a result of cell death, as confirmed by broth MIC assays (Section 4.2.2).

The third hypothesis (Section 4.1.3) was not tested due to a lack of time (see COVID Impact Statement), but is discussed in Section 5.2.

Both the experimental and review work presented above contributed to ongoing work investigating plasmid dynamics in the human gut microbiome, and ways in which to observe and manipulate these dynamics. The following section outlines how these insights can together build the grounds for further research on reducing the conjugation of AMR plasmids in this environment.

4.4.1 Future work with natural extracts

The turmeric and black pepper data discussed in this chapter demonstrate the promising abilities of these extracts to reduce the conjugation of AMR plasmids. However, alongside the further work needed to optimise the experiments performed in this project (discussed in Section 4.2.5), further experimental work would be necessary to gather more data to support these observations. In order to circumvent the above issues concerning potential fluorescence interference when using the dual-fluorescence assay, the conjugation experiments would need to be repeated using a classical conjugation assay (Section 2.2.6). Using selective plating to count transconjugant colonies would be more laborious, but provide more stringent data than those potentially compromised by the fluorescent properties of the extracts.

In order to both begin to investigate a potential mechanism of action and optimise the anti-plasmid effects of the extracts, the active components of these extracts would need to be identified. This would be difficult, due to the complex composition of both turmeric and black pepper extracts. The best-studied and best-understood components, curcumin and piperine,

could be tested first. Alternatively, the extracts could be fractionated, and fractions tested individually to identify whether components in different proportions increased the observed anti-plasmid effects.

The next steps to take to elucidate the potential of these extracts (or components thereof) for therapeutic use would be to investigate their actions *in vivo*, either in an animal model or an specialised *in vitro* system. This stage would identify interactions of the extracts with other components of the gut microbiome, such as other microbial strains or host factors such as intestinal absorption or metabolism. Further details are discussed in Section 5.2.

It would also be necessary at this stage to consider and investigate the bioavailability and potential toxicity of components of these extracts. Investigating the bioavailability of whole extract would be extremely difficult due to the vast number of component phytochemicals, and so bioavailability studies would need to be focused on individual molecules of interest. The bioavailabilities of curcumin and piperine have been previously investigated and were discussed in Section 4.1.1.

Computational analysis of 200 compounds from turmeric identified only 16 with no predicted toxic effects (Balaji and Chempakam, 2010), not including curcumin which was predicted to have hepatotoxic effects. Dose-dependent hepatotoxicity has been reported in mice (Kandarkar et al., 1998), and a case study of hepatitis attributed to turmeric supplements reported (Chand et al., 2020), though the dosing in these studies was unclear. When investigating black pepper, Piyachaturawat et al. (1983) observed an acute lethal dose (LD_{50}) of piperine of 330.0 mg/kg body weight in mice and 514 mg/kg body weight in rats when administered intragastrically.

More up-to-date research on the toxicity of these extracts is needed, though it may be more beneficial to test toxicity *in vitro* using human tissue culture or organoids. This would overcome the ethical challenges of performing *in vivo* experiments with death as an endpoint, and to bypass the limitation that animal models may not represent the responses in human

systems. Aspects of *in vitro* models discussed in Section 4.3.3 could be considered when designing these experiments. Additionally, the doses investigated must be considered in light of the efficacy in reducing conjugation: toxicity in higher doses is no concern if conjugation can be significantly reduced at much lower doses.

5. Discussion

5.1 Discussion of the research questions

In addressing research question 1 (Section 1.5.2), a conclusion was drawn in Chapter 3 that co-culture with *B. fragilis* impacted neither the growth of the *K. pneumoniae* donor or *E. coli* recipient, nor the conjugation frequency of pCPE01_2 between them. This was observed to be the case for these particular combinations of strains, but it was discussed that similar investigations using different strains and definitions of co-culture were required in order to gain a better understanding of the relationship between the presence of microbiota strains and the plasmid dynamics between opportunistic pathogens in the gut (Section 3.5).

In addressing the broader research question 2, methods and models of investigating conjugation were discussed, and an investigation was undertaken in which several natural compounds were tested, with promising results, for anti-plasmid activity. In order to bring these aspects together and fully address the research question, insights from research question 1 were incorporated, and discussed in the following Section 5.2.

5.2 Incorporating co-culture *in vitro* models into anti-plasmid research

The dual-fluorescence system used in this project has been successfully applied to many other drugs and extracts as a rapid and medium-throughput screen for potential anti-plasmid activity, as described by Buckner et al. (2020). This system could be developed further, incorporating more aspects of the gut microbiome to generate further insight into how these extracts could behave *in situ* without the use of animal models.

Stringent data generated by various drug and extract experiments, including turmeric and black pepper, could be used to validate the incorporation of various microbiome aspects, with the eventual aim to perform these conjugation assays in an established *in vitro* system as discussed in Section 4.3. The first aspects to investigate would be anaerobic incubation and co-culture with microbiome strains, both of which were discussed in Chapter 3.

Firstly, incubating the fluorescent strains anaerobically would require the use of AFR to be able to use the dual-fluorescence assay. As two variables would be changing in this experiment (anaerobic environment and use of AFR) compared with the initial *in vitro* experiment, this would also need to be validated using classical conjugation and selective plating, as used to investigate conjugation in Chapter 3. Classical conjugation experiments would identify whether anaerobiosis alone has an effect on conjugation frequency, independently of AFR.

Next, performing these experiments with bacterial co-culture included in the incubation step could be tested. Introducing additional bacterial strains would present issues at the flow cytometry stage however, since many of these cells would be included in the 10,000 events count, contributing to the percentage of non-fluorescent events. A potential solution to this issue would be to increase the counts collected, subsequently increasing the total number of fluorescent events. If possible, the increase in counts would be somewhat proportional to the ratio of fluorescent:non-fluorescent cells in the liquid culture in order to bring the number of fluorescent events as close to 10,000 as possible, however this may be difficult to achieve. Nevertheless, co-culture growth assays (Section 2.2.9) would need to be performed prior to the co-culture conjugation to investigate any growth inhibition, as done in Chapter 3, and so these data may be used to predict the factor by which to increase the number of events collected at the flow cytometry stage. In addition, a fluorescence microplate reader could be used in these growth assays as the cells of interest are fluorescent, which would quicken the growth assay experiments as there would be no need to selectively plate to work out viable counts. This would likely be necessary anyway, since the donors and recipients all express

the same single selective marker (kanamycin resistance), making selective plating impossible when growing these strains together in co-culture.

Eventually, the aim would be to include an established *in vitro* model, such as those discussed in Section 4.3, in experiments investigating anti-plasmid compounds. If such a model were to be successfully validated using data from classical conjugations or dual-fluorescence assays, in both the absence and presence of drugs or compounds, there is vast potential for such a method to further *in vitro* research into anti-plasmid compound discovery, among other applications in plasmid dynamics research. An *in vitro* environment more closely simulating the conditions *in situ* would not only give a better representation of how certain compounds behave *in vivo*, but also the strains themselves. As one example, the observations by Lambrecht et al. (2019) that 30 times more transconjugants were isolated from mucin microcosms than the lumen when using the M-SHIME gut model demonstrate that environmental factors have an effect on the behaviour of donor and recipient bacteria. Such conditions in an *in vitro* model allow the collection of translatable data without the need for as much *in vivo* research and its accompanying costs.

List of References

van den Abbeele, Pieter et al. (2009). "In vitro model to study the modulation of the mucin-adhered bacterial community". *Applied Microbiology and Biotechnology* 83.2, pp. 349–359.

Adar, Assaf et al. (2021). "Clinical and Demographic Characteristics of Patients With a New Diagnosis of Carriage or Clinical Infection With Carbapenemase-Producing Enterobacterales: A Retrospective Study". *Frontiers in public health* 9, p. 616793.

Aghamohammad, Shadi et al. (2019). "Considerable rate of putative virulent phylo-groups in fecal carriage of extended-spectrum β-lactamase producing Escherichia coli". *Infection, Genetics and Evolution* 73, pp. 184–189.

Aguirre, Marisol et al. (2014). "To pool or not to pool? Impact of the use of individual and pooled fecal samples for in vitro fermentation studies". *Journal of Microbiological Methods* 107, pp. 1–7.

Ahsan, Haseeb and S M Hadi (1998). "Strand scission in DNA induced by curcumin in the presence of Cu(II)". *Cancer Letters* 124.1, pp. 23–30.

Alakomi, H L et al. (2000). "Lactic acid permeabilizes gram-negative bacteria by disrupting the outer membrane." *Applied and environmental microbiology* 66.5, pp. 2001–2005.

Ali, Zulfiqar et al. (2019). "Determination of curcuminoid content in turmeric using fluorescence spectroscopy." *Spectrochimica acta. Part A, Molecular and biomolecular spectroscopy* 213, pp. 192–198.

Ambler, R P, James Baddiley, and Edward Penley Abraham (1980). "The structure of β-lactamases". *Philosophical Transactions of the Royal Society of London. B, Biological Sciences* 289.1036, pp. 321–331.

Anderson, E S (1975). "Viability of, and transfer of a plasmid from, E. coli K12 in human intestine." *Nature* 255.5508, pp. 502–504.

Anderson, J D (1975). “Factors that may prevent transfer of anti-biotic resistance between gram-negative bacteria in the gut.” *Journal of medical microbiology* 8.1, pp. 83–88.

Arpaia, Nicholas et al. (2013). “Metabolites produced by commensal bacteria promote peripheral regulatory T-cell generation”. *Nature* 504.7480, pp. 451–455.

Bacic, Melissa K and C Jeffrey Smith (2008). “Laboratory maintenance and cultivation of bacteroides species”. *Current protocols in microbiology* 9, pp. 13C.1.1–13C.1.21.

Badmaev, Vladimir, Muhammed Majeed, and Edward P Norkus (1999). “Piperine, an alkaloid derived from black pepper increases serum response of beta-carotene during 14-days of oral beta-carotene supplementation”. *Nutrition Research* 19.3, pp. 381–388.

Balaji, S and B Chempakam (2010). “Toxicity prediction of compounds from turmeric (Curcuma longa L)”. *Food and Chemical Toxicology* 48.10, pp. 2951–2959.

Balis, E et al. (1996). “Indications of in vivo transfer of an epidemic R plasmid from Salmonella enteritidis to Escherichia coli of the normal human gut flora”. *Journal of clinical microbiology* 34.4, pp. 977–979.

Becker, Natalie et al. (2011). “Human intestinal microbiota: characterization of a simplified and stable gnotobiotic rat model.” *Gut microbes* 2.1, pp. 25–33.

Bergstrom, C T, M Lipsitch, and B R Levin (2000). “Natural selection, infectious transfer and the existence conditions for bacterial plasmids”. *Genetics* 155.4, pp. 1505–1519.

Bharathan, Subhashree et al. (2019). “Sub lethal levels of platinum nanoparticle cures plasmid and in combination with carbapenem, curtails carbapenem resistant Escherichia coli”. *Scientific reports* 9.1, p. 5305.

Blair, Jessica M A, Grace E Richmond, and Laura J V Piddock (2014). “Multidrug efflux pumps in Gram-negative bacteria and their role in antibiotic resistance.” *Future microbiology* 9.10, pp. 1165–1177.

Blair, Jessica M A et al. (2015). “Molecular mechanisms of antibiotic resistance”. *Nature Reviews Microbiology* 13.1, pp. 42–51.

Blanquet-Diot, Stéphanie et al. (2012). "Use of artificial digestive systems to investigate the biopharmaceutical factors influencing the survival of probiotic yeast during gastrointestinal transit in humans." *Pharmaceutical research* 29.6, pp. 1444–1453.

Bocanegra-Ibarias, Paola et al. (2019). "The successful containment of a hospital outbreak caused by NDM-1-producing Klebsiella pneumoniae ST307 using active surveillance." *PloS one* 14.2, e0209609.

Boyd, Eric and Tamar Barkay (2012). "The Mercury Resistance Operon: From an Origin in a Geothermal Environment to an Efficient Detoxification Machine". *Frontiers in Microbiology* 3, p. 349.

Bradford, P A (2001). "Extended-spectrum beta-lactamases in the 21st century: characterization, epidemiology, and detection of this important resistance threat". *Clinical microbiology reviews* 14.4, pp. 933–951.

Brugiroux, Sandrine et al. (2016). "Genome-guided design of a defined mouse microbiota that confers colonization resistance against Salmonella enterica serovar Typhimurium." *Nature microbiology* 2, p. 16215.

Buckner, Michelle M C, Maria Laura Ciusa, and Laura J V Piddock (2018a). "Strategies to combat antimicrobial resistance: anti-plasmid and plasmid curing". *FEMS Microbiology Reviews* 42.6, pp. 781–804.

Buckner, Michelle M C et al. (2018b). "Clinically Relevant Plasmid-Host Interactions Indicate that Transcriptional and Not Genomic Modifications Ameliorate Fitness Costs of Klebsiella pneumoniae Carbapenemase-Carrying Plasmids". *mBio* 9.2, e02303–17.

Buckner, Michelle M C et al. (2020). "HIV Drugs Inhibit Transfer of Plasmids Carrying Extended-Spectrum β-Lactamase and Carbapenemase Genes". *mBio* 11.1.

Butt, Masood Sadiq et al. (2013). "Black Pepper and Health Claims: A Comprehensive Treatise". *Critical Reviews in Food Science and Nutrition* 53.9, pp. 875–886.

Cai, Bin et al. (2017). “Prevalence of Carbapenem-Resistant Gram-Negative Infections in the United States Predominated by Acinetobacter baumannii and Pseudomonas aeruginosa”. *Open Forum Infectious Diseases* 4.3.

Carattoli, Alessandra (2009). “Resistance Plasmid Families in Enterobacteriaceae”. *Antimicrobial Agents and Chemotherapy* 53.6, pp. 2227–2238.

Card, Roderick M et al. (2017). “An In Vitro Chicken Gut Model Demonstrates Transfer of a Multidrug Resistance Plasmid from Salmonella to Commensal Escherichia coli”. *mBio* 8.4, e00777–17.

Cassini, Alessandro et al. (2019). “Attributable deaths and disability-adjusted life-years caused by infections with antibiotic-resistant bacteria in the EU and the European Economic Area in 2015: a population-level modelling analysis”. *The Lancet. Infectious diseases* 19.1, pp. 56–66.

Castanheira, Mariana et al. (2017). “Meropenem-Vaborbactam Tested against Contemporary Gram-Negative Isolates Collected Worldwide during 2014, Including Carbapenem-Resistant, KPC-Producing, Multidrug-Resistant, and Extensively Drug-Resistant Enterobacteriaceae.” *Antimicrobial agents and chemotherapy* 61.9.

Chand, Sheital, Chris Hair, and Lauren Beswick (2020). “A rare case of turmeric-induced hepatotoxicity”. *Internal Medicine Journal* 50.2, pp. 258–259.

Chen, Chi-Chung et al. (2019). “Antimicrobial Activity of Lactobacillus Species Against Carbapenem-Resistant Enterobacteriaceae.” *Frontiers in microbiology* 10, p. 789.

Chen, Liang et al. (2014). “Comparative genomic analysis of KPC-encoding pKpQIL-like plasmids and their distribution in New Jersey and New York Hospitals.” *Antimicrobial agents and chemotherapy* 58.5, pp. 2871–2877.

Cieplak, T et al. (2018). “The Smallest Intestine (TSI)—a low volume in vitro model of the small intestine with increased throughput”. *FEMS Microbiology Letters* 365.21.

Cinquin, C et al. (2004). “Immobilization of Infant Fecal Microbiota and Utilization in an in vitro Colonic Fermentation Model”. *Microbial Ecology* 48.1, pp. 128–138.

Citorik, Robert J, Mark Mimee, and Timothy K Lu (2014). “Sequence-specific antimicrobials using efficiently delivered RNA-guided nucleases”. *Nature biotechnology* 32.11, pp. 1141–1145.

Costa, Joana and Arti Ahluwalia (2019). “Advances and Current Challenges in Intestinal in vitro Model Engineering: A Digest”. *Frontiers in Bioengineering and Biotechnology* 7, p. 144.

Cottell, Jennifer L et al. (2011). “Complete sequence and molecular epidemiology of IncK epidemic plasmid encoding blaCTX-M-14.” *Emerging infectious diseases* 17.4, pp. 645–652.

Craggs, Timothy D (2009). “Green fluorescent protein: structure, folding and chromophore maturation”. *Chemical Society Reviews* 38.10, pp. 2865–2875.

Cronin, Mark (2017). *Non-animal approaches The way forward*. Tech. rep. Brussels: European Scientific Commission.

Dahlberg, Cecilia and Lin Chao (2003). “Amelioration of the Cost of Conjugative Plasmid Carriage in Eschericha coli K12”. *Genetics* 165.4, pp. 1641–1649.

de Souza Grinevicius, Valdelúcia Maria Alves et al. (2016). “Piper nigrum ethanolic extract rich in piperamides causes ROS overproduction, oxidative damage in DNA leading to cell cycle arrest and apoptosis in cancer cells”. *Journal of Ethnopharmacology* 189, pp. 139–147.

De, Jaysankar et al. (2003). “Tolerance to various toxicants by marine bacteria highly resistant to mercury.” *Marine biotechnology (New York, N.Y.)* 5.2, pp. 185–193.

Dewhirst, F E et al. (1999). “Phylogeny of the defined murine microbiota: altered Schaedler flora.” *Applied and environmental microbiology* 65.8, pp. 3287–3292.

Dicks, Leon M T et al. (2019). “Clostridium difficile, the Difficult “Kloster” Fuelled by Antibiotics”. *Current Microbiology* 76.6, pp. 774–782.

Douglas, Gavin M and Morgan G I Langille (2019). “Current and Promising Approaches to Identify Horizontal Gene Transfer Events in Metagenomes”. *Genome Biology and Evolution* 11.10, pp. 2750–2766.

Douillard, François P et al. (2013). “Comparative genomic and functional analysis of Lactobacillus casei and Lactobacillus rhamnosus strains marketed as probiotics.” *Applied and environmental microbiology* 79.6, pp. 1923–1933.

Doumith, M et al. (2017). “Major role of pKpQIL-like plasmids in the early dissemination of KPC-type carbapenemases in the UK.” *The Journal of antimicrobial chemotherapy* 72.8, pp. 2241–2248.

Duval-Iflah, Y et al. (1980). “R-plasmic transfer from Serratia liquefaciens to Escherichia coli in vitro and in vivo in the digestive tract of gnotobiotic mice associated with human fecal flora”. *Infection and immunity* 28.3, pp. 981–990.

ECDC (2019). *Surveillance of antimicrobial resistance in Europe 2018*. `https://www.ecdc.europa.eu/sites/default/files/documents/surveillance-antimicrobial-resistance-Europe-2018.pdf`.

Eklund, T (1983). “The antimicrobial effect of dissociated and undissociated sorbic acid at different pH levels”. *Journal of Applied Bacteriology* 54.3, pp. 383–389.

Elzinga, Janneke et al. (2019). “The Use of Defined Microbial Communities To Model Host-Microbe Interactions in the Human Gut”. *Microbiology and Molecular Biology Reviews* 83.2, e00054–18.

EUCAST (2020a). *The European Committee on Antimicrobial Susceptibility Testing. Breakpoint tables for interpretation of MICs and zone diameters. Version 10.0, 2020.* `http://www.eucast.org`.

EUCAST (2020b). *The European Committee on Antimicrobial Susceptibility Testing. Routine and extended internal quality control for MIC determination and disk diffusion as recommended by EUCAST. Version 10.0, 2020.* `http://www.eucast.org`.

Fayol-Messaoudi, Domitille et al. (2005). "pH-, Lactic acid-, and non-lactic acid-dependent activities of probiotic Lactobacilli against Salmonella enterica Serovar Typhimurium." *Applied and environmental microbiology* 71.10, pp. 6008–6013.

Fernández-Lázaro, Diego et al. (2020). "Iron and Physical Activity: Bioavailability Enhancers, Properties of Black Pepper (Bioperine(®)) and Potential Applications". *Nutrients* 12.6, p. 1886.

Fisher, Robert A, Bridget Gollan, and Sophie Helaine (2017). "Persistent bacterial infections and persister cells." *Nature reviews. Microbiology* 15.8, pp. 453–464.

Fleming-Dutra, Katherine E et al. (2016). "Prevalence of Inappropriate Antibiotic Prescriptions Among US Ambulatory Care Visits, 2010-2011". *JAMA* 315.17, pp. 1864–1873.

Fookes, Maria et al. (2013). "Genome Sequence of Klebsiella pneumoniae Ecl8, a Reference Strain for Targeted Genetic Manipulation." *Genome announcements* 1.1.

Fux, C A et al. (2005). "Can laboratory reference strains mirror "real-world" pathogenesis?" *Trends in microbiology* 13.2, pp. 58–63.

Galani, Irene et al. (2013). "In vivo transmission of a plasmid containing the KPC-2 gene in a single patient". *Journal of Global Antimicrobial Resistance* 1.1, pp. 35–38.

Garcea, Giuseppe et al. (2005). "Consumption of the Putative Chemopreventive Agent Curcumin by Cancer Patients: Assessment of Curcumin Levels in the Colorectum and their Pharmacodynamic Consequences". *Cancer Epidemiology Biomarkers & Prevention* 14.1, 120 LP –125.

Gibson, Glenn R, J H Cummings, and G T Macfarlane (1988). "Use of a three-stage continuous culture system to study the effect of mucin on dissimilatory sulfate reduction and

methanogenesis by mixed populations of human gut bacteria." *Applied and environmental microbiology* 54.11, pp. 2750–2755.

Goldenberg, Joshua Z et al. (2017). "Probiotics for the prevention of Clostridium difficile-associated diarrhea in adults and children". *The Cochrane database of systematic reviews* 12.12, pp. CD006095–CD006095.

Goren, Moran G et al. (2010). "Transfer of carbapenem-resistant plasmid from Klebsiella pneumoniae ST258 to Escherichia coli in patient". *Emerging infectious diseases* 16.6, pp. 1014–1017.

Gorgani, Leila et al. (2017). "Piperine—The Bioactive Compound of Black Pepper: From Isolation to Medicinal Formulations". *Comprehensive Reviews in Food Science and Food Safety* 16.1, pp. 124–140.

Göttig, Stephan et al. (2015). "In vivo horizontal gene transfer of the carbapenemase OXA-48 during a nosocomial outbreak." *Clinical infectious diseases : an official publication of the Infectious Diseases Society of America* 60.12, pp. 1808–1815.

Gumpert, Heidi et al. (2017). "Transfer and Persistence of a Multi-Drug Resistance Plasmid in situ of the Infant Gut Microbiota in the Absence of Antibiotic Treatment". *Frontiers in microbiology* 8, p. 1852.

Han, Hyo-Kyung (2011). "The effects of black pepper on the intestinal absorption and hepatic metabolism of drugs". *Expert Opinion on Drug Metabolism & Toxicology* 7.6, pp. 721–729.

Harrison, Ellie and Michael A Brockhurst (2012). "Plasmid-mediated horizontal gene transfer is a coevolutionary process". *Trends in Microbiology* 20.6, pp. 262–267.

Harrison, Ellie et al. (2015). "Parallel Compensatory Evolution Stabilizes Plasmids across the Parasitism-Mutualism Continuum". *Current Biology* 25.15, pp. 2034–2039.

Haug, Martina C et al. (2011). "Monitoring horizontal antibiotic resistance gene transfer in a colonic fermentation model". *FEMS Microbiology Ecology* 78.2, pp. 210–219.

Headd, Brendan and Scott A Bradford (2020). “The Conjugation Window in an E. coli K-12 Strain With an IncFII Plasmid”. *Applied and Environmental Microbiology*, AEM.00948–20.

Heuer, Holger, Randal E Fox, and Eva M Top (2007). “Frequent conjugative transfer accelerates adaptation of a broad-host-range plasmid to an unfavorable Pseudomonas putida host”. *FEMS Microbiology Ecology* 59.3, pp. 738–748.

Høiby, Niels et al. (2010). “Antibiotic resistance of bacterial biofilms.” *International journal of antimicrobial agents* 35.4, pp. 322–332.

Howden, Benjamin P et al. (2013). “Genomic insights to control the emergence of vancomycin-resistant enterococci”. *mBio* 4.4, e00412–13.

Huddleston, Jennifer R (2014). “Horizontal gene transfer in the human gastrointestinal tract: potential spread of antibiotic resistance genes”. *Infection and drug resistance* 7, pp. 167–176.

Husain, Fasahath et al. (2014). “The Ellis Island Effect: A novel mobile element in a multi-drug resistant Bacteroides fragilis clinical isolate includes a mosaic of resistance genes from Gram-positive bacteria.” *Mobile genetic elements* 4, e29801.

Hutchings, Matthew I, Andrew W Truman, and Barrie Wilkinson (2019). “Antibiotics: past, present and future”. *Current Opinion in Microbiology* 51, pp. 72–80.

Huttenhower, Curtis et al. (2012). “Structure, function and diversity of the healthy human microbiome”. *Nature* 486.7402, pp. 207–214.

Imran, Mudassar, Don Jones, and Hal Smith (2005). “Biofilms and the plasmid maintenance question.” *Mathematical biosciences* 193.2, pp. 183–204.

Ireson, Christopher R et al. (2002). “Metabolism of the Cancer Chemopreventive Agent Curcumin in Human and Rat Intestine”. *Cancer Epidemiology Biomarkers & Prevention* 11.1, 105 LP –111.

Jalasvuori, Matti et al. (2011). “Bacteriophage selection against a plasmid-encoded sex apparatus leads to the loss of antibiotic-resistance plasmids”. *Biology letters* 7.6, pp. 902–905.

Kaczmarek, Frank M et al. (2006). “High-level carbapenem resistance in a Klebsiella pneumoniae clinical isolate is due to the combination of bla(ACT-1) beta-lactamase production, porin OmpK35/36 insertional inactivation, and down-regulation of the phosphate transport porin phoe”. *Antimicrobial agents and chemotherapy* 50.10, pp. 3396–3406.

Kandarkar, S V et al. (1998). “Subchronic oral hepatotoxicity of turmeric in mice–histopathological and ultrastructural studies”. *Indian journal of experimental biology* 36.7, pp. 675–679.

Karami, Nahid et al. (2007). “Transfer of an ampicillin resistance gene between two Escherichia coli strains in the bowel microbiota of an infant treated with antibiotics”. *Journal of Antimicrobial Chemotherapy* 60.5, pp. 1142–1145.

Keller, D et al. (2019). “Spores of Bacillus coagulans GBI-30, 6086 show high germination, survival and enzyme activity in a dynamic, computer-controlled in vitro model of the gastrointestinal tract”. *Beneficial Microbes* 10.1, pp. 77–87.

Khan, Asad U, Lubna Maryam, and Raffaele Zarrilli (2017). “Structure, Genetics and Worldwide Spread of New Delhi Metallo-β-lactamase (NDM): a threat to public health.” *BMC microbiology* 17.1, p. 101.

Kim, Jun-Seob et al. (2016). “CRISPR/Cas9-Mediated Re-Sensitization of Antibiotic-Resistant Escherichia coli Harboring Extended-Spectrum β-Lactamases.” *Journal of microbiology and biotechnology* 26.2, pp. 394–401.

Kitano, K and A Tomasz (1979). “Escherichia coli mutants tolerant to beta-lactam antibiotics.” *Journal of bacteriology* 140.3, pp. 955–963.

Kitchel, Brandon et al. (2009). “Molecular epidemiology of KPC-producing Klebsiella pneumoniae isolates in the United States: clonal expansion of multilocus sequence type 258.” *Antimicrobial agents and chemotherapy* 53.8, pp. 3365–3370.

Kopotsa, Katlego, John Osei Sekyere, and Nontombi Marylucy Mbelle (2019). "Plasmid evolution in carbapenemase-producing Enterobacteriaceae: a review". *Annals of the New York Academy of Sciences* 1457.1, pp. 61–91.

Krause, Jannike Lea et al. (2020). "Following the community development of SIHUMIx – a new intestinal in vitro model for bioreactor use". *Gut Microbes*, pp. 1–14.

Kruse, Thomas, Jette Bork-Jensen, and Kenn Gerdes (2005). "The morphogenetic MreBCD proteins of Escherichia coli form an essential membrane-bound complex". *Molecular Microbiology* 55.1, pp. 78–89.

Kunishima, Hiroyuki et al. (2019). "The effect of gut microbiota and probiotic organisms on the properties of extended spectrum beta-lactamase producing and carbapenem resistant Enterobacteriaceae including growth, beta-lactamase activity and gene transmissibility." *Journal of infection and chemotherapy : official journal of the Japan Society of Chemotherapy* 25.11, pp. 894–900.

Kurien, Biji T, Yaser Dorri, and R Hal Scofield (2012). "Spicy SDS-PAGE gels: curcumin/turmeric as an environment-friendly protein stain". *Methods in molecular biology (Clifton, N.J.)* 869, pp. 567–578.

Lagier, J.-C. et al. (2012). "Microbial culturomics: paradigm shift in the human gut microbiome study". *Clinical Microbiology and Infection* 18.12, pp. 1185–1193.

Lambrecht, Ellen et al. (2019). "Commensal E. coli rapidly transfer antibiotic resistance genes to human intestinal microbiota in the Mucosal Simulator of the Human Intestinal Microbial Ecosystem (M-SHIME)". *International Journal of Food Microbiology* 311, p. 108357.

Lange, Felix et al. (2019). "Characterization of mutations in Escherichia coli PBP2 leading to increased carbapenem MICs". *Journal of Antimicrobial Chemotherapy* 74.3, pp. 571–576.

Lazdins, Alessandro et al. (2020). "Potentiation of curing by a broad-host-range self-transmissible vector for displacing resistance plasmids to tackle AMR". *PLOS ONE* 15.1, pp. 1–23.

Leavitt, Azita et al. (2010a). "Complete nucleotide sequence of KPC-3-encoding plasmid pKpQIL in the epidemic Klebsiella pneumoniae sequence type 258". *Antimicrobial agents and chemotherapy* 54.10, pp. 4493–4496.

Leavitt, Azita et al. (2010b). "Plasmid pKpQIL encoding KPC-3 and TEM-1 confers carbapenem resistance in an extremely drug-resistant epidemic Klebsiella pneumoniae strain." *The Journal of antimicrobial chemotherapy* 65.2, pp. 243–248.

Leslie, Jhansi L et al. (2015). "Persistence and toxin production by Clostridium difficile within human intestinal organoids result in disruption of epithelial paracellular barrier function". *Infection and immunity* 83.1, pp. 138–145.

Lester, Camilla H et al. (2006). "In vivo transfer of the vanA resistance gene from an Enterococcus faecium isolate of animal origin to an E. faecium isolate of human origin in the intestines of human volunteers". *Antimicrobial agents and chemotherapy* 50.2, pp. 596–599.

Li, Shiyou (2011). "Chemical Composition and Product Quality Control of Turmeric (Curcuma longa L.)" *Pharmaceutical Crops* 2.1, pp. 28–54.

Lili, Loukia N, Nicholas F Britton, and Edward J Feil (2007). "The persistence of parasitic plasmids". *Genetics* 177.1, pp. 399–405.

Limmathurotsakul, Direk et al. (2019). "Improving the estimation of the global burden of antimicrobial resistant infections". *The Lancet Infectious Diseases* 19.11, e392–e398.

Liu, LinShu et al. (2018). "Establishing a mucosal gut microbial community in vitro using an artificial simulator". *PloS one* 13.7, e0197692–e0197692.

Liu, Yunbao et al. (2010). "Inhibitory effects of black pepper (Piper nigrum) extracts and compounds on human tumor cell proliferation, cyclooxygenase enzymes, lipid peroxi-

dation and nuclear transcription factor-kappa-B." *Natural product communications* 5.8, pp. 1253–1257.

Logan, Latania K and Robert A Weinstein (2017). "The Epidemiology of Carbapenem-Resistant Enterobacteriaceae: The Impact and Evolution of a Global Menace". *The Journal of Infectious Diseases* 215.suppl_1, S28–S36.

Lopatkin, Allison J et al. (2017). "Persistence and reversal of plasmid-mediated antibiotic resistance". *Nature communications* 8.1, p. 1689.

Macfarlane, Sandra, Emma J Woodmansey, and George T Macfarlane (2005). "Colonization of mucin by human intestinal bacteria and establishment of biofilm communities in a two-stage continuous culture system". *Applied and environmental microbiology* 71.11, pp. 7483–7492.

Machado, Ana Manuel Dantas and Morten O A Sommer (2014). "Human intestinal cells modulate conjugational transfer of multidrug resistance plasmids between clinical Escherichia coli isolates". *PloS one* 9.6, e100739–e100739.

MacLean, R Craig and Alvaro San Millan (2019). "The evolution of antibiotic resistance". *Science* 365.6458, 1082 LP –1083.

Marathe, Sandhya Amol et al. (2016). "Curcumin Reduces the Motility of Salmonella enterica Serovar Typhimurium by Binding to the Flagella, Thereby Leading to Flagellar Fragility and Shedding". *Journal of Bacteriology* 198.13, 1798 LP –1811.

Marchesi, Julian R and Jacques Ravel (2015). "The vocabulary of microbiome research: a proposal". *Microbiome* 3.1, p. 31.

Martinson, Jonathan N V et al. (2019). "Rethinking gut microbiome residency and the Enterobacteriaceae in healthy human adults." *The ISME journal* 13.9, pp. 2306–2318.

Marzorati, Massimo et al. (2014). "The HMI^{TM} module: a new tool to study the Host-Microbiota Interaction in the human gastrointestinal tract in vitro". *BMC Microbiology* 14.1, p. 133.

Mathers, Amy J et al. (2017). “Chromosomal Integration of the Klebsiella pneumoniae Carbapenemase Gene, bla(KPC), in Klebsiella Species Is Elusive but Not Rare”. *Antimicrobial agents and chemotherapy* 61.3, e01823–16.

Mazmanian, Sarkis K, June L Round, and Dennis L Kasper (2008). “A microbial symbiosis factor prevents intestinal inflammatory disease”. *Nature* 453.7195, pp. 620–625.

McInnes, Ross S et al. (2020). “Horizontal transfer of antibiotic resistance genes in the human gut microbiome”. *Current Opinion in Microbiology* 53, pp. 35–43.

Mehmood, Malik Hassan and Anwarul Hassan Gilani (2010). “Pharmacological basis for the medicinal use of black pepper and piperine in gastrointestinal disorders.” *Journal of medicinal food* 13.5, pp. 1086–1096.

Meletis, Georgios (2016). “Carbapenem resistance: overview of the problem and future perspectives”. *Therapeutic advances in infectious disease* 3.1, pp. 15–21.

Meng, Fan-Cheng et al. (2018). “Chapter 10 - Turmeric: A Review of Its Chemical Composition, Quality Control, Bioactivity, and Pharmaceutical Application”. *Handbook of Food Bioengineering*. Academic Press, pp. 299–350.

Minekus, M et al. (1999). “A computer-controlled system to simulate conditions of the large intestine with peristaltic mixing, water absorption and absorption of fermentation products”. *Applied Microbiology and Biotechnology* 53.1, pp. 108–114.

Modi, R I et al. (1991). “Plasmid macro-evolution: selection of deletions during adaptation in a nutrient-limited environment”. *Genetica* 84.3, pp. 195–202.

Moore, W E and L V Holdeman (1974). “Human fecal flora: the normal flora of 20 Japanese-Hawaiians”. *Applied microbiology* 27.5, pp. 961–979.

Morrill, Haley J et al. (2015). “Treatment Options for Carbapenem-Resistant Enterobacteriaceae Infections”. *Open forum infectious diseases* 2.2, ofv050–ofv050.

Moubareck, C et al. (2007). “Inhibitory impact of bifidobacteria on the transfer of beta-lactam resistance among Enterobacteriaceae in the gnotobiotic mouse digestive tract.” *Applied and environmental microbiology* 73.3, pp. 855–860.

Naas, Thierry et al. (2008). “Genetic structures at the origin of acquisition of the beta-lactamase bla KPC gene.” *Antimicrobial agents and chemotherapy* 52.4, pp. 1257–1263.

Nair, Akhila et al. (2019). “Non-Curcuminoids from Turmeric and Their Potential in Cancer Therapy and Anticancer Drug Delivery Formulations”. *Biomolecules* 9.1, p. 13.

Nair, Mohit M et al. (2021). “Behavioural interventions to address rational use of antibiotics in outpatient settings of low-income and lower-middle-income countries”. *Tropical Medicine & International Health* n/a.n/a.

Nava, Gerardo M, Hans J Friedrichsen, and Thaddeus S Stappenbeck (2011). “Spatial organization of intestinal microbiota in the mouse ascending colon”. *The ISME Journal* 5.4, pp. 627–638.

Nguyen, Thi Loan Anh et al. (2015). “How informative is the mouse for human gut microbiota research?” *Disease models & mechanisms* 8.1, pp. 1–16.

O’Neill, Jim (2016). *Tackling Drug-Resistant Infections Globally: Final Report and Recommendations*. Tech. rep. Review on Antimicrobial Resistance.

Ogawa, M et al. (2001). “Inhibition of in vitro growth of Shiga toxin-producing Escherichia coli O157:H7 by probiotic Lactobacillus strains due to production of lactic acid.” *International journal of food microbiology* 68.1-2, pp. 135–140.

Oliver, D B et al. (1990). “Azide-resistant mutants of Escherichia coli alter the SecA protein, an azide-sensitive component of the protein export machinery.” *Proceedings of the National Academy of Sciences* 87.21, 8227 LP –8231.

Orlek, Alex et al. (2017). “Plasmid Classification in an Era of Whole-Genome Sequencing: Application in Studies of Antibiotic Resistance Epidemiology”. *Frontiers in Microbiology* 8, p. 182.

Pal, Chandan et al. (2015). “Co-occurrence of resistance genes to antibiotics, biocides and metals reveals novel insights into their co-selection potential”. *BMC Genomics* 16.1, p. 964.

Parkes, Gareth C, Jeremy D Sanderson, and Kevin Whelan (2009). “The mechanisms and efficacy of probiotics in the prevention of Clostridium difficile-associated diarrhoea”. *The Lancet Infectious Diseases* 9.4, pp. 237–244.

Pinilla-Redondo, Rafael, Leise Riber, and Søren J Sørensen (2018). “Fluorescence Recovery Allows the Implementation of a Fluorescence Reporter Gene Platform Applicable for the Detection and Quantification of Horizontal Gene Transfer in Anoxic Environments”. *Applied and Environmental Microbiology* 84.6. Ed. by Maia Kivisaar, e02507–17.

Pitout, Johann D D, Patrice Nordmann, and Laurent Poirel (2015). “Carbapenemase-Producing Klebsiella pneumoniae, a Key Pathogen Set for Global Nosocomial Dominance”. *Antimicrobial Agents and Chemotherapy* 59.10, 5873 LP –5884.

Piyachaturawat, Pawinee, Thirayudh Glinsukon, and Chaivat Toskulkao (1983). “Acute and subacute toxicity of piperine in mice, rats and hamsters”. *Toxicology Letters* 16.3, pp. 351–359.

Poirel, Laurent, Johann D Pitout, and Patrice Nordmann (2007). “Carbapenemases: molecular diversity and clinical consequences”. *Future Microbiology* 2.5, pp. 501–512.

Porse, Andreas et al. (2016). “Survival and Evolution of a Large Multidrug Resistance Plasmid in New Clinical Bacterial Hosts.” *Molecular biology and evolution* 33.11, pp. 2860–2873.

Prakash, Om, Yogesh Nimonkar, and Yogesh S Shouche (2013). “Practice and prospects of microbial preservation”. *FEMS Microbiology Letters* 339.1, pp. 1–9.

Prevel, Renaud et al. (2019). “Is systematic fecal carriage screening of extended-spectrum beta-lactamase-producing Enterobacteriaceae still useful in intensive care unit: a systematic review.” *Critical care (London, England)* 23.1, p. 170.

Price, Lance B et al. (2017). “Colonizing opportunistic pathogens (COPs): The beasts in all of us”. *PLOS Pathogens* 13.8, e1006369.

Quale, John et al. (2006). “Interplay of efflux system, ampC, and oprD expression in carbapenem resistance of Pseudomonas aeruginosa clinical isolates”. *Antimicrobial agents and chemotherapy* 50.5, pp. 1633–1641.

Rajilić-Stojanović, Mirjana et al. (2010). “Evaluating the microbial diversity of an in vitro model of the human large intestine by phylogenetic microarray analysis.” *Microbiology (Reading, England)* 156.Pt 11, pp. 3270–3281.

Rangel, Ignacio et al. (2015). “The relationship between faecal-associated and mucosal-associated microbiota in irritable bowel syndrome patients and healthy subjects”. *Alimentary Pharmacology & Therapeutics* 42.10, pp. 1211–1221.

Ranjan, Amit et al. (2017). “Comparative Genomics of Escherichia coli Isolated from Skin and Soft Tissue and Other Extraintestinal Infections.” *mBio* 8.4.

Rashid, Harunur and Mahbubur Rahman (2015). “Possible transfer of plasmid mediated third generation cephalosporin resistance between Escherichia coli and Shigella sonnei in the human gut.” *Infection, genetics and evolution : journal of molecular epidemiology and evolutionary genetics in infectious diseases* 30, pp. 15–18.

Richter, Sara N et al. (2012). “KPC-mediated resistance in Klebsiella pneumoniae in two hospitals in Padua, Italy, June 2009-December 2011: massive spreading of a KPC-3-encoding plasmid and involvement of non-intensive care units”. *Gut pathogens* 4.1, p. 7.

Ringel, Yehuda et al. (2015). “High throughput sequencing reveals distinct microbial populations within the mucosal and luminal niches in healthy individuals”. *Gut Microbes* 6.3, pp. 173–181.

Rodriguez-Grande, Jorge and Raul Fernandez-Lopez (2020). “Measuring Plasmid Conjugation Using Antibiotic Selection”. *Horizontal Gene Transfer. Methods in Molecular Biology*. Vol. 2075. New York: Humana. Chap. 6, pp. 93–98.

Russell, William Moy Stratton and Rex Leonard Burch (1959). *The principles of humane experimental technique*. London: Methuen.

San Millan, Alvaro (2018). "Evolution of Plasmid-Mediated Antibiotic Resistance in the Clinical Context". *Trends in Microbiology* 26.12, pp. 978–985.

San Millan, Alvaro and R Craig MacLean (2017). "Fitness Costs of Plasmids: a Limit to Plasmid Transmission." *Microbiology spectrum* 5.5.

Saw, Howard T H (2015). "The Biology of Antibiotic Resistance Plasmids". Thesis (Ph.D.) University of Birmingham.

van Schaik, Willem (2015). "The human gut resistome." *Philosophical transactions of the Royal Society of London. Series B, Biological sciences* 370.1670, p. 20140087.

Scott, Karen P et al. (1998). "The green fluorescent protein as a visible marker for lactic acid bacteria in complex ecosystems". *FEMS Microbiology Ecology* 26.3, pp. 219–230.

Sekirov, Inna et al. (2010). "Gut Microbiota in Health and Disease". *Physiological Reviews* 90.3, pp. 859–904.

Shah, Pranjul et al. (2016). "A microfluidics-based in vitro model of the gastrointestinal human–microbe interface". *Nature Communications* 7.1, p. 11535.

Shaner, Nathan C et al. (2004). "Improved monomeric red, orange and yellow fluorescent proteins derived from Discosoma sp. red fluorescent protein". *Nature Biotechnology* 22.12, pp. 1567–1572.

Sheppard, Anna E et al. (2016). "Nested Russian Doll-Like Genetic Mobility Drives Rapid Dissemination of the Carbapenem Resistance Gene blaKPC". *Antimicrobial Agents and Chemotherapy* 60.6, pp. 3767–3778.

Shintani, Masaki, Zoe K Sanchez, and Kazuhide Kimbara (2015). "Genomics of microbial plasmids: classification and identification based on replication and transfer systems and host taxonomy". *Frontiers in Microbiology* 6, p. 242.

Shoba, G et al. (1998). “Influence of piperine on the pharmacokinetics of curcumin in animals and human volunteers.” *Planta medica* 64.4, pp. 353–356.

Sinha, R P (1986). “Toxicity of organic acids for repair-deficient strains of Escherichia coli”. *Applied and Environmental Microbiology* 51.6, pp. 1364–1366.

Smet, A et al. (2011). “In situ ESBL conjugation from avian to human Escherichia coli during cefotaxime administration.” *Journal of applied microbiology* 110.2, pp. 541–549.

Smillie, Chris S et al. (2010). “Mobility of Plasmids”. *Microbiology and Molecular Biology Reviews* 74.3, 434 LP –452.

Smillie, Chris S et al. (2011). “Ecology drives a global network of gene exchange connecting the human microbiome.” *Nature* 480.7376, pp. 241–244.

Smith, H W (1969). “Transfer of antibiotic resistance from animal and human strains of Escherichia coli to resident E. coli in the alimentary tract of man.” *Lancet (London, England)* 1.7607, pp. 1174–1176.

Soucy, Shannon M, Jinling Huang, and Johann Peter Gogarten (2015). “Horizontal gene transfer: building the web of life”. *Nature Reviews Genetics* 16.8, pp. 472–482.

Stecher, Bärbel et al. (2012). “Gut inflammation can boost horizontal gene transfer between pathogenic and commensal Enterobacteriaceae.” *Proceedings of the National Academy of Sciences of the United States of America* 109.4, pp. 1269–1274.

Stevenson, Cagla et al. (2018). “Plasmid stability is enhanced by higher-frequency pulses of positive selection”. *Proceedings. Biological sciences* 285.1870, p. 20172497.

Strack, Rita L et al. (2010). “Chromophore Formation in DsRed Occurs by a Branched Pathway”. *Journal of the American Chemical Society* 132.24, pp. 8496–8505.

Suresh, D and K Srinivasan (2007). “Studies on the in vitro absorption of spice principles – Curcumin, capsaicin and piperine in rat intestines”. *Food and Chemical Toxicology* 45.8, pp. 1437–1442.

Swain Ewald, Holly A and Paul W Ewald (2018). “Natural Selection, The Microbiome, and Public Health”. *The Yale journal of biology and medicine* 91.4, pp. 445–455.

Tacconelli, Evelina et al. (2018). “Discovery, research, and development of new antibiotics: the WHO priority list of antibiotic-resistant bacteria and tuberculosis”. *The Lancet Infectious Diseases* 18.3, pp. 318–327.

Tamma, Pranita D et al. (2017). “Comparing the Outcomes of Patients With Carbapenemase-Producing and Non-Carbapenemase-Producing Carbapenem-Resistant Enterobacteriaceae Bacteremia”. *Clinical infectious diseases : an official publication of the Infectious Diseases Society of America* 64.3, pp. 257–264.

Tang, Qiang et al. (2020). “Current Sampling Methods for Gut Microbiota: A Call for More Precise Devices”. *Frontiers in Cellular and Infection Microbiology* 10, p. 151.

Tannenbaum, Jerrold and B Taylor Bennett (2015). “Russell and Burch’s 3Rs then and now: the need for clarity in definition and purpose”. *Journal of the American Association for Laboratory Animal Science : JAALAS* 54.2, pp. 120–132.

Tap, Julien et al. (2017). “Identification of an Intestinal Microbiota Signature Associated With Severity of Irritable Bowel Syndrome”. *Gastroenterology* 152.1, 111–123.e8.

Tayyem, Reema F et al. (2006). “Curcumin content of turmeric and curry powders.” *Nutrition and cancer* 55.2, pp. 126–131.

Tomasz, A (1979). “The mechanism of the irreversible antimicrobial effects of penicillins: how the beta-lactam antibiotics kill and lyse bacteria.” *Annual review of microbiology* 33, pp. 113–137.

Towse, Adrian et al. (2017). “Time for a change in how new antibiotics are reimbursed: Development of an insurance framework for funding new antibiotics based on a policy of risk mitigation”. *Health Policy* 121.10, pp. 1025–1030.

Traxler, Matthew F and Roberto Kolter (2015). “Natural products in soil microbe interactions and evolution”. *Nat. Prod. Rep.* 32.7, pp. 956–970.

Trevors, J T (1986). “Plasmid curing in bacteria”. *FEMS Microbiology Reviews* 1.3-4, pp. 149–157.

Trobos, Margarita et al. (2008). “Natural transfer of sulphonamide and ampicillin resistance between Escherichia coli residing in the human intestine”. *Journal of Antimicrobial Chemotherapy* 63.1, pp. 80–86.

Tsien, Roger Y (1998). “THE GREEN FLUORESCENT PROTEIN”. *Annual Review of Biochemistry* 67.1, pp. 509–544.

Tyagi, Poonam et al. (2015). “Bactericidal Activity of Curcumin I Is Associated with Damaging of Bacterial Membrane”. *PLOS ONE* 10.3, e0121313.

Ulluwishewa, Dulantha et al. (2015). “Live Faecalibacterium prausnitzii in an apical anaerobic model of the intestinal epithelial barrier”. *Cellular Microbiology* 17.2, pp. 226–240.

Veilleux, B G and I Rowland (1981). “Simulation of the rat intestinal ecosystem using a two-stage continuous culture system.” *Journal of general microbiology* 123.1, pp. 103–115.

Venema, Koen (2015). “The TNO In Vitro Model of the Colon (TIM-2)”. *The Impact of Food Bioactives on Health: in vitro and ex vivo models*. Springer. Chap. 26.

Venema, Koen and Pieter van den Abbeele (2013). “Experimental models of the gut microbiome”. *Best Practice & Research Clinical Gastroenterology* 27.1, pp. 115–126.

Ventola, C Lee (2015). “The antibiotic resistance crisis: part 1: causes and threats”. *P & T : a peer-reviewed journal for formulary management* 40.4, pp. 277–283.

Vincent, Jean-Louis (2003). “Nosocomial infections in adult intensive-care units”. *The Lancet* 361.9374, pp. 2068–2077.

Wang, Yuanzhe et al. (2020). “Electrochemical quantification of piperine in black pepper”. *Food Chemistry* 309, p. 125606.

Wang, Yuli et al. (2018). “Bioengineered Systems and Designer Matrices That Recapitulate the Intestinal Stem Cell Niche”. *Cellular and Molecular Gastroenterology and Hepatology* 5.3, 440–453.e1.

Wehrli, W (1983). “Rifampin: mechanisms of action and resistance.” *Reviews of infectious diseases* 5 Suppl 3, S407–11.

Westfall, Corey S and Petra Anne Levin (2018). “Comprehensive analysis of central carbon metabolism illuminates connections between nutrient availability, growth rate, and cell morphology in Escherichia coli”. *PLoS genetics* 14.2, e1007205–e1007205.

WHO (2020). *Antibiotic resistance*. `https://www.who.int/news-room/fact-sheets/detail/antibiotic-resistance`.

van de Wiele, Tom et al. (2015). “The Simulator of the Human Intestinal Microbial Ecosystem (SHIME®)”. *The Impact of Food Bioactives on Health: in vitro and ex vivo models*. Springer. Chap. 27.

Wilkins, Thad and Jacqueline Sequoia (2017). “Probiotics for Gastrointestinal Conditions: A Summary of the Evidence.” *American family physician* 96.3, pp. 170–178.

Wu, Chengxin et al. (2018). “Sensitive analysis of curcuminoids via micellar electrokinetic chromatography with laser-induced native fluorescence detection and mixed micelles-induced fluorescence synergism.” *Journal of chromatography. A* 1564, pp. 207–213.

Xilin, Zhao and Karl Drlica (2002). “Restricting the Selection of Antibiotic-Resistant Mutant Bacteria: Measurement and Potential Use of the Mutant Selection Window”. *The Journal of Infectious Diseases* 185.4, pp. 561–565.

Yaffe, Eitan and David A Relman (2020). “Tracking microbial evolution in the human gut using Hi-C reveals extensive horizontal gene transfer, persistence and adaptation”. *Nature Microbiology* 5.2, pp. 343–353.

Yelin, Idan et al. (2019). “Genomic and epidemiological evidence of bacterial transmission from probiotic capsule to blood in ICU patients.” *Nature medicine* 25.11, pp. 1728–1732.

Yi, Hana et al. (2012). “Genome Sequence of Escherichia coli J53, a Reference Strain for Genetic Studies”. *Journal of Bacteriology* 194.14, 3742 LP –3743.

Yousi, Fu et al. (2019). “Evaluation of the effects of four media on human intestinal microbiota culture in vitro.” *AMB Express* 9.1, p. 69.

Zarai, Zied et al. (2013). “Antioxidant and antimicrobial activities of various solvent extracts, piperine and piperic acid from Piper nigrum”. *LWT - Food Science and Technology* 50.2, pp. 634–641.

Zeng, Ximin and Jun Lin (2017). “Factors influencing horizontal gene transfer in the intestine”. *Animal Health Research Reviews* 18.2, pp. 153–159.

Zihler Berner, Annina et al. (2013). “Novel Polyfermentor Intestinal Model (PolyFermS) for Controlled Ecological Studies: Validation and Effect of pH”. *PLOS ONE* 8.10, e77772.

Zitomersky, Naamah Levy, Michael J Coyne, and Laurie E Comstock (2011). “Longitudinal analysis of the prevalence, maintenance, and IgA response to species of the order Bacteroidales in the human gut”. *Infection and immunity* 79.5, pp. 2012–2020.

Zotta, T, E Parente, and A Ricciardi (2017). “Aerobic metabolism in the genus Lactobacillus: impact on stress response and potential applications in the food industry.” *Journal of applied microbiology* 122.4, pp. 857–869.

Zwanzig, Martin et al. (2019). “Mobile Compensatory Mutations Promote Plasmid Survival”. *mSystems* 4.1, e00186–18.

Appendices

A.

SUMMARY TABLE OF MIC VALUES

Table A.1: Summary table of MIC values for broth microdilution MIC assays performed as described in Section 2.2.4. Antibiotic abbreviations are outlined in Table 2.1. Where biological replicates gave different values, the MIC is indicated as a range. *Range as accepted by EUCAST (2020b); N/A indicates that recommendations are not available for that antibiotic. **Experiments done by Nicholas Lim (placement student, Buckner Lab). - indicates that the MIC was not performed.

Strain	MIC (μg/ml) of antibiotic					
	KAN	RIF	CEF	AMP	DOR	$HgCl_2$
I448	2	4	16-32	2	0.03125-0.0625	1
I448 range*	N/A	N/A	N/A	2-8	N/A	N/A
H207	256	32	256	-	-	1-2
H222	-	-	-	32-64	-	-
H235	128-256	>256	2-4	64-128	-	1-2
CPE01**	-	>512	-	-	>16	-
Az^R J53	-	-	-	-	0.015625 - 0.03125	-

B.

INITIAL CONFIRMATION OF PKPQIL PLASMID CARRIAGE

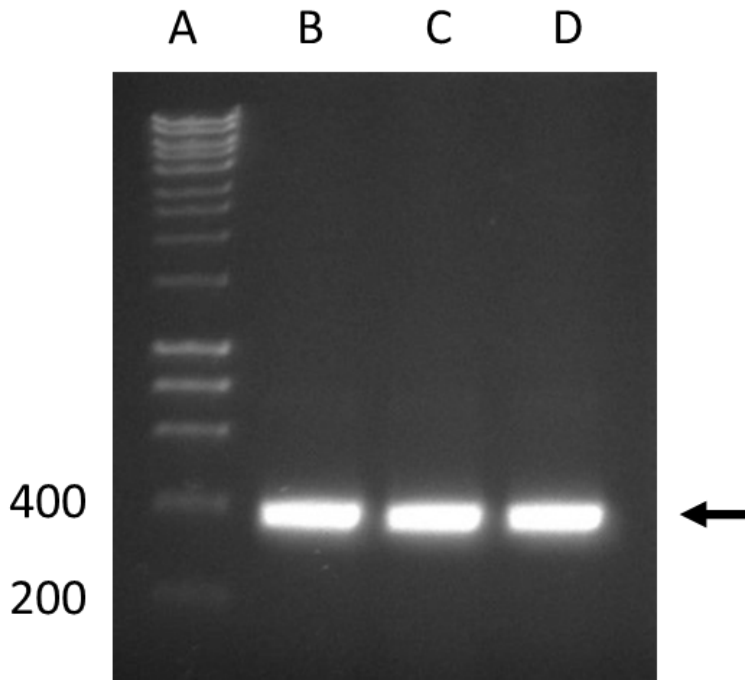

Figure B.1: Colony PCR of replica plated putative transconjugants, that grew when replica plated onto double-selective plates, for the pKpQIL backbone.
Lanes A: 1kb hyperladder, B-D: putative transconjugants. Appropriate hyperladder band sizes (in base pairs) are indicated on the left. Band of interest has a size of 383bp and is identified with an arrow.

C.

BRAIN HEART INFUSION SUPPLEMENTED MEDIA

The preparation of BHIS media was performed as instructed in Table C.1, based on an ATCC recommended preparation which can be found at `https://www.atcc.org/~/media/D773986160FE485BAC6AFFB074F52F94.ashx`.

	Ingredient (source)	**Quantity**
Mix pre-autoclave	Brain heart infusion broth (Sigma Aldrich)	37.0 g
	Yeast extract (Sigma Aldrich)	5.0 g
	Distilled water	1 l
	L resazurin (Acros Organics)	4.0 ml of 0.025% solution in SDW
Mix post-autoclave	L-cysteine . HCl (Thermo Scientific)	0.5 g
	Hemin (Sigma Aldrich)	10.0 ml of 0.05% solution in 0.001 mol/l NaOH
	Vitamin K1 (Cerilliant)	0.2 ml of 0.5% solution in 95% EtOH

Table C.1: Supplemented Brain-Heart Infusion media preparation

D.

FLOW CYTOMETRY: DMSO SOLVENT CONTROLS

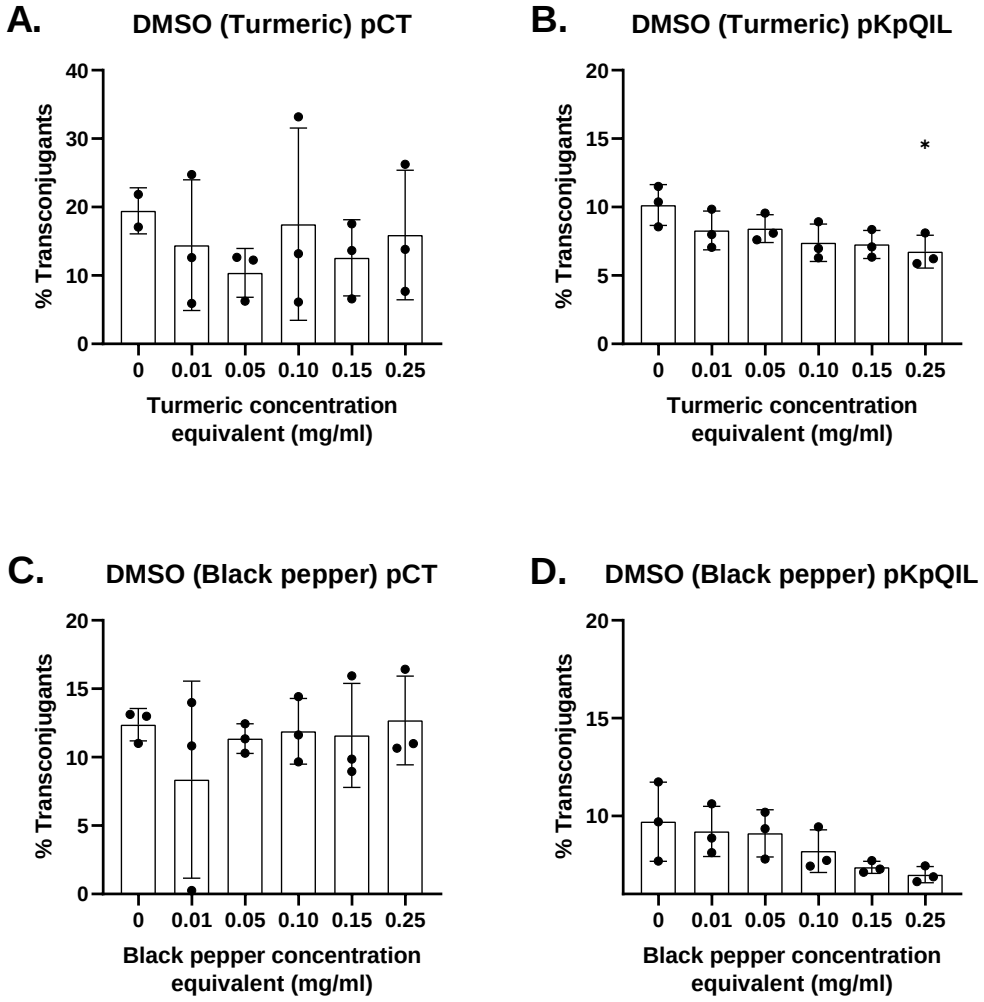

Figure D.1: Effect of DMSO on the conjugation of pCT and pKpQIL, in the quantities present in the tested concentrations of turmeric and black pepper extracts. **A.** DMSO equivalent to concentrations in turmeric extract tested on pCT. **B.** DMSO equivalent to concentrations in turmeric extract tested on pKpQIL. **C.** DMSO equivalent to concentrations in black pepper extract tested on pCT. **D.** DMSO equivalent to concentrations in black pepper extract tested on pKpQIL. Each data point represents one experiment with four biological repeats. Error bars represent one standard deviation above and below the mean. * = $P \leq 0.05$, when the difference to the control (0 mg/ml equivalent) was calculated with Welch's t-test.

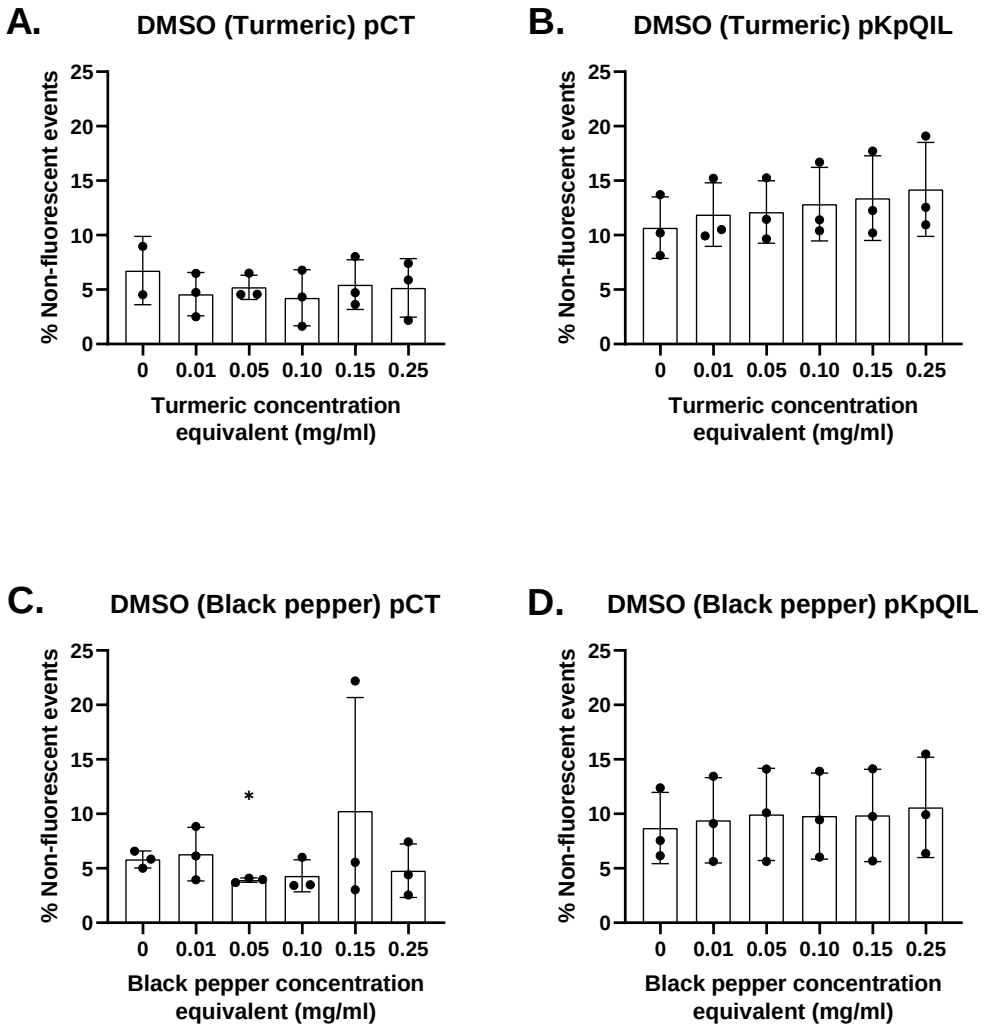

Figure D.2: Effect of DMSO on the detection of non-fluorescent events, in the quantities present in the tested concentrations of turmeric and black pepper extracts. **A.** DMSO equivalent to concentrations in turmeric extract tested on pCT. **B.** DMSO equivalent to concentrations in turmeric extract tested on pKpQIL. **C.** DMSO equivalent to concentrations in black pepper extract tested on pCT. **D.** DMSO equivalent to concentrations in black pepper extract tested on pKpQIL. Each data point represents one experiment with four biological repeats. Error bars represent one standard deviation above and below the mean. * = $P \leq 0.05$, when the difference to the control (0 mg/ml equivalent) was calculated with Welch's t-test.